

**TOMAS BATA UNIVERSITY IN ZLÍN**  
**FACULTY OF TECHNOLOGY**

**Petr Zádrapa**

---

**THE MORPHOLOGY AND PROPERTIES OF SELECTED  
FILLER/POLY(ETHYLENE-CO-METHACRYLIC ACID)  
COPOLYMER SYSTEMS**

**Morfologie a vlastnosti vybraných systémů plnivo/kopolymer  
poly(ethylen-co-kyselina metakrylová)**

---

Doctoral Thesis

2011

---

Programme:	Chemistry and Materials Technology
Course:	Technology of Macromolecular Substances
Supervisor:	Assoc. Prof. Jiří Maláč

---

# ABSTRACT

Fillers are the most frequently used additives for polymeric materials. Their addition into the polymer matrix leads to the modification of its processing or physical properties. Nowadays, active fillers sized in nanometres are often used. Originally, active fillers were mainly carbon blacks in rubber compounds. However, since the 1990s, a steep increase in the number of publications about nanoparticle based fillers has been seen, and clay minerals tend to be among those most studied. The reason is that, if their dispersion in a polymer matrix is good enough, even a small amount of these fillers can significantly change the desired properties of the resulting materials.

The work herein presented is focused on the modification of clays for their application in a polyethylene copolymer matrix. Two representatives of the layered silicate group - vermiculite and montmorillonite, were studied. The structure of both is formed of thin layers of silicates, whose interlayer spacing can be increased by suitable modification. Interlayers usually contain inorganic cations which can be changed by bigger organic ones, in order to increase the interlayer distance and thus make the fillers more organophilic.

While the initially studied montmorillonite was in a sodium form (*i.e.* with sodium cations only), the interlayers of the initial vermiculite contained various types of inorganic cations. Because of easier organophilization, the different types of cations in the vermiculite had first to be replaced by only one type. After this step, only one inorganic cation-type was present in both the vermiculite and the montmorillonite, and the inorganic cations were subsequently substituted for organic ones. The modified filler samples thus obtained were studied by X-ray scattering and thermo-gravimetric analysis. Fillers with the highest increase in interlayer distance caused by organic cation modification were compounded with the copolymer, and their effect on the composite properties was compared with commercially available nanofillers.

Surlyn®, the commercial copolymer of ethylene and methacrylic acid with acid groups partially neutralized by metal ions (e.g. by sodium or zinc), was used in this work as the polymer matrix. Several types of Surlyn® were tested with different concentrations of methacrylic acid and different levels of its neutralization. These nanocomposites with Surlyn® were characterized by X-ray scattering, microscopy, tensile property and gas permeability measurements. The effects of methacrylic acid concentration, ion type and methacrylic acid neutralization level on the resulting properties of the tested nanocomposites were then evaluated.

**Keywords:** Poly(ethylene-co-methacrylic acid) copolymer, clay intercalation, vermiculite, montmorillonite, gas permeability.

# ABSTRAKT

Plniva jsou jedny z nejčastěji používaných aditiv do polymerních směsí a jejich přidavek do polymerní matrice vede ke změně zpracovatelských a fyzikálních vlastností. Nyní se nejčastěji používají takzvaná aktivní plniva, jejichž rozměry jsou často v nanometrech. Původně plnily efekt aktivního plniva hlavně saze u kaučukových směsí. Ale od 90 let minulého století se výrazně zvyšuje zájem i o jiné typy plniv s rozměry v nanometrech. Velmi často jsou to zvláště jílové minerály. Důvodem je jejich výrazný vliv na výsledné vlastnosti kompozitu i při přidavku malého množství, zvláště pokud se dosáhne vysokého stupně disperze plniva v polymerní matrici.

Předložená práce je zaměřená na úpravu jílu pro jejich použití v polymerní matrici s kopolymerem polyetylénu. Studovány byly plniva reprezentující skupinu vrstevnatých silikátů, vermikulit a montmorillonit. Struktura obou plniv je složena ze silikátových vrstev, jejichž mezivrstvi obsahuje vyměnitelné kationty kovů. Tyto můžou být vyměněny za mnohem větší organické ionty, což vede ke zvýšení mezivrstevné vzdálenosti a navíc ke zvýšení kompatibility mezi plnivem a polymerem.

Studovaný typ montmorillonitu v mezivrstvi obsahoval jenom jeden typ iontu ( $\text{Na}^+$ ), v mezivrstvi vermikulitu bylo přítomno několik různých anorganických kationtů. Pro snadnější modifikaci organickými kationty, musely být nejdříve převedeny na jeden typ iontu. Takto upravený vermikulit a následně i montmorillonit byly interkalovány organickými kationty. Vzorke plniv byly zkoumány pomocí rentgenové difrakce a termogravimetrické analýzy. Plniva s největší dosaženou mezivrstevnou vzdáleností byly vybrány pro přípravu kompozitních materiálů.

Jako polymer byl použit Surlyn®, což je kopolymer etylénu a kyseliny metakrylové, jejíž kyselé skupiny jsou částečně neutralizovány kovovými ionty (sodné nebo zinečnaté). Zkoušky se prováděly na několika typech Surlyn®, lišících se v množství kyseliny metakrylové ve struktuře, stupni její neutralizace a iontu k tomu použitému. Nanokompozity ze Surlyn®u byly testovány pomocí rentgenové difrakce, zkoumaly se mechanické vlastnosti a propustnost na plyny. Vyhodnocován byl vliv stupně neutralizace kyseliny metakrylové a použitého iontu na konečné vlastnosti nanokompozitu.

**Klíčová slova:** Kopolymer poly(ethylen-co-metakrylové kyseliny), interkalaci jílu, vermikulit, montmorillonit, plynopropustnost.

*I would like to take this opportunity to express my gratitude to everybody who participated in the research for their fruitful discussions, kind help and inspiration.*

*Last but not least, I would like to thank to Lucie and my entire family for their love and support throughout my study.*

# TABLE OF CONTENTS

<b>ABSTRACT</b> .....	<b>2</b>
<b>ABSTRAKT</b> .....	<b>3</b>
<b>TABLE OF CONTENTS</b> .....	<b>5</b>
<b>INTRODUCTION</b> .....	<b>8</b>
<b>1. IONOMER</b> .....	<b>10</b>
1.1. Ionomer definition .....	10
1.2. Poly(ethylene-co-methacrylic acid) ionomer – Surlyn® .....	10
1.3. Ionomer copolymerization .....	12
1.4. Ionomer physical–mechanical description .....	13
<b>2. POLYMER COMPOSITES</b> .....	<b>15</b>
2.1. Processing development: From composite to nanocomposite .....	15
2.2. Mineral description.....	17
2.3. Polymer clay composite preparation .....	20
2.4. Surlyn® – clay nanocomposites.....	22
<b>3. THE AIMS OF RESEARCH WORK</b> .....	<b>24</b>
<b>4. EXPERIMENTAL PART</b> .....	<b>25</b>
4.1 Materials .....	25
4.1.1 Polymers .....	25
4.1.2 Fillers.....	26
4.1.3 Intercalation agent.....	29
4.2 Characterization Methods .....	30
4.2.1 X-Ray diffraction (XRD).....	30
4.2.2 Fourier transforms infrared spectroscopy (FTIR).....	31

4.2.3	Thermal gravimetric analysis (TGA) .....	31
4.2.4	Optical microscopy .....	31
4.2.5	Scanning electron microscopy (SEM).....	32
4.2.6	Transmission electron microscopy (TEM) .....	32
4.2.7	Mechanical testing .....	33
<b>5</b>	<b>RESULTS AND DISCUSSION .....</b>	<b>35</b>
5.1	Filler modification.....	35
5.1.1	Preparation of sodium vermiculite .....	36
5.1.2	VMT modification by HCl .....	42
5.1.3	Preparation of organically modified VMT.....	46
5.1.4	Thermo gravimetric analysis of fillers.....	54
5.2	Polymer/clay composite preparation .....	58
5.2.1	Evaluation of the best compounding condition.....	58
5.2.2	Materials .....	61
5.2.3	Preparation of tested compounds.....	61
5.3	Characterization of structure and properties .....	62
5.3.1	X-Ray diffraction .....	62
5.3.2	Optical microscopy .....	64
5.3.3	Scanning electron microscopy .....	67
5.3.4.	Transmission electron microscopy .....	72
5.3.5	Tensile test .....	74
5.3.6	Gas permeability .....	77
5.4	Ion effect on filler dispersion in matrix .....	80
5.5	Effect of degree of MAA group neutralization on resulting polymer/clay properties.....	89

<b>CONCLUSION .....</b>	<b>96</b>
<b>CONTRIBUTION TO THE SCIENCE AND PRACTICE .....</b>	<b>98</b>
<b>REFERENCES.....</b>	<b>99</b>
<b>AUTHOR’S PUBLICATIONS.....</b>	<b>104</b>
<b>CURRICULUM VITAE .....</b>	<b>107</b>
<b>LIST OF FIGURES .....</b>	<b>108</b>
<b>LIST OF TABLES.....</b>	<b>112</b>
<b>LIST OF SYMBOLS AND ABBREVIATIONS .....</b>	<b>113</b>

# INTRODUCTION

One hundred years ago, an era of synthetic materials started. The Belgian chemist, Leo Hendrik Baekeland, synthesized a material, chemically termed as polyoxybenzylmethylenglycolanhydride, which is well known as Bakelite all over the world.

Due to its favourable properties, such as high temperature resistance, isolative properties, *etc.*, Bakelite found a broad application area, mainly in electrotechnic industry. Not only light switcher or mains outlets were the products made from this material. Many luxurious objects were made from Bakelite, for instance industry lamps, shave machines, hair dryers, telephone covers and also toys or bijouterie [1, 2].

Despite of the fact, that the invention of Bakelite started intensive research on chemical field, new knowledge reflected in lower interest about Bakelite alone and thus it was continuously replaced with more suitable polymers. In the next 20 years, a plenty of new polymeric materials were synthesised (Fig. 1) and their amount increased up to 50's of the last century. Hence, the discovery of new polymer is rather rare case [1–3].

Generally, wide grade of polymers is divided into the three groups according to ratio cost *vs.* performance: commodity (polyethylene, polypropylene, polystyrene and polyvinyl chloride), constructive (polycarbonate, polyethylene terephthalate, polymethyl metacrylate and others) and specials polymers (polyaryletheretherketone, liquid crystal polymers, *etc.*). Commodity polymers are permanently the most frequently used polymers, mainly because of their relatively good properties and low prize. Prediction in 70's supposed that the production of commodity polymers is going to decline and the importance of constructive and specials are going to increase. The reason, why the predictions were not fulfilled influenced the finding of many methods improving the physical-mechanical properties of commodity ones [3].

Nowadays, the three main areas of intensive research on polymeric field are as follows: structural modifications, blending two or more polymers and finally compounding polymers with fillers and recently nanofillers, which is also the main goal of presented doctoral study.

Worldwide, the most widespread polymer is polyethylene with consumption approximately 70 million tons in 2010 [4]. As mentioned above, popularity of polyethylene is given by its relatively good properties and low prize. Moreover, its ability to be copolymerized markedly spreads out its variability to be used in potential applications. Poly(ethylene-co-methacrylic acid) ionomer is one of them. Its methacrylic acid groups are partially neutralized by metal ions. Due to this fact, ionomer obtains unique properties, such as high impact, abrasion and chemical resistance, melt strength, clarity, *etc.* The presence of polar groups increases its compatibility to other polymers [5–7].



Ionomers were also considered as a suitable matrix in nanocomposite materials. In contrast to pure polyethylene, whose compatibility to fillers is low, the usage of ionomer improves particle exfoliation [8–9]. Although several studies dealing with ionomer nanocomposites were carried out, many factors have not been successfully answered until now.

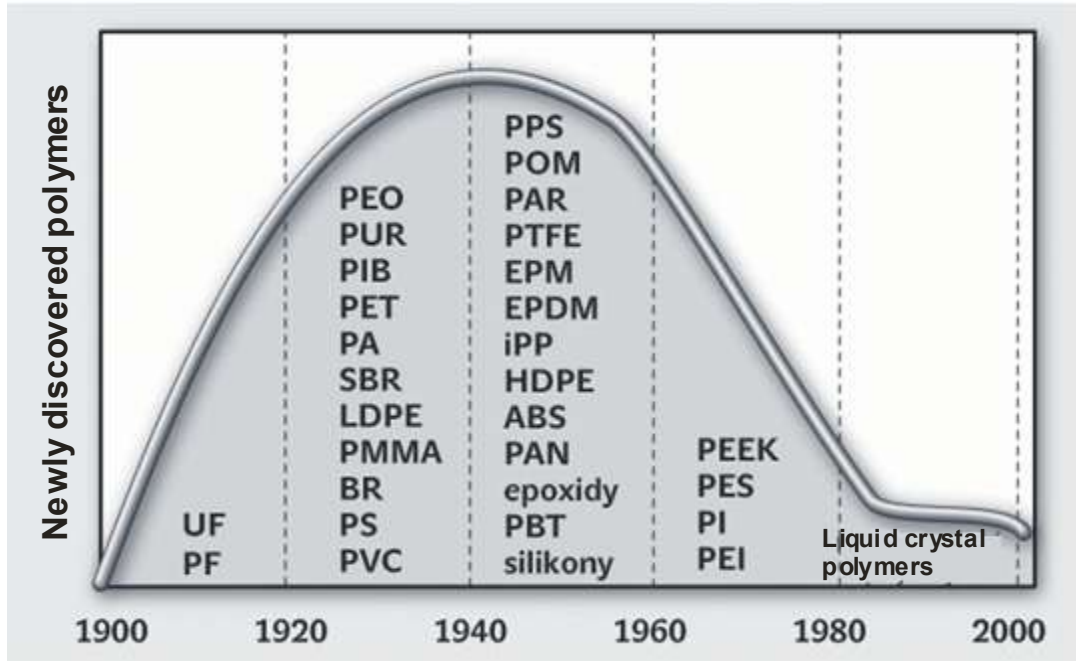


Fig. 1: The discovery of new polymer in time [3].

# 1. IONOMER

## 1.1. Ionomer definition

In the 1960's, Rees and Vaughan [10] defined ionomer as “an olefin based polymers containing a relatively small percentage of ionic groups in which strong ionic interchain forces play a dominant role in controlling properties”. During the time, other polymers were employed as parents for ionomers. A definition was extended, however the problem was not solved, because the ionomers, notably those with higher ion content can behave also as polyelectrolytes. Eisenberg and Rinaudo [11] define ionomers “as polymers in which the bulk properties are governed by ionic interaction in discrete regions of the material”. It follows, that ionomer behaviour is connected with its properties rather than composition and as the main part of ionomer is defined ionic aggregate, which is similar to original definition [6].

Mostly, ionomers are copolymers of materials with low dielectric constant (polyethylene, styrene) containing ionic groups based on methacrylic and sulfonic acid or amines, which are partially or fully neutralized. Depending on the copolymer type, the ionic groups can be located in various positions in polymer chain. Independently on the position, ionic groups create aggregates with similar effect as physical crosslinking. Thus ionomer obtains unique properties [6, 12].

## 1.2. Poly(ethylene-co-methacrylic acid) ionomer – Surlyn®

Poly(ethylene-co-methacrylic acid) ionomer, commercially available as Surlyn®, is a thermoplastic copolymer, which was firstly synthesized by DuPont in early 60's of the last century. Surlyn® is a random copolymer of ethylene and methacrylic acid (MAA), whose groups are partially neutralized by metal ions, such as sodium, lithium or zinc. The degree of neutralization is generally from 20 % to 80 %. The content of MAA groups is low, approximately up to 15 molar %. The structure of this polymer contains three regions: an amorphous, crystalline and ionic cluster (Fig. 1.1), which is clearly seen via wide angle X-ray scattering (WAXS) (Fig. 1.2). Ionic clusters are confirmed by the presence of the peak around  $3^{\circ}2\theta$  [5, 7, 13].

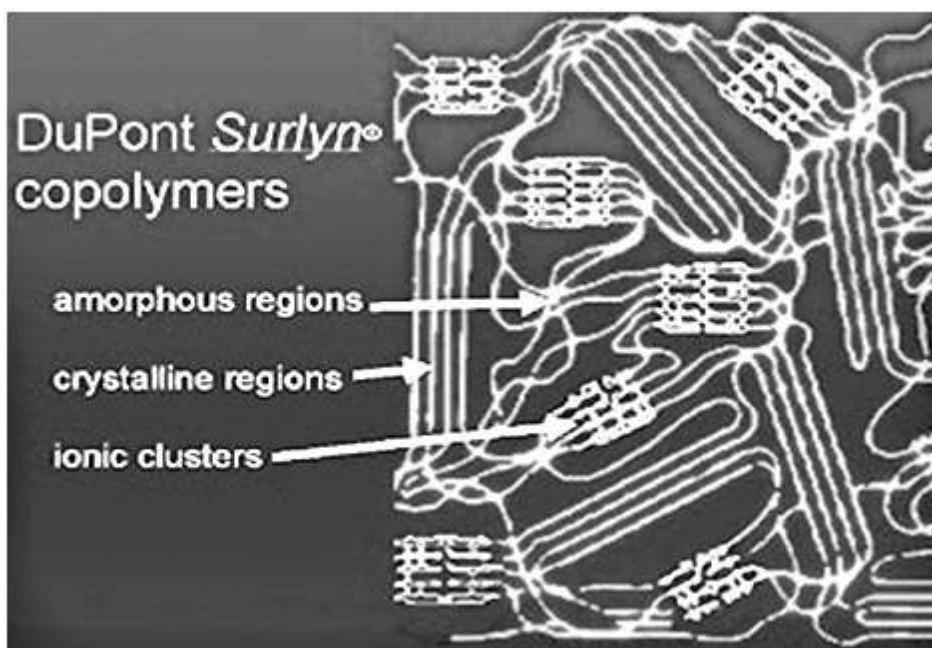


Fig. 1.1: Theoretical structure of poly(ethylene-co-methacrylic acid) ionomer [5].

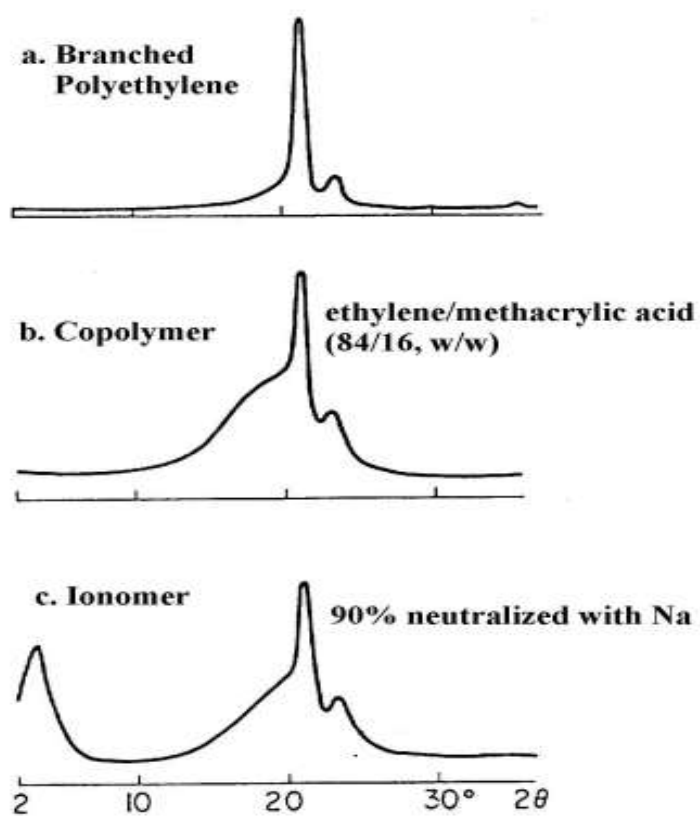


Fig. 1.2: WAXS profile for a) branched polyethylene, b) ethylene/methacrylic acid copolymer and c) ethylene/methacrylic acid copolymer neutralized with Na ions [7].

### 1.3. Ionomer copolymerization

The polymerization of Surlyn® is similar to the reaction of low density polyethylene. Surlyn® ionomer is synthesized by radical copolymerization of ethylene with low amount of methacrylic acid at high pressure ( $p = 150\text{--}300$  MPa) and temperature ( $T = 200$  °C). After the reaction, the copolymer is neutralized by metal ions and subsequently dissolved in solution (e.g. tetrahydrofuran). Finally alkaline solution is added. Then, the solvent is removed and neutralized copolymer is obtained.

Neutralization can be also done in a melt state via an extruder or a double roll mill. Ethylene - methacrylic acid copolymer is melted together with an aqueous alkaline solution. After water evaporation, the final product is extracted. Neutralization is done by NaOH and LiOH in the case of sodium and lithium ions or by  $\text{Zn}(\text{OH})_2$  in the case of zinc ions. The process is shown in the Figs. 1.3 and 1.4 [6, 7, 12, 14].

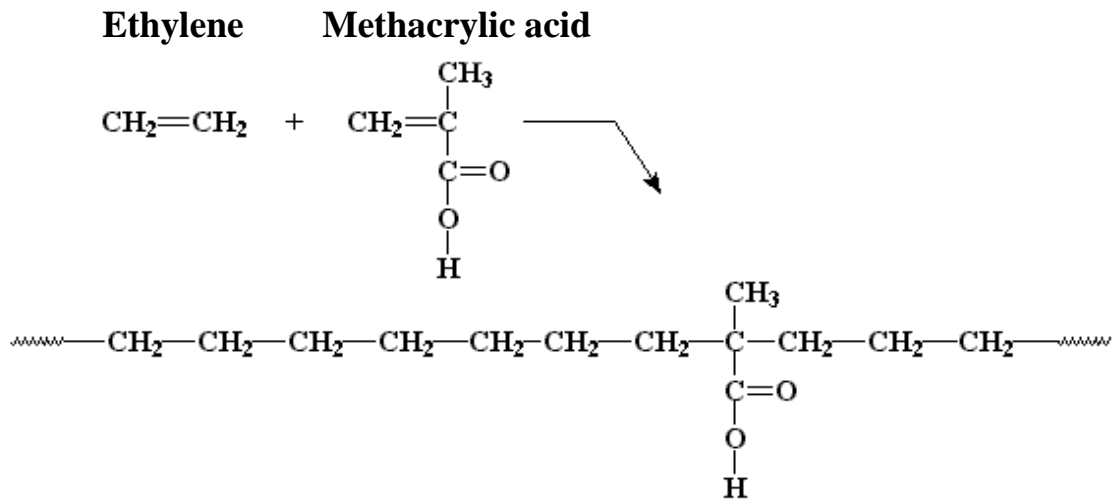


Fig. 1.3: Copolymerization of ethylene and methacrylic acid (step 1).

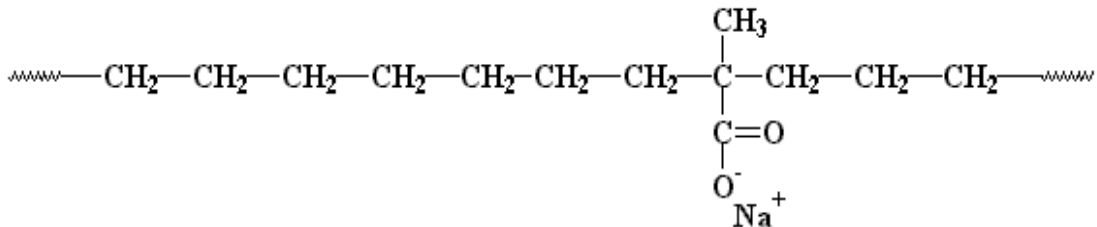


Fig. 1.4: Structure of Surlyn® neutralized by NaOH (step 2).

## 1.4. Ionomer physical–mechanical description

As a pure copolymer or blend, Surlyn® exceeds other polymers from polyolefinic group with extraordinary properties, such as tensile strength, impact, abrasion, chemical and oil resistance. Moreover, the presence of MAA groups makes Surlyn® amorphous, which results in its high clarity and transparency. Surlyn® is usually processed by extrusion, injection or blow moulding. Furthermore, Surlyn® can be applied as a polymer modifier as well. General characteristic of Surlyn® are given in Table 1.1.

The applications arise from its properties. Surlyn® is widely used as surface cover (golf ball, ski boots, *etc.*), packaging material (perfumes and cosmetics, food industry), coating material for glass and metal and polymer modifier [5, 13, 14].

Naturally, Surlyn® is frequently studied material [15–19], because of its still not successfully explained behaviour, or its ability to improve compatibility with both blends [20–24], and fillers [9, 25–32].

Table 1.1: Selected properties of Surlyn® [5]

Property	Value range	Test method
Specific gravity (g/cm <sup>3</sup> )	0.94–0.97	ASTM D 792
Hardness (Shore D)	36–68	ASTM D 2240
Flex Modulus (room temp, MPa)	30–517	ASTM D790 Procedure B
Tensile strength (MPa)	16–37	ASTM D 638
Elongation at Break (%)	285–770	ASTM D 638
Melt Flow Index (g/10 min)	0.7–20	ASTM D 1238
Vicat Softening Point(°C)	47–74	ASTM D 1525-70
Melting Point (°C)	70–100	DSC
Optical Haze (6.4 mm)	1.3–27	ASTM D1003A

As mentioned above, the properties of Surlyn® are influenced by the amount of comonomer (methacrylic acid), degree of methacrylic acid group neutralization and finally by the type of neutralized ions. Surlyn® is produced at several grades differing in three parameters (Fig. 1.5). With higher amount of MAA properties, like yield point, tensile strength, stiffness, tear strength or hardness increases, however elongation, freeze point or haze decreases. Similarly, with neutralization degree of MAA group higher tensile strength, stiffness and hardness, *etc.* increases, but at the same time other properties (adhesion, haze, freeze point and tear strength) are reduced [5, 12, 14].

The methacrylic acid groups are commercially neutralized by three types of ion – sodium, zinc and lithium. Each of these ions gives specific properties to the copolymer and together with amount of the ions, changes *e.g.* compatibility to other polymers. As it is well known, sodium ions increase compatibility to

polyesters and stress crack resistance, but reduce haze, while zinc ions improve melt flow, tear resistance and adhesion to polyamides, *etc.* Finally, ionomers neutralized by lithium ions are harder and stiffer than zinc and sodium [5, 12–14].

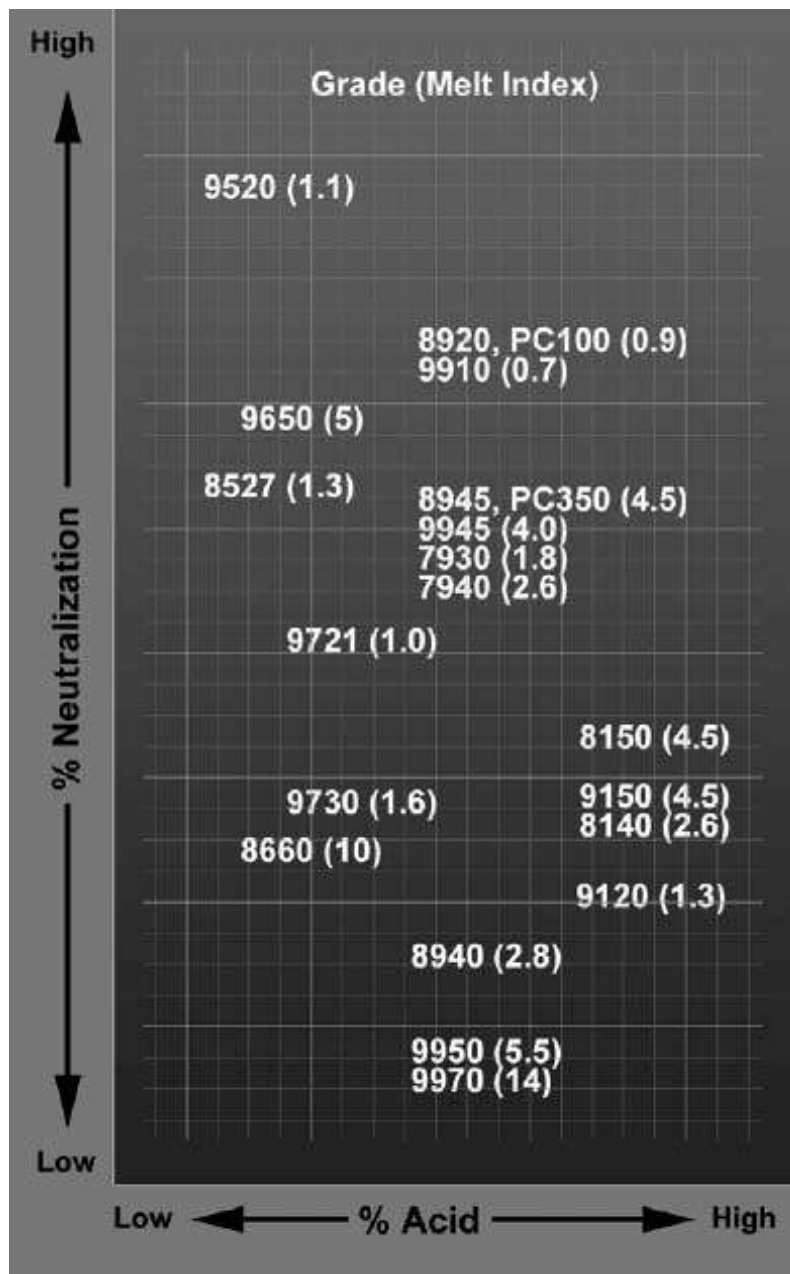


Fig. 1.5: Various grades of Surlyn® are influenced by MAA content and MAA degree neutralization [5].

## 2. POLYMER COMPOSITES

The term *composite* means material composed from two or more diverse components is used since the beginning of the last century. Today, nobody knows anymore, who came as the first with an idea to combine various materials and polymers with the aim to improve their properties. Probably, an inventor was not only one, but this idea got more people at different places in the same time. The main motivation to fill polymers was to reduce the production costs. However, a positive effect of polymer filling on many mechanical, thermal and processing properties was gradually pointed out. New superior materials exhibit significantly better properties than in separate form [33–35].

Since early 90's, enormous interest about nanocomposites is registered, when the first nanocomposite, namely Nylon/montmorillonite, was produced in Toyota group laboratories. Nano-, and in this case nanocomposite, means that one or more component dimensions are in a maximal size of nanometres ( $10^{-9}$ ) [36].

### 2.1. Processing development: From composite to nanocomposite

The structure and the properties of the polymer–filler compounds depend on several factors (compatibility, filler size, shape, aspect ratio, *etc.*). Unfortunately, the interaction between polymer and filler are usually weak, because of structure defects in fillers. As the reinforcing elements became smaller and smaller, the structural perfection strongly increases. Maximal properties are supposed to be reached at molecular or atomic size of fillers, *e.g.* carbon nanotubes show highest values of elastic modulus  $E \approx 1.7$  TPa [37, 38] or clay sheets 1 nm in thickness display a perfect crystalline structure. Nevertheless, the smaller particles, the higher internal surface, which tends to particle agglomeration rather than their dispersion in polymer matrix. Contact surface between matrix and filler enormously rises as well which makes problems to create a strong interaction at the interface. To solve this task, several methods improving mutual interaction were found [39, 40].

To the most frequently used particular fillers belong minerals and in the case of particle minimization especially layered minerals as clays [35, 40–45]. Several procedures, how to disperse individual silicate layers into polymer matrix, exist. However, the first step is always the same - swelling of layers termed as intercalation (Fig. 2.1). Ions located between the crystalline layers are exchanged by organic ions. In dependence on interaction with monomer,

oligomer or polymer, these ions have various functional groups in order to reach a required effect on platelets separation and consequently good dispersion in matrix. This means ions have to reduce solid-solid interaction between layers and improve interaction between mineral and matrix [39, 40, 46].

To describe intercalation more simply, it can be imagined as inserting beans between each pair of play card in a stack. Definitely, it would not be easy. Cards must be pre-spaced and moreover some driving force must be employed [39].

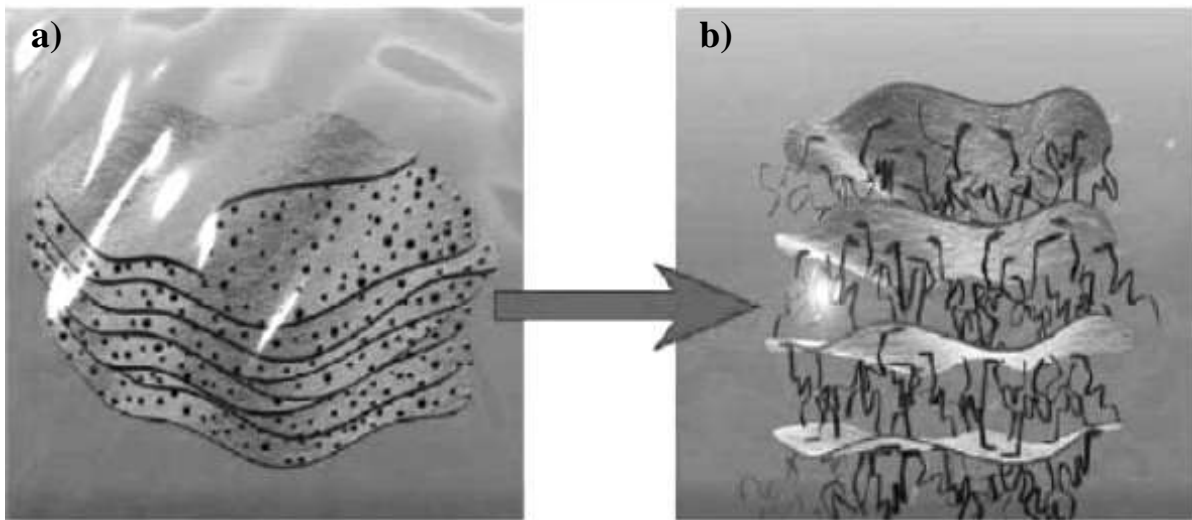


*Fig. 2.1: The platelets of layered silicate, a) exchangeable ions between layers, and b) organic cations intercalated between layers [39].*

To successful clay intercalation cation-exchange capacity (CEC) should be in interval 0.5–2.0 meq/g. CEC lower than 0.5 is deficient for ion exchange and interlayer bonds with CEC higher than 2.0 are too strong for easy intercalation as well. For example, CEC for kaolin is  $< 0.1$  meq/g, and for mica, illites, attapulgite and sepiolite about 0.2 meq/g, what contrasts to smectites and vermiculites (VMT) whose theoretical CEC value is 1.39 but experimentally only 0.8–1.2 meq/g. Therefore, smectites (montmorillonite (MMT), saponite and hectorite) are preferred clays for preparation of polymer–filler (nano-) composites. Especially MMT attracts high attention because of large aspect ratio and easy availability from natural deposits [40, 47–51].



## 2.2. Mineral description

Almost all minerals (mica, kaolin, talc or MMT) used as fillers belong to the silicate class and phyllosilicate subclass. Layered structure is a typical feature for this group; nevertheless, it varies according to specific mineral. Mineral layers consist mainly from tetrahedron and octahedron (Fig. 2.2). As a central atom (cation) of tetrahedron crystal is mainly  $\text{Si}^{4+}$ , but  $\text{Al}^{3+}$ , or  $\text{Fe}^{3+}$  are also possible. Octahedron central cations can be  $\text{Al}^{3+}$ ,  $\text{Fe}^{3+}$ ,  $\text{Fe}^{2+}$ ,  $\text{Mg}^{2+}$  and *etc.* Anions are mostly  $\text{O}^{2-}$  or  $\text{OH}^-$ . These crystals create octahedral or tetrahedral sheets. In dependence on number of sheet minerals are divided on 1:1 or 2:1. Kaolin belongs to the 1:1 group (one tetrahedral  $\text{SiO}_4$  sheet and one octahedral  $\text{AlO}_6$  layer) while the smectites rank to the 2:1 group (one octahedral  $\text{Al}_2(\text{OH})_6$  sheet is placed between two tetrahedral  $\text{SiO}_4$  sheets) (Fig. 2.3) [33, 40, 43, 52].

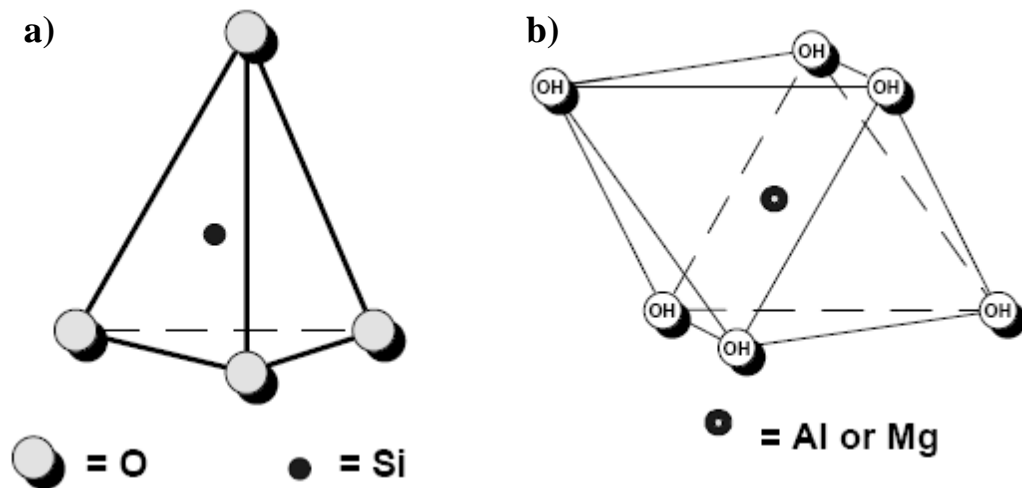


Fig. 2.2: Structure of a) tetrahedron, and b) octahedron [43].

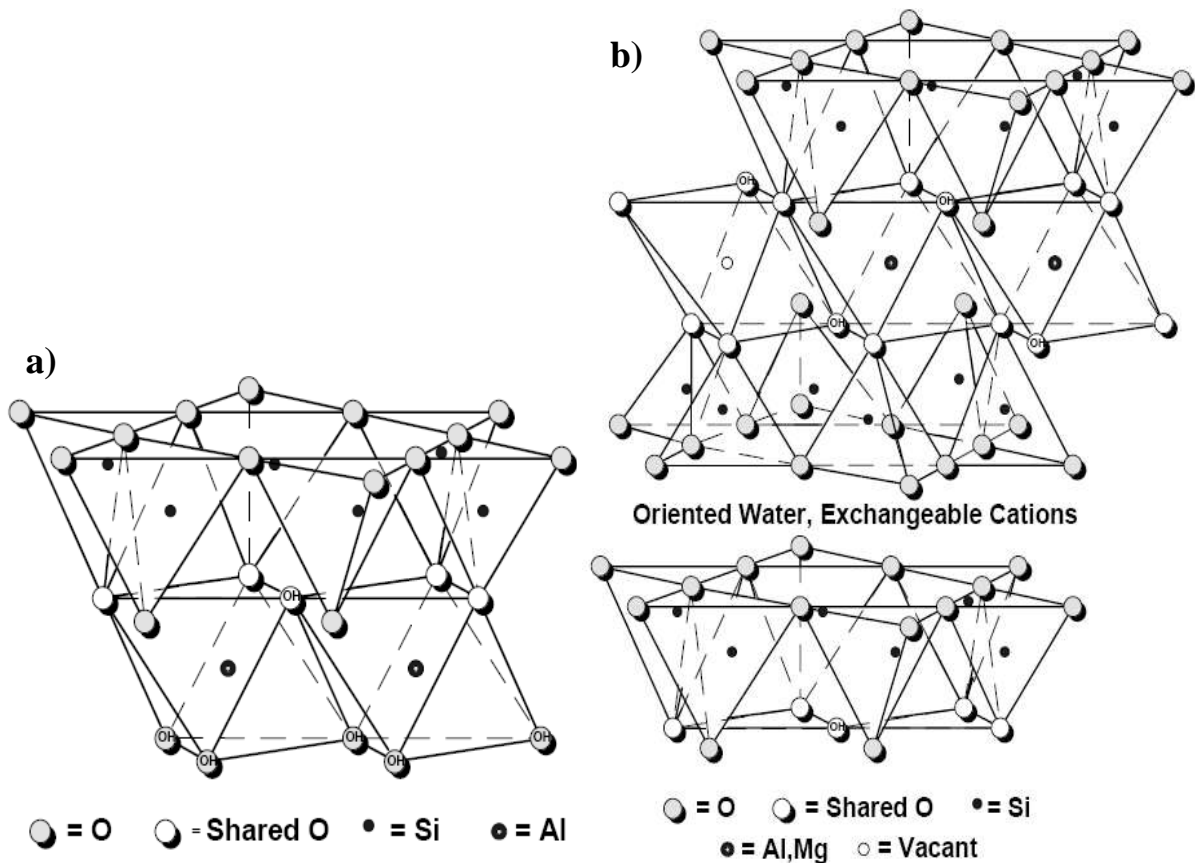


Fig. 2.3: Schematically visualized layers of a) kaolin and b) MMT [43].

The thickness of the layer is approximately 1 nm. The distance between layers ( $d_{001}$ ) is 0.72 nm for kaolin and 0.96 nm for MMT, respectively. When appropriate amount of water is added to MMT,  $d_{001}$  increases up to 1.25 nm [40, 53].

When the clay is used as filler to polymer, especially in the case of nanocomposites, it is necessary to increase clay organophilicity and the interlayer spacing to 3 or 4 nm [54–58]. Usually, it is three steps process. The first step consists in clay dispersion in water or aqueous solution to reduce the solid-solid interaction between layers. Then, the organic cations are added and the  $\text{Na}^+$  or other ions are exchanged by organic ones. Finally, organoclay can be treated by reactive compound to improve its compatibility with polymer.

Gradually, several ways of clay intercalation were investigated:

- Intercalation by solvents or solutions (water, alcohols, glycols or crown ethers),
- Intercalation by organic cation, such as ammonium, phosphonium or sulfonium,
- Use of organic liquids and their solutions (monomers, macromers, oligomers, polymers, copolymers and their solutions),
- Melt intercalation – direct compounding of polymer with clay. However, the goal is to prepare exfoliated structure, not intercalated,
- Combination of previous methods.

After intercalation, clay is prepared for compounding with polymer. X-ray diffraction patterns of sodium MMT (Fig. 2.4a) and MMT intercalated by dimethyl dehydrogenated tallow ammonium chloride (Fig. 2.4b) are presented. Before the modification by organic ion, the lamellar distance was 1.2 nm. After the organophilization, the interlayer distance increased twice. Then, when the organic clay is compounded with polymer, higher degrees (from intercalated (Fig. 2.5a) to fully exfoliated (Fig. 2.5b) of filler dispersion can be obtained according to processing conditions or applied modifier [59–64].

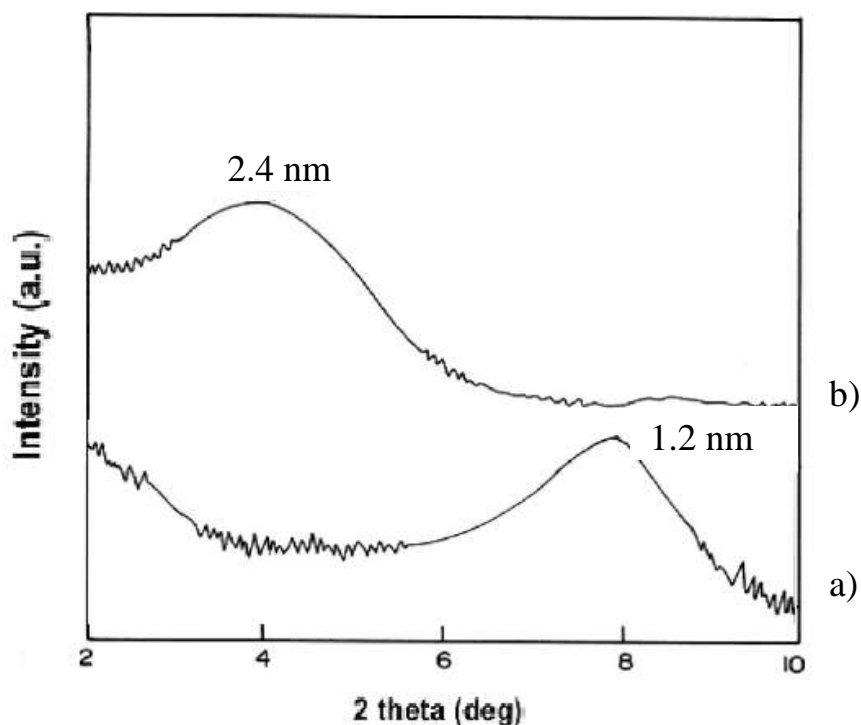


Fig. 2.4: Comparison of a) sodium MMT and b) MMT intercalated by organic cation [59].

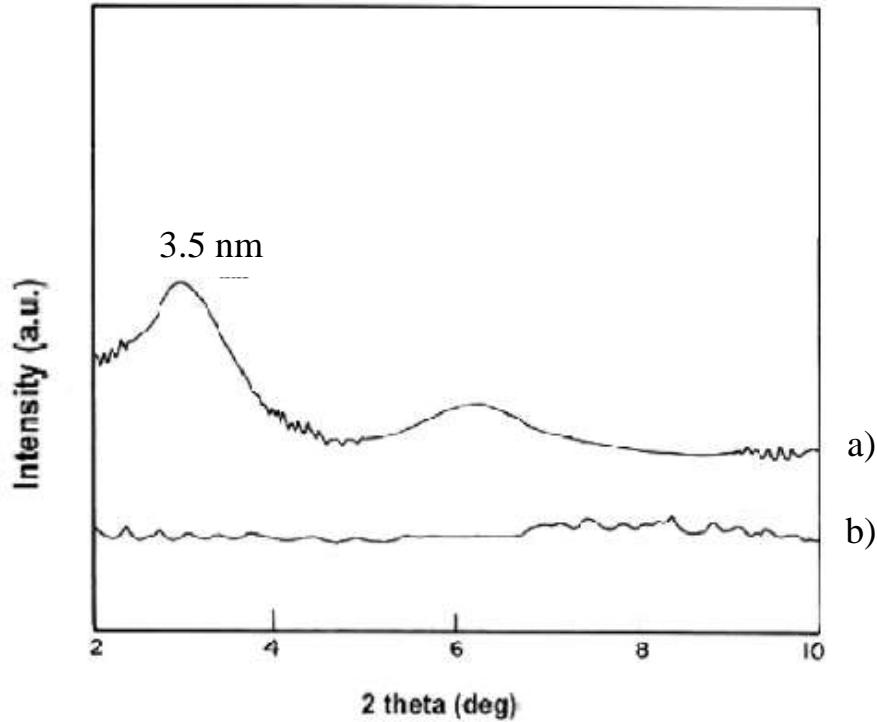


Fig. 2.5: Clay/polymer compound with a) intercalated structure, and b) exfoliated structure [59].

### 2.3. Polymer clay composite preparation

The goal of polymer–clay compounding is to prepare fully exfoliated structure. The first step is to intercalate clay, as it was mentioned above. The second step is compounding filler with polymer. Mostly, the intercalation is one part of composite preparation, *e.g.* intercalation by monomers is followed by its polymerization.

Direct melt intercalation is the most frequently used method of composite production. Besides, this method can be suitably combined with another intercalation, especially with organic cation modification, to reach easily the maximal exfoliation [40, 65, 66].

When the polymer and clay are compounded, various types of composite can be prepared (Fig. 2.6):

- Conventional composite - with aggregates in size in microns. The polymer chains are not able to intercalate between clay layers. Mostly, this type is obtained, when the clay is not treated.
- Intercalated composite - polymer chains incorporate into clay layers, without their separation. Platelets distance is 2–3 nm.
- Exfoliated nanocomposite - with locally ordered structure.
- Exfoliated nanocomposite - with disordered structure.

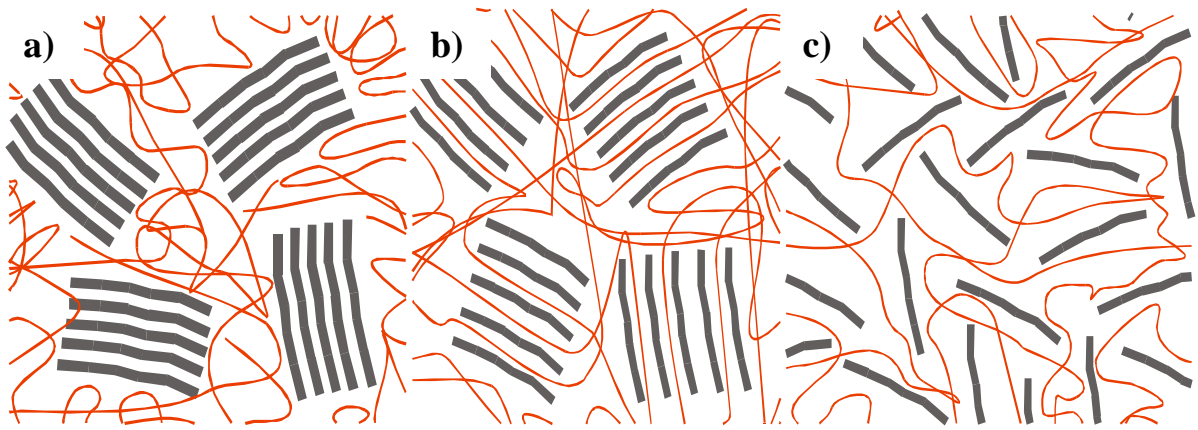


Fig. 2.6: Scheme of the a) conventional composite, b) intercalated composite, and c) exfoliated composite.

The level of exfoliation can be measured by X-ray diffraction or transmission electron microscopy (TEM). The composite types shown in Fig. 2.6 are also visualized by X-ray diffraction in Fig. 2.7.

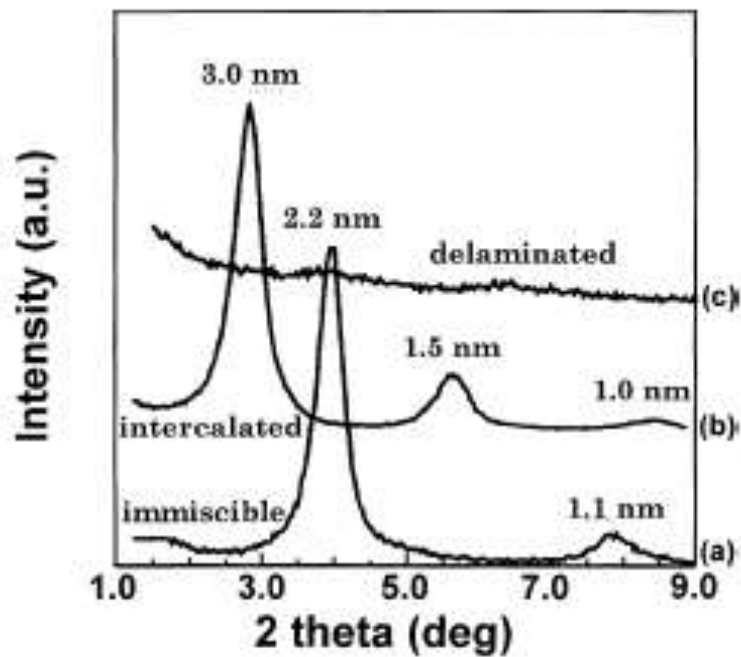


Fig. 2.7: X-ray diffraction pattern of a) conventional clay composite, b) intercalated clay nanocomposite, and c) exfoliated (delaminated) clay nanocomposite [67].

## Surlyn® – clay nanocomposites

Poly(ethylene-co-methacrylic acid) ionomer is a proper candidate for clay nanocomposite preparation mainly because of suitable polarity. Several studies, dealing with Surlyn®–clay nanocomposite behaviour, were published [5, 28, 32, 68–71]. Sodium MMT or organically modified MMT as fillers were studied predominantly.

As already mentioned in previous chapter, content and level of MAA neutralization as well as various ion types in Surlyn® can vary. All factors dramatically influence processing behaviour and final properties of Surlyn® nanocomposites [5, 28, 32].

The effect of ion type on final composite properties was studied by Shah and Paul [28]. The selected polymer matrixes differed in type of used neutralizing ion. Results from TEM showed (Fig. 2.8) that clay filled zinc and sodium ionomer gained higher level of MMT exfoliation than lithium based one. This idea was confirmed by X-ray diffraction and tensile tests, where lithium ionomer demonstrate the lowest value of relative modulus ( $E/E_m$ ) in comparison to the other types. Despite the similar morphology of MMT in sodium and zinc ionomers, zinc composite exhibits higher relative modulus and the difference increases with amount of filler.

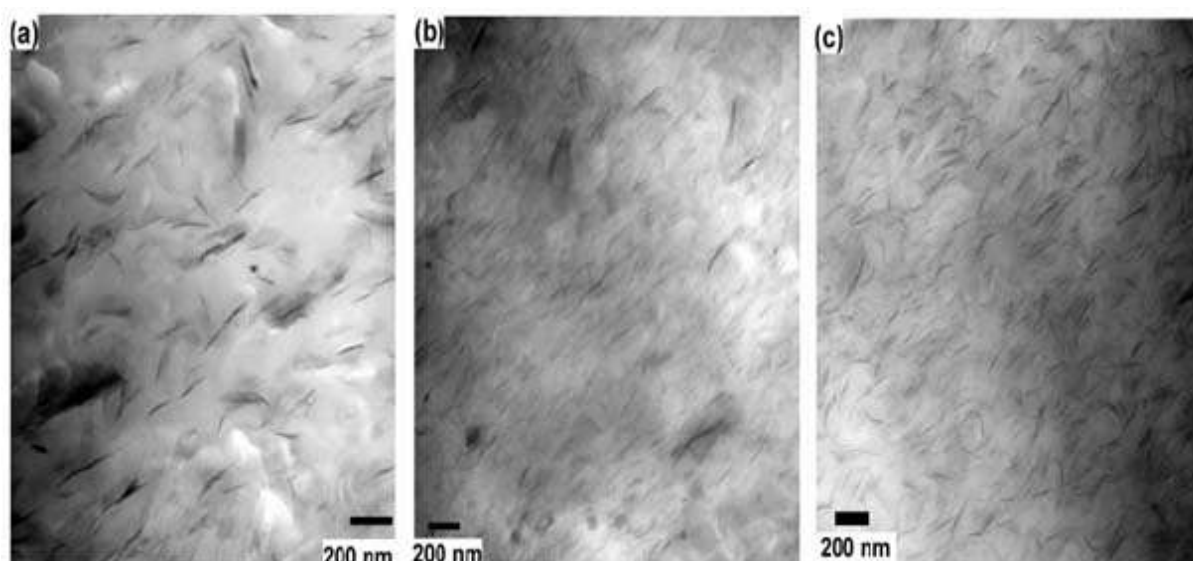


Fig. 2.8: TEM micrographs of nanocomposite prepared from a) lithium, b) sodium and c) zinc neutralized Surlyn® [28].

Also the influence of surfactant structure on morphology and mechanical properties was studied [32, 68]. The chosen surfactants varied in number of long alkyl tails and their carbon atoms on the quaternary ammonium ion. As found in previous work, the higher level of exfoliation in nylon or styrene acrylonitrile based nanocomposites was achieved using clay modified by quaternary ion with one long alkyl tails [69, 70]. On the other hand, nanocomposite based on

polyethylene showed opposite trends, two-tailed organoclays embody higher level of exfoliation and better properties [71]. Surfactants with one, two or three long carbon chains were studied. It was pointed out the numerous tails surfactant, the higher level of clay exfoliation reached. This also corresponds with obtained properties of the nanocomposite compounds, which means improved mechanical properties and reduced gas and water vapour permeability as well. At the same time, the effect of surfactant amount on the final nanocomposite properties was compared. MMT with higher organic content (CEC = 1.4 meq/g) were more exfoliated and presented higher mechanical properties than nanocomposite with lower organic fraction in clay (CEC = 0.95 meq/g) [32, 69].

In some studies, the effect of maleic anhydride (MA) grafted polyolefins and Surlyn®, as additives on filler exfoliation in polyolefinic matrixes was compared. Compatibility to clay and its exfoliation notably increase, when additives were used. Surlyn® additive reach higher exfoliation, however it was not reflected on improvement of mechanical properties of composites [8, 9, 26].

### **3. THE AIMS OF RESEARCH WORK**

The goals presented thesis as follows:

- To prepare intercalated clay – montmorillonite and vermiculite, by various intercalations or co-intercalations agents to obtain organically modified clay as filler for polymer/clay nanocomposites.
- To compound pre-intercalated clay with polymer matrix (Surlyn®); finding the best compounding conditions to reach maximal level of filler exfoliation in matrix.
- To evaluate the influence of differently modified clay, clay concentration and compounding conditions on the morphology and mechanical properties of nanocomposite.
- To compare the effect of various neutralizing ions and level of MAA neutralization of Surlyn® on the final properties of polymer nanocomposites.



## 4. EXPERIMENTAL PART

### 4.1 Materials

#### 4.1.1 Polymers

The nanocomposite preparation brings a lot of difficulties. There are several factors influencing the filler dispersion in polymer matrix, namely particle size shape, aspect ratio, compatibility to polymer, *etc.* The polymer polarity also plays an important role. To disperse *e.g.* clay particles in polyamide is easier than in polyolefins. However, their polarity can increase by copolymerization with polar monomers such as vinyl acetate, acrylic or methacrylic acid, which leads to the improvement of final properties of composite [40].

With respect to these aspects, several commercially available types of Surlyn® were chosen for this study (Tab. 4.1). Surlyn® 1605 and Surlyn® 8920 are sodium neutralized, while Surlyn® 1705, Surlyn® 9020, Surlyn® 9721 and Surlyn® 9910 are neutralized copolymers by zinc.

Besides, all these types differed in the amount of methacrylic acid and the level of its neutralization as well. Surlyn® 8920 and Surlyn® 9910 contained the same amount of methacrylic acid (15 wt %) and were neutralized to the same level (60 %). Surlyn® 1605, with the same content of MAA was neutralized only to 30 %. In another two types, Surlyn® 9721 and Surlyn® 9020, 10 wt % of MAA was included and 70 % of acid groups were neutralized. In addition, isobutyl acrylate (IA) as a third copolymer was incorporated to polymer chain of Surlyn® 9020 (in amount of 10 %) and its final composition was PE/MAA/IA 80/10/10 wt %. The last employed ionomer contained 12 wt % of MAA and only 3 % were neutralized. This type is commercially available as Surlyn® 1705 [72–76].

Table 4.1: Properties of various types of Surlyn® [5, 72–76]

	<b>Surlyn 1605</b>	<b>Surlyn 8920</b>	<b>Surlyn 1705</b>	<b>Surlyn 9020</b>	<b>Surlyn 9721</b>	<b>Surlyn 9910</b>
Ion	Na <sup>+</sup>	Na <sup>+</sup>	Zn <sup>2+</sup>	Zn <sup>2+</sup>	Zn <sup>2+</sup>	Zn <sup>2+</sup>
Content of MAA (wt %)	15	15	12	10	10	15
Neutralization degree (%)	30	60	3	70	70	60
Specific gravity (g/cm <sup>3</sup> )	0.95	0.95	0,9	0.96	0.96	0.97
Hardness (Shore D)	–	66	–	55	61	64
Flex modulus (MPa)	–	380	–	100	250	330
Melt flow index (g/10 min)	2.5	0.9	5.5	1.0	1.0	0.7
Melting point (°C)	95	88	95	85	92	86
Vicat softening point (°C)	64	58	65	57	71	62
Optical haze (%, 6.4 mm)	–	4	–	7	12	6

#### 4.1.2 Fillers

Various types of fillers differ in chemical composition, structure, size, shape, *etc.* Fillers like carbon tubes, carbon black and minerals are under intensive investigation because of their wide applicability in polymer industry. Among frequently used particular fillers belong clays (kaolin, mica, MMT, VMT, *etc.*). VMT and MMT were selected for the purpose of this work. Although, VMT is not as popular as MMT, the similar structure and ability to adopt organic ions into interlayer spacing, make from this clay a proper candidate for organophilization [40]. Both MMT and VMT were employed as fillers in this study unmodified and organically modified form as well.

The structure of MMT and VMT is presented in Fig. 4.1. Evidently, the structure of VMT (Fig 4.1a) consists from 2:1 silicate sheet. Two flat layers of silica or alumina tetrahedral layers are joined together by octahedral layer, composed from apical oxygen atoms or hydroxyl molecules and central magnesium or iron atoms. Between sheets can be find exchangeable magnesium (or sodium, barium, strontium and potassium) cations and one or two layers of oriented water [40, 43, 52, 70].

MMT structure is also consisted by 2:1 layers (Fig 4.1 b). One layer is composed by apical oxygen atom or hydroxyl molecules and aluminium central

atom (octahedral alumina layer) is located between two tetrahedral silica layers. Interlayer of MMT contains exchangeable cations ( $\text{Na}^+$ ,  $\text{Ca}^{2+}$ ) and oriented water [43, 52, 77].

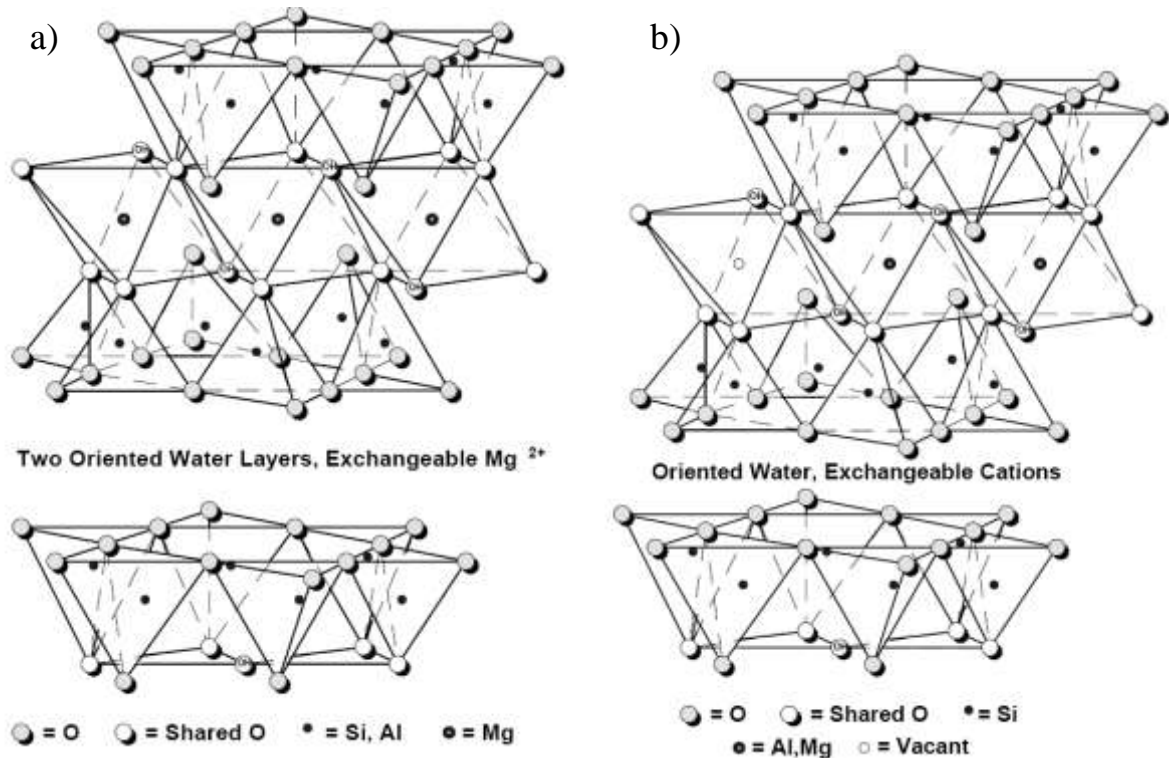


Fig. 4.1: Structure of a) VMT, and b) MMT [43].

Unmodified MMT and VMT are characterized in Table 4.2. Employed MMT is commercially available as Cloisite  $\text{Na}^+$ , purchased from the Southern Clay Products, Inc., and expanded type of VMT branched as K-0 produced by Dämmstoff-fabrik Klein.

Table 4.2: Basic characteristic of MMT and VMT [52, 77, 78]

	Montmorillonite	Vermiculite
Interlayer ion	$\text{Na}^+$	Various ( $\text{Mg}^{2+}$ , $\text{Na}^+$ , $\text{K}^+$ )
Colour	Off white	Brown
Hardness	1 – 2	1.5
Specific gravity [ $\text{g}/\text{cm}^3$ ]	2.86	2.3
Particle size [ $\mu\text{m}$ ]	< 13	25 – 40*
Weight loss on ignition [%]	7	8.1*
Interlayer distance [nm]	1.17	1.45 – 1.02*

\*measured at TBU Zlín, Faculty of Technology

According to the previous studies, the best properties of Surllyn®/clay nanocomposites were achieved using organically modified MMT with commercial name Cloisite 20A and Cloisite 15A (Southern Clay Product, Inc.) [27, 28]. Both types were compared with the properties of laboratory modified fillers. Cloisites 15A and 20A were intercalated by dimethyl di(hydrogenated tallow) ammonium chloride (Fig. 4.2), however, difference was in amount of modifying agent in their structures. Characteristics for both fillers are stated in Table 4.3 [79].

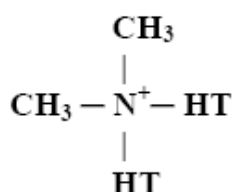


Fig. 4.2: Intercalating agent of commercially available fillers. HT is Hydrogenated Tallow (~65 % C18; ~30 % C16; ~5 % C14)[79].

Table 4.3: Main characteristic properties of Cloisite 20A and Cloisite 15A [79]

	<b>Cloisite 20A</b>	<b>Cloisite 15A</b>
Modifier concentration [meq/100 g clay]	95	125
Weight loss on ignition [%]	38	43
Moisture [%]	< 2	< 2
Specific gravity [g/cm <sup>3</sup> ]	1.77	1.66
Interlayer distance [nm]	2.42	3.15
Colour	Off white	Off white

### 4.1.3 Intercalation agent

Both unmodified clays were intercalated using modifying agents, namely cetyltrimethylammonium bromide (CTAB) and MA (Fig. 4.3). CTAB belongs to quarter ammonium salts group. The quaternary ammonium compounds are characterized by their property of greatly depressing the surface tension of water. This property puts them in the group of chemicals variously described as wetting agents, detergents, emulsifiers or dispersing agents [80]. Both chemicals were obtained from Aldrich chemical company.

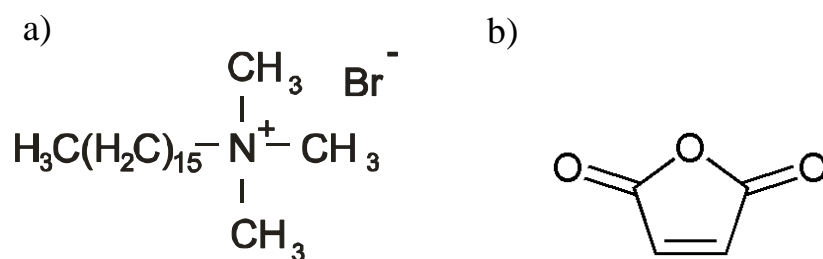


Fig. 4.3: Modifying agent a) cetyltrimethylammonium bromide and b) malein anhydride [81].

## 4.2 Characterization Methods

### 4.2.1 X-Ray diffraction (XRD)

XRD is a non-destructive method allowing to detect inner structure of materials (crystallographic, amorphous) or chemical composition. The method, which enables to inform about size of macromolecule, characteristic distances of partially ordered materials, *etc.* in nm range is small-angle X-ray scattering (SAXS). Scattering angle is typically up to  $10^\circ 2\theta$  and the wavelength of beam is in the range of 0.1–0.2 nm. This method is also suitable for characterization of powder materials, composites or nanocomposite materials based on layered class as well. Information about interlayer distances, regularities of clay and composite, intercalation or exfoliation level can be measured. Diffraction of X-ray beams on the crystalline or layered structure is defined by Bragg's law Eq. (4.1).

$$n\lambda=2d\sin\Theta \quad (4.1)$$

where  $n$  is an integer called the order of reflection,  $\lambda$  is the wavelength,  $d$  is the spacing between crystal planes,  $\Theta$  is the angle between the incident beam and the normal to the reflection lattice plane (see Fig. 4.4) [82–84].

XRD of fillers and composite compounds was measured on PANalytical X'Pert PRO (PANalytical B.V., Netherlands). Beam produced by  $\text{CuK}_\alpha$  radiation monochromatized with Ni filter with the  $\lambda = 0.154$  nm was used in reflection mode. Interlayer distance of clay was calculated according to Bragg's law.

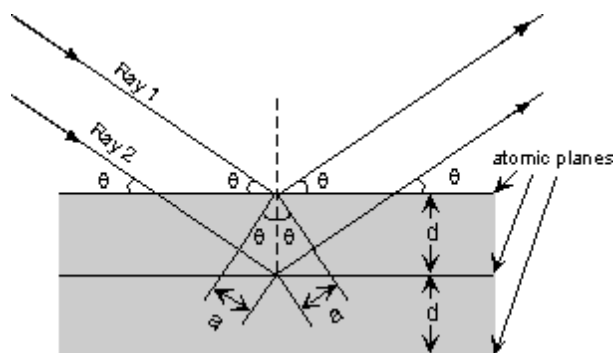


Fig. 4.4: Bragg's law

## **4.2.2 Fourier transforms infrared spectroscopy (FTIR)**

Infrared spectroscopy is another non-destructive technique which allows identification and characterization structure of both organic and inorganic substances. FTIR is based on the absorption or transmission of the infrared radiation. Irradiation of material excites molecules into a higher vibrations state because of their absorption by a specific wavelength of the light. The molecular structure of sample is consequently characterized by the signals where the absorbed wavelengths create characteristic peaks [83, 85].

The tests were performed on the powder fillers for identification of the changes in their structure during modification. Nicolet AVATAR 320 (ThermoScientific, USA) was employed in ATR mode.

## **4.2.3 Thermal gravimetric analysis (TGA)**

In principle, TGA monitored the weight changes in during predefined heating. Sample is placed to the testing chamber and heated. The inert gas flows around and sample and carries away the combustion products. Weight changes in time are recorded and plotted in dependence on temperature. From the final curve, degradation temperatures, absorbed moisture, level of organic or inorganic component, *etc.* can be deduced [83].

TGA was carried out on samples of the fillers to identify the moisture and organic content, and evaporation temperature. Test conditions were set as follows: heating rate 20 °C/min, temperature range from 25–400 °C for VMT samples or 25–600 °C for MMTs, respectively, under nitrogen atmosphere (40 ml/min).

## **4.2.4 Optical microscopy**

Optical microscopy is the most common method for studying of polymer morphology. This technique can be employed for characterization crystalline polymers structure, because of the difference between crystal lamellae and amorphous phase. However, optical microscopy is also applied for identification of filler particles, in size of microns, which are not dispersed in polymer matrix. Furthermore, information about aggregates formation in matrix during compounding, or the effect of compounding condition on the filler dispersion can be obtained in this way as well [86].

The morphology of prepared composite samples was studied to obtain first information about composite structure via Jena Zeiss NU-2 (Germany) optical microscope. Thin slices with thickness approximately 50  $\mu\text{m}$  were cut from press moulded sheets by Leica RM2255 (Leica Microsystems, Germany) rotary microtome. The pictures were taken by digital camera Sony DSC F717 (Japan).

#### **4.2.5 Scanning electron microscopy (SEM)**

SEM is a suitable method for the observation of morphology. Sample surface is imaged by scanning with a high-energy beam of electron in a raster scan pattern. The electrons interact with the sample atoms and produce signals with information about the topography, composition and other properties of the surface. Electron beam produces more types of signals like secondary electrons, back-scattered electrons (BSE), or characteristic X-rays. Signals for secondary electron detectors set in the interaction of the electron beam with atom on or nearby the surface. Obtained images have high-resolution and because of narrow electron beam also a large depth to the field. BSE signal is obtained by the electrons that are reflected from the surface. Thus, information about the various elements distribution is provided [86].

In this work, the morphology of specimens, which were cryogenically fractured in liquid nitrogen and moreover selectively etched (1% solution of  $\text{KMnO}_4$  in 85%  $\text{H}_3\text{PO}_4$  at 25 °C for 10 min) and subsequently coated with thin layer of AU/PD, was studied via SEM TESCAN VEGA/LMU (TESCAN, Czech Republic) employed with BSE detectors.

#### **4.2.6 Transmission electron microscopy (TEM)**

TEM belongs to optical techniques, whose principle is transmission of a beam of electrons through an ultra thin specimen. Thus, an image emerges, which is magnified and displayed on fluorescent screen, photographic film or detector of CCD camera. In comparison to SEM, TEM allows to operate with higher magnification. Nevertheless, TEM is also – much more expensive and time consuming, mainly in requirements to sample preparation [86].

Specimens for TEM were prepared by replication method. Samples were firstly selectively etched by 1% solution of  $\text{KMnO}_4$  in 85%  $\text{H}_3\text{PO}_4$  at 25 °C for 10 min. After that, etched layer was coated by a thin gold layer and replicated 5% water solution of polyvinyl alcohol. Replicas were reinforced by a carbon



layer. Finally, surface of prepared samples was studied by Tesla BM 500 (Czech Republic) electron microscope.

#### **4.2.7 Mechanical testing**

Generally, mechanical properties of polymers are functions of temperature, testing rate, magnitude of excitation, *etc.* These factors strongly influence the form of mechanical testing. From this reason, detailed information about testing condition purveys worldwide standards and should be strictly followed to obtain comparable results from various departments [87].

##### ***Tensile testing***

Mechanical properties of press moulded samples were measured by the tensile testing which is the most frequently used method. Tensile tests were performed according to international standard CSN EN ISO 527-1 and were carried out by help of two machines: Instron 8871 (Instron, USA) for *E*-modulus and Tensometer T2000 (Alpha Technology, USA) for stress-strain behaviour. At least six specimens (type 4A) from each compound were tested. *E*-modulus was obtained by elongation rate 1 mm/min and stress-strain curve by the rate of 100 mm/min.

##### ***Gas permeability***

Gas permeability of solid materials allows passing gas through its body in the presence of pressure differential. In dependence on the material structure, three types of gas permeability are known: diffusion flow, molecular effusion and laminar flow. Diffusion flow is a typical for the polymeric materials because of pores absence in their structure. Initially, gas is dissolved on the surface, and then diffuses through the mass. Finally, gas leaves the body on the other side [88].

Permeability of prepared samples was measured (CSN 64 0115) by the help of apparatus sketched in Fig. 4.5. This special device consists from two chambers separated by tested sample. The high pressure chamber was pressurized by measuring gas to 2 bars, while low pressure chamber was vacuumed. Temperature during the test was kept at 35 °C for 1 hour. Nitrogen, carbon dioxide and technical gas were employed as measuring gases.

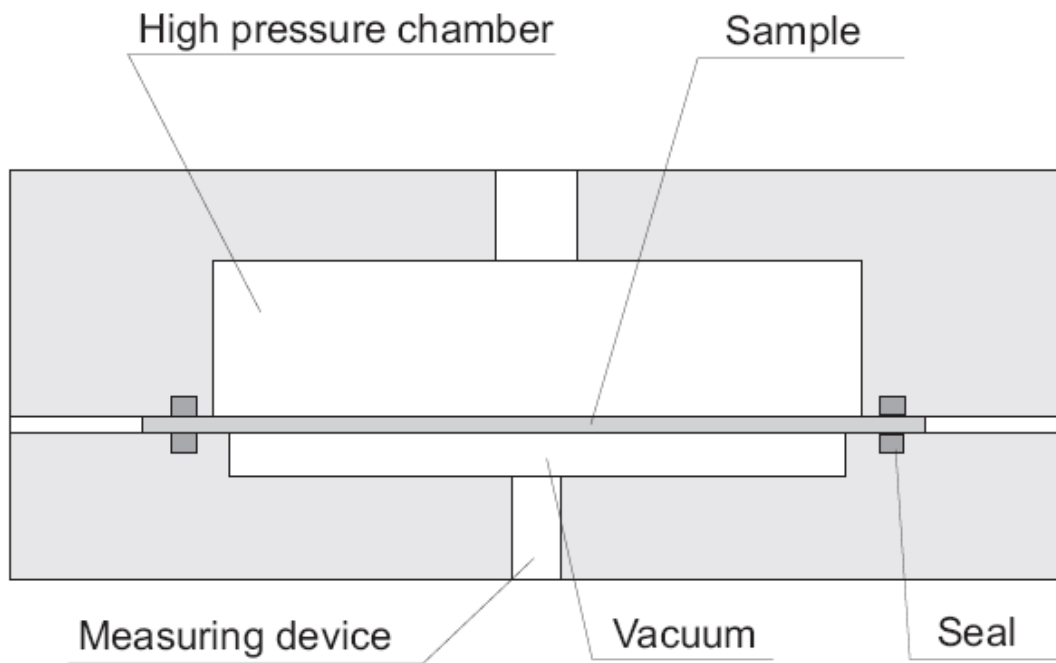


*Fig. 4.5: Measuring cell for gas permeability*

## 5 RESULTS AND DISCUSSION

### 5.1 Filler modification

To the main aims of presented doctoral study belongs modification of clays, namely MMT and VMT. MMT is relatively deeply studied and therefore was selected as comparative filler. By reason of similar structure to MMT, VMT was chosen for the preparation of organically modified form. The interlayer of vermiculite contains various ions (*e.g.* magnesium, sodium, strontium or potassium). The structure of expanded and hydrated vermiculite K-0 is presented in Fig. 5.1. The interlayer distance depends on the ion type, which is contained in the clay. The layers of expanded VMT are separated in next distances: 1.45 nm (corresponding to position of peak at  $6.1^\circ 2\theta$  and magnesium ions), 1.16 nm ( $7.6^\circ 2\theta$ ) – 1.29 nm ( $6.8^\circ 2\theta$ , barium, sodium and strontium ions) and 1.02 nm ( $8.6^\circ 2\theta$ , potassium and ammonium ions) [89]. The intensity is quite low. However, it changed after hydration of the sample. This shift results from the presence of water molecules, which penetrate into silicate layers.

The last curve represents the sodium type of MMT. Wide peak around  $7.4^\circ 2\theta$  corresponds to the d-spacing 1.18 nm.

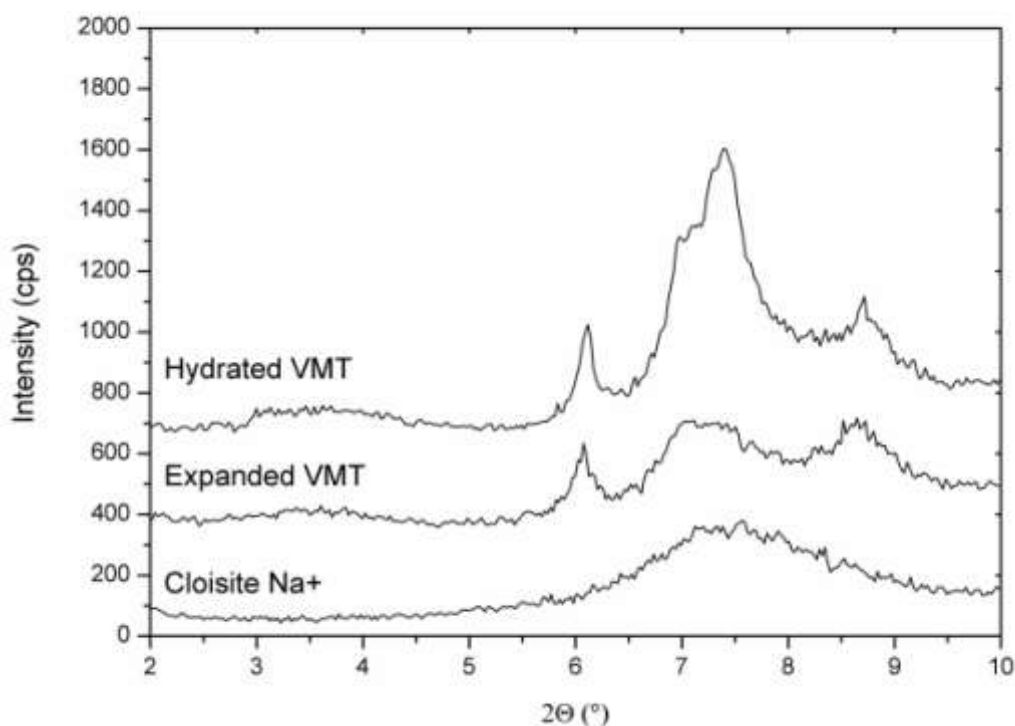


Fig. 5.1: Comparison of VMT and MMT structures.

VMT structure composed from various cations is not suitable for the organophilization and has to be replaced by one type of ion. The most suitable way, how to exchange contained ions to fully sodium ones, is by saturation. Another opportunity of clay modification is hydration of hydroxyl ions on and in the phyllosilicate structure using aliphatic, simple aromatic organic or mineral acids (HCl or HNO<sub>3</sub>) [90–93].

When HCl is used, concentration or time of acid action on clay has to be controlled; otherwise it causes full destruction of the unit structure. Preliminary treatment of sodium ions or HCl on VMT improves intercalation of clay by organic ions [93].

### **5.1.1 Preparation of sodium vermiculite**

The saturation of VMT by sodium ion was described in several papers [90–92, 94, 95]. In principle, VMT is stirred in NaCl solution. Individual research teams employed various concentrations of solution, or period of stirring. However, it is not completely obvious, which procedure is the most effective one. Definitely, a critical role also plays type and deposit of clay.

In this work, the saturation of VMT was also done. Several methods differed in NaCl solution concentration; stirring time and temperature or drying temperature influence were observed.

Sodium VMT was prepared as follows: expanded VMT in particles in size of mm was milled by ball mill firstly. Then, the particles were sieved on micro mesh sieves. Particle fraction from 25 to 40 μm of expanded VMT in amount of 10 g was added to 100 ml of NaCl solution in various concentrations (1M, 2M, 3M and 4M). Suspension was stirred at ambient and enhanced (40 °C, 60 °C and 80 °C) temperature for 5, 24 and 48 hours. After that, suspension was centrifuged (3000 rpm, 2.5 min) to separate solid fraction, which was dispersed in distilled water and centrifuged again. Centrifugation was repeated several times, till the absence of Cl<sup>-</sup> ions was confirmed (AgNO<sub>3</sub> test). Modified VMT was subsequently dried at the temperature of either 100 °C or 200 °C. Some samples passed through this process repeatedly. The conditions of the sample preparation are given in Tables 5.1 – 5.3.

Table 5.1: Preparation condition for 2M NaCl water solution

<b>Sample</b>	<b>Solution concentration [mol/l]</b>	<b>Stirring temperature [°C]</b>	<b>Stirring time [hours]</b>	<b>Drying temperature [°C]</b>
2MNaVMT 20/5/100	2	20	5	100
2MNaVMT 40/5/100	2	40	5	100
2MNaVMT 60/5/100	2	60	5	100
2MNaVMT 80/5/100	2	80	5	100
2MNaVMT 20/24/100	2	20	24	100
2MNaVMT 20/24/200	2	20	24	200

Table 5.2: Preparation condition for 3M NaCl water solution

<b>Sample</b>	<b>Solution concentration [mol/l]</b>	<b>Stirring temperature [°C]</b>	<b>Stirring time [hours]</b>	<b>Drying temperature [°C]</b>
3MNaVMT 20/24/200	3	20	24	200
3MNaVMT 20/48/200	3	20	48	200
3MNaVMT 20/24×3/200	3	20	24×3*	200
3MNaVMT 70/24×1/200	3	70	24	200
3MNaVMT 70/24×2/200	3	70	24×2*	200
3MNaVMT 70/24×3/200	3	70	24×3*	200
3MNaVMT 70/24×4/200	3	70	24×4*	200

\* number of repeated saturation

The saturation of VMT interlayers seem to be rather slow in the case of 1 M NaCl solution. On the other hand, use of 4 M solution is reflected only in a slight increase of sodium ions in the VMT structure in comparison to 3 M solution. Therefore, only selected VMTs modified by 1 M and 4 M solutions are presented in the following table (Table 5.3).

Table 5.3: Preparation condition for 1M and 4M NaCl water solution

Sample	Solution concentration [mol/l]	Stirring temperature [°C]	Stirring time [hours]	Drying temperature [°C]
1MNaVMT 20/24/200	1	20	24	200
4MNaVMT 20/24/100	4	20	24	100
4MNaVMT 20/24/200	4	20	24	200

Firstly, the influence of solution temperature during stirring was studied (Table 5.1). Evidently, the temperature affects the speed of ion replacement (Fig. 5.2). At low temperature, peak for  $Mg^{2+}$  ions is still presented; however, it continuously disappears as the temperature increases. In the same time, the main peak (6.8 – 7.6 °2 $\Theta$ ) splits up to two and moves to higher °2 $\Theta$  and its intensity rise. The peak at 7.2 °2 $\Theta$  (with d-spacing = 1.23 nm) corresponds to sodium ions and the other at 7.8 °2 $\Theta$  to strontium or barium. The last peak at 8.7 °2 $\Theta$  does not move, only its intensity slightly increases.

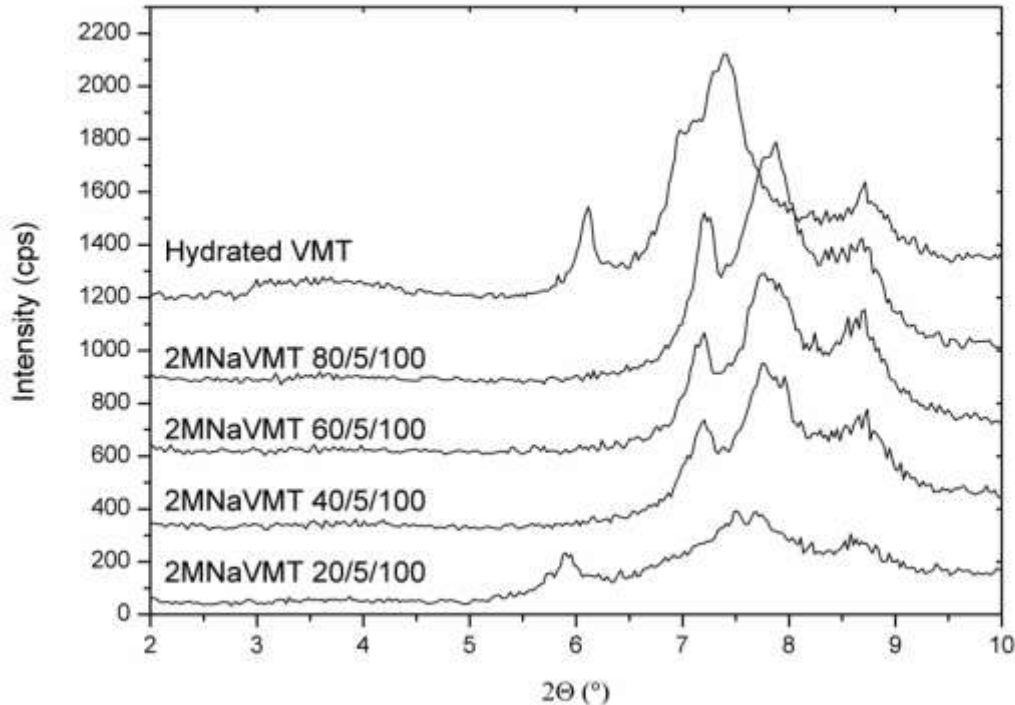


Fig. 5.2: The effect of the solution temperature on the VMT structure. Sample codes denoted in Table 5.1.

The influence of drying temperature on sodium VMT structure was also evaluated, because, as generally known, heating of VMT causes its expansion in consequence of water evaporation.

In Fig. 5.3 is compared VMT dispersed in either 2M or 4M solution for 24 hours at 20 °C. Both samples were subsequently dried at two temperatures (100 °C and 200 °C). Apparently, the drying temperature significantly influenced the final structure of saturated VMT powders. The peaks at 6 °2 $\Theta$  and 7.5 °2 $\Theta$  reached higher intensity, when the samples were dried at lower temperature. Possible explanation can be that the interlayer water did not evaporate completely.

The increasing evaporation in impact of higher temperature reduces peak intensity of Mg<sup>2+</sup> ions (4MNaVMT 20/24/200), because Mg<sup>2+</sup> ions are supposedly either exchanged or removed from VMT structure. In consequence, intensity of the peak around 8.7 °2 $\Theta$  increases.

Structure changes during saturation also depend on the solution molarity as shown in Fig. 5.4. The intensity of peak at 7.7 °2 $\Theta$  rises with higher molarity of solution. However, the peak at 6.0 °2 $\Theta$  is reduced and shifted to the higher angles. This shift indicates increasing amount of sodium ions in VMT structure.

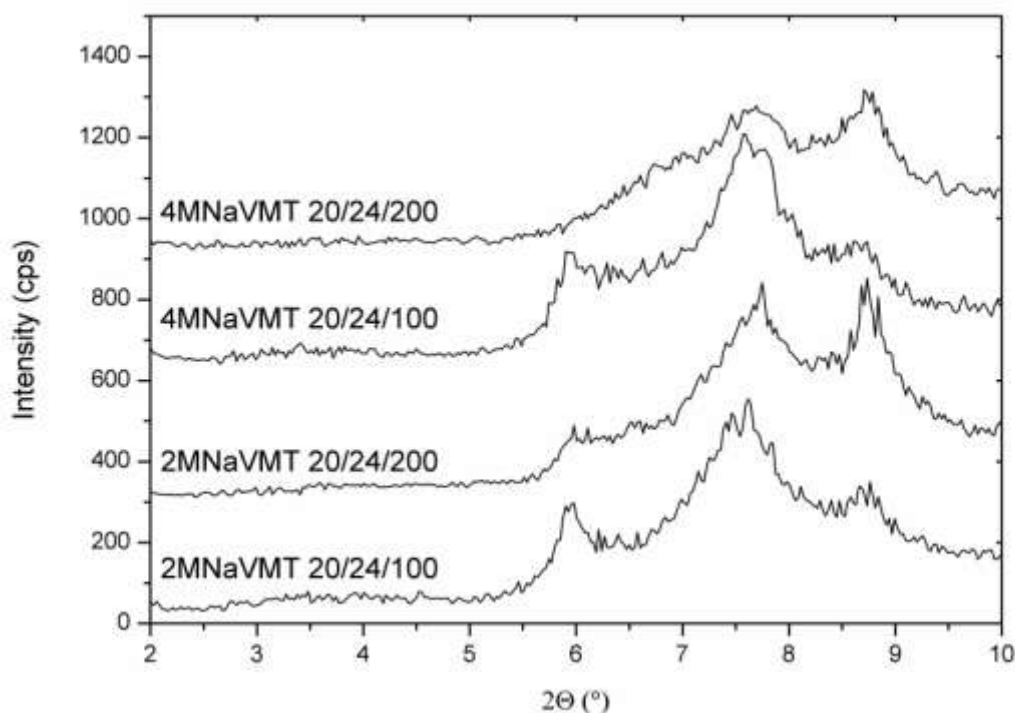


Fig. 5.3: The effect of the drying temperature on vermiculite structure. Sample codes denoted in Table 5.1 and 5.3.

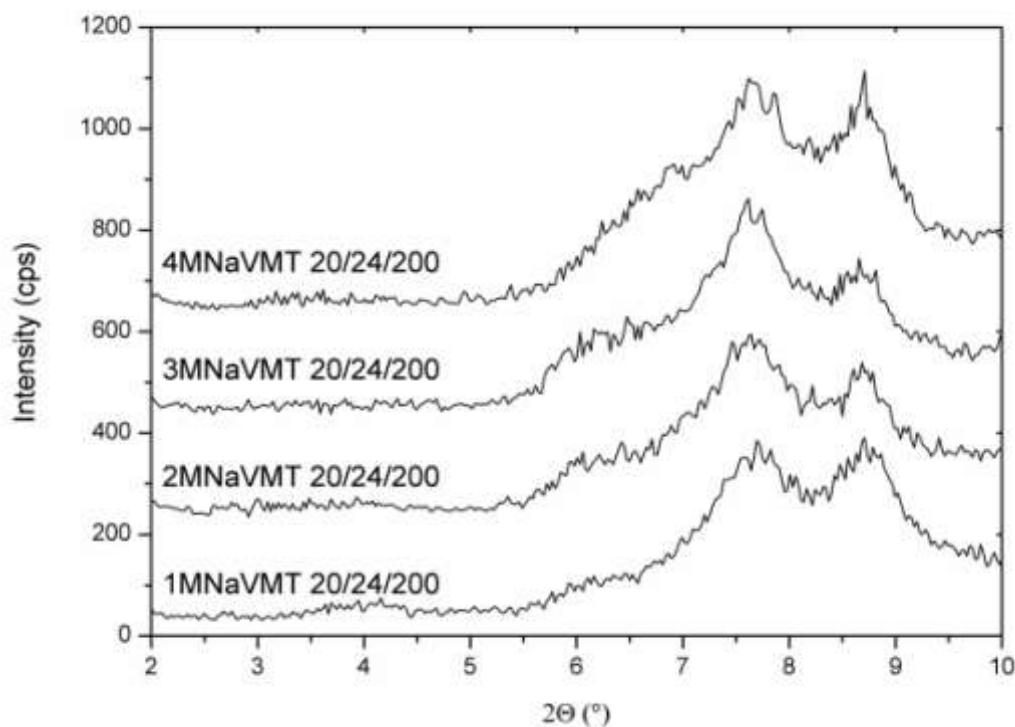


Fig. 5.4: The effect of the solution molarity on the structure changes of vermiculite. Sample codes denoted in Table 5.1–5.3.

Time dependence on the amount of sodium ions exchanged and penetrated to the VMT structure is shown in Fig. 5.5. VMT was dispersed for 24, 48 and 72 hours in NaCl water solution, where NaCl was exchanged by fresh one every 24 hours in case of last sample. Extension of saturation time leads to disappearance of the peak typical for  $Mg^{2+}$  ions. When the saturation is hold for three days, noticeable peak appears at  $7.2^{\circ}2\theta$  (d-spacing = 1.23 nm), which confirms the presence of sodium ions in clay structure. However, the substitution of original ions in VMT structure for sodium ones still not finished (peaks at  $7.8^{\circ}2\theta$  and  $8.7^{\circ}2\theta$ ).

Based on these results, saturation of VMT was further carried out at higher molar solutions, several times repeated and stirred under enhanced temperature (Fig. 5.6). After one day saturation, sample present significant peak at  $8.7^{\circ}2\theta$  and small one at  $7.3^{\circ}2\theta$  ( $Na^{+}$  ions), another ions almost disappeared. Continuously, the intensity of  $Na^{+}$  peak increases while the next peak declines.

Thus, VMT saturated for four times with the most uniform structure was selected as the most promising candidate for successful intercalation by organic ions.



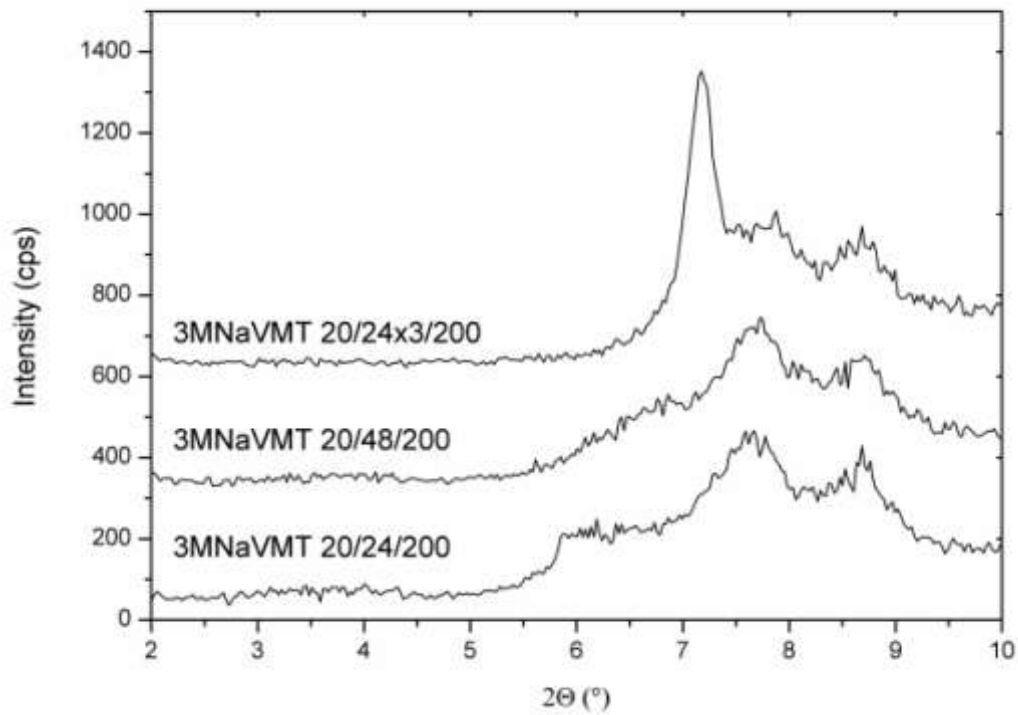


Fig. 5.5: The effect of the mixing time on the level of  $\text{Na}^+$  saturation during room temperature. Sample codes denoted in Table 5.2.

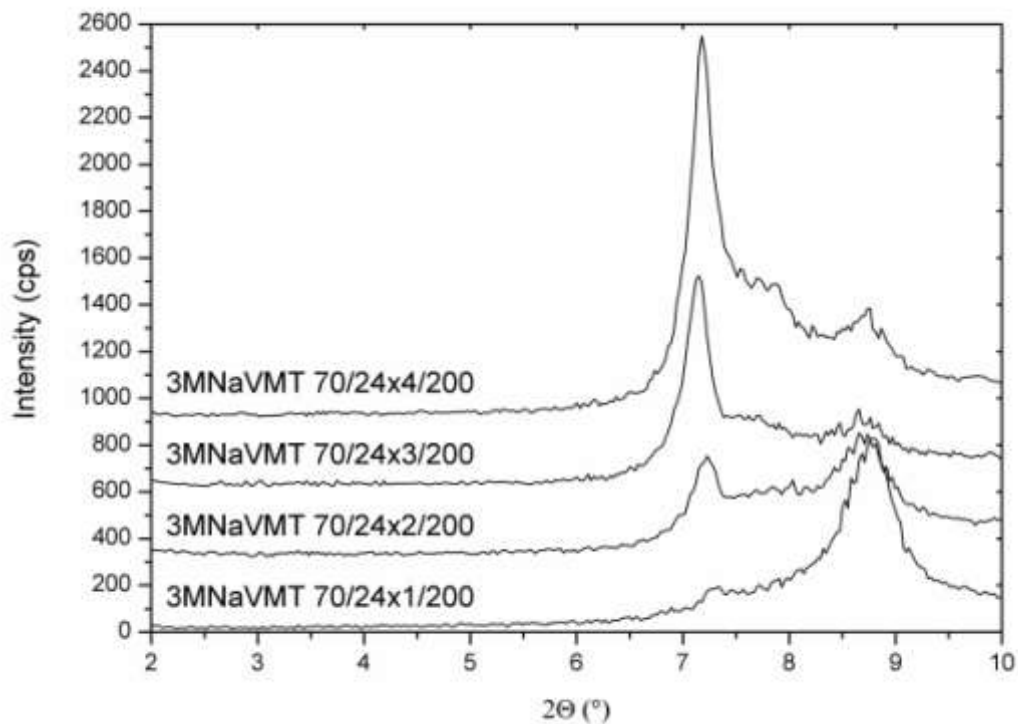


Fig. 5.6: The effect of the renewal solution on the level of  $\text{Na}^+$  saturation at higher temperature. Sample codes denoted in Table 5.2.

Prepared samples were also characterized by FTIR to find out structural changes during modification. As can be seen in Fig. 5.7 VMT presents one characteristic peak from 850 to 1100  $\text{cm}^{-1}$ . This area is typical for Si–O and O–H bonds together with another clay bonds (Al–O or Mg–O) which are contained in VMT structure. The structure is not changed during saturation, but the intensity of the peak increases with higher concentration of NaCl in solution. Similar trends were observed also for time and temperature dependence.

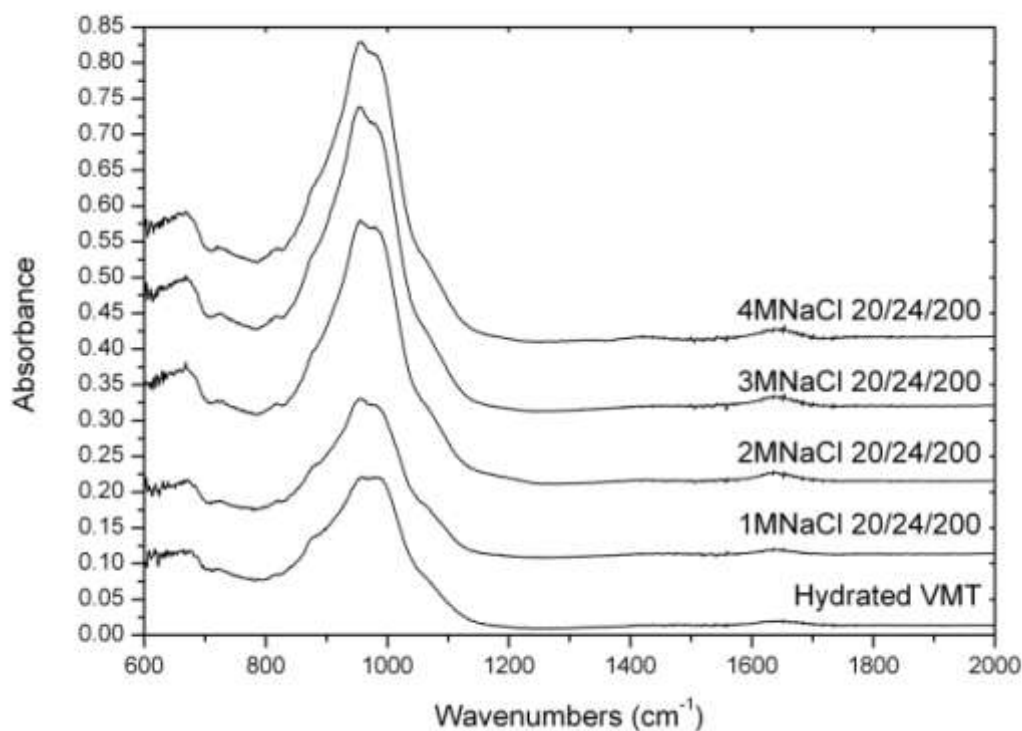


Fig. 5.7: FTIR spectra: effect of solution molarity. Sample codes denoted in Table 5.1–5.3.

### 5.1.2 VMT modification by HCl

The saturation of VMT is only one from possible ways, how to prepare organically intercalated clay. Besides, VMT can be modified by hydrogen ions from mineral or organic acids. When HCl is employed, the hydroxyl ions are hydrated and thus form molecular water and metal chlorides. Metal chlorides are created from interlayer cations and aluminium or ferrous ions, which are removed from the octahedral layers [92, 93].

In presented study, the effect of HCl molar concentration during preparation under various conditions was investigated (Table 5.4).

HCl modified VMT was prepared as follows: 10 g of expanded VMT (in particle size 25–40  $\mu\text{m}$ ) was added to 1M or 2M HCl solution (300 ml) under

intensive stirring at defined temperature and time. Then, the solution was centrifuged to obtain solid fraction. Solid fraction was subsequently dispersed in distilled water and centrifuged. This procedure was repeated several times, till pH value was neutral. Finally, modified VMT was dried at 200 °C for 24 hours.

Table 5.4: Condition of VMT preparation modified by HCl

Sample	Solution concentration [mol/l]	Stirring temperature [°C]	Stirring time [hours]	Drying temperature [°C]
1MHClVMT 20/4/200	1	20	4	200
1MHClVMT 20/6/200	1	20	6	200
1MHClVMT 20/8/200	1	20	8	200
1MHClVMT 20/24/200	1	20	24	200
2MHClVMT 20/4/200	2	20	4	200
2MHClVMT 20/6/200	2	20	6	200
2MHClVMT 20/8/200	2	20	8	200
2MHClVMT 20/24/200	2	20	24	200
1MHClVMT 40/24/200	1	40	24	200
1MHClVMT 60/24/200	1	60	24	200
1MHClVMT 80/24/200	1	80	24	200
2MHClVMT 60/24/200	2	60	24	200

At first, the influence of stirring time on the changes in VMT structure was compared for both employed HCl solution (Fig. 5.8 and 5.9). Sample stirred (dispersed) for 4 hours presented similar spectra (with three peaks) to unmodified VMT. However, the peak around  $6.1^{\circ}2\theta$  almost disappeared and by contrast the intensity of the peak at  $7.3^{\circ}2\theta$  slightly increased, when VMT was stirred for longer time (6 and 8 hours). After 24 hours of stirring,  $Mg^{2+}$  peak ( $6.1^{\circ}2\theta$ ) fully vanished, and the other ( $7.3^{\circ}2\theta$ ) increased again. Intensity of the last peak around  $8.7$  kept constant irrespectively to stirring time. Probably,

1M HCl solution can easily hydrate hydroxyl ions contained in layers with higher interlayer distance. On the contrary, hydration of smaller interlayer distance needs more time or application of stronger acid solution (Fig. 5.9).

Evolution of the structure changes is similar, but significantly accelerated, when 2M acid solution is used. And after 24 hours, the structure is considerably disturbed because of intensive hydration of octahedral layers.

In addition to time, temperature effect during mixing plays an important role. Higher temperature positively influences a presence of irregularities in VMT structure. The octahedral layers happen fully hydrated and  $\text{Al}^{3+}$  and ferrous ions are partially removed from the structure in the same time [93]. Thus, the structure of the sample mixed in 2M HCl solution at 60 °C for 24 hours was absolutely delaminated. Hydration of VMT layers was so intensive that negative charges were removed by interlayer cations and bonded water.

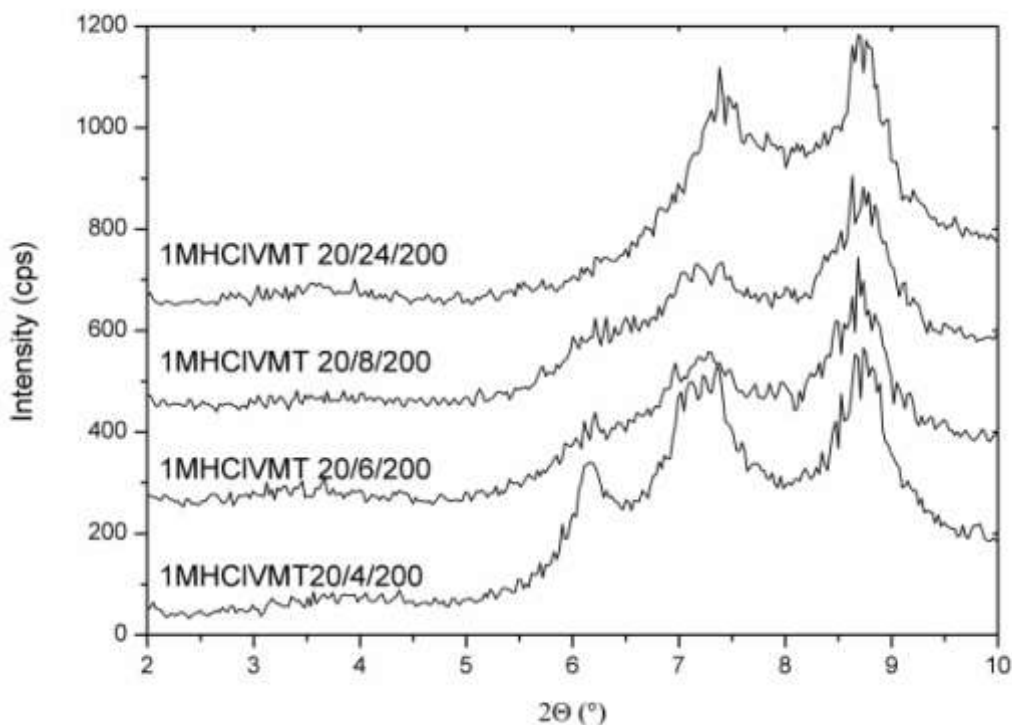


Fig. 5.8: Time dependence of structural changes using 1M HCl solution. Sample codes denoted in Table 5.4.

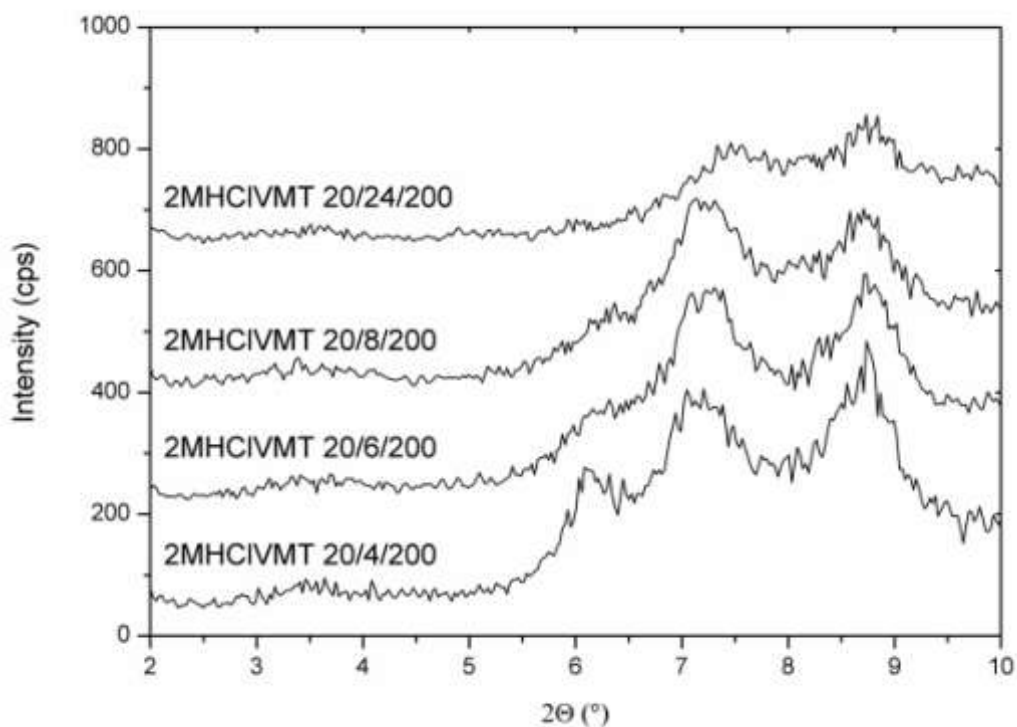


Fig. 5.9: Time dependence of structural changes using 2M HCl solution. Sample codes denoted in Table 5.4.

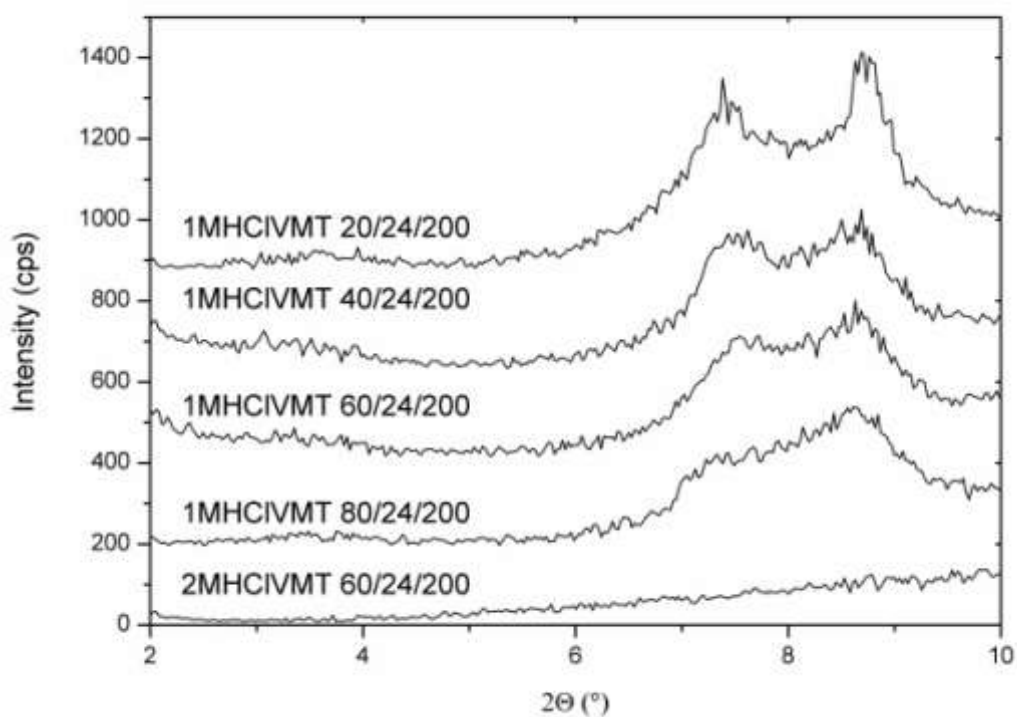


Fig. 5.10: Effect of temperature on the structural changes using 1M and 2 M HCl solution. Sample codes denoted in Table 5.4.

HCl modified VMT samples were also characterized by FTIR. Temperature and time differences between samples of 2 M solution are compared in Fig. 5.11. The most significant change appeared by comparison of samples prepared under room and enhanced temperature. When HCl hydrates hydroxyl and metal ions and continuously removed those from structure, which subsequently delaminated. Therefore, initial peak shifted from  $980\text{ cm}^{-1}$  to  $1080\text{ cm}^{-1}$ , what was also confirmed by XRD. Simultaneously, peak intensity (around  $980\text{ cm}^{-1}$ ) decreases in the time, what also indicates changes in structure.

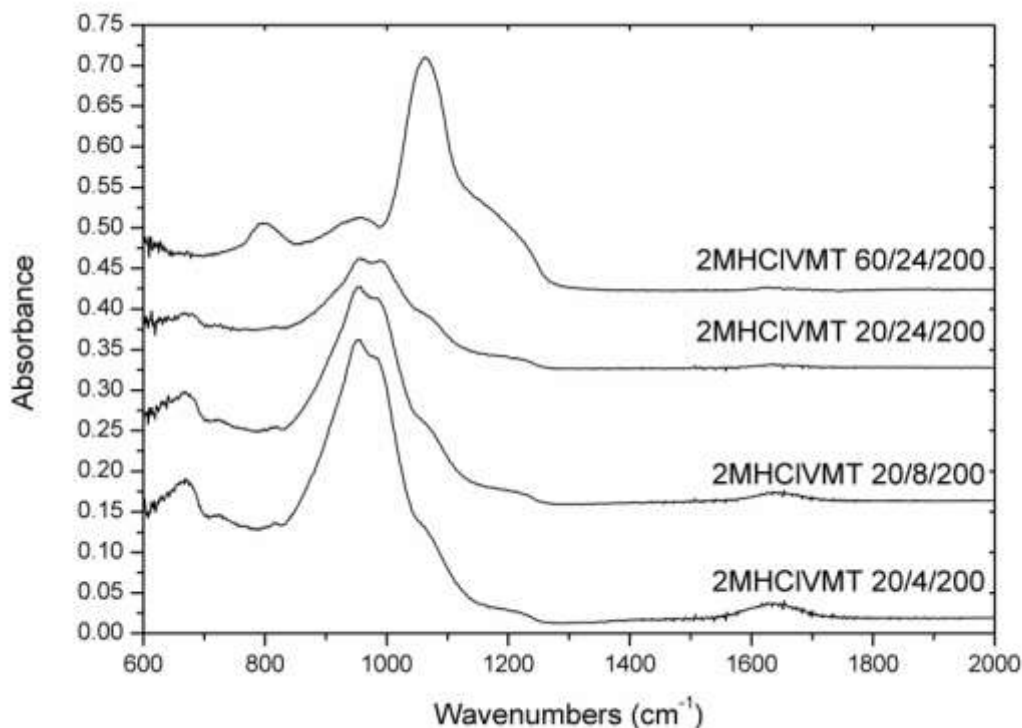


Fig. 5.11: FTIR spectra of HCl modified VMT. Sample codes denoted in Table 5.4.

### 5.1.3 Preparation of organically modified VMT

Pre-preparation of VMT for subsequent intercalation was described in previous chapter in detail. Three of these samples were used for its organophilization. Sodium type of VMT was prepared at 3M NaCl solution at  $70\text{ }^{\circ}\text{C}$  for 24 hours and then four times stirred (3MNaVMT 70/24 $\times$ 4/200). Another sample was VMT modified by 2M HCl solution at room temperature for 8 hours (2MHCIVMT 20/8/200). Sample with delaminated structure (2MHCIVMT 60/24/200) was selected as a last suitable candidate.

Sodium VMT was modified by cetyltrimethylammonium bromide, while HCl VMT by maleic anhydride and acetic acid, respectively.

## *Intercalation of sodium vermiculite by CTAB*

Sodium VMT modified by CTAB was intercalated under various conditions (Table 5.5). Sodium VMT (3MNaVMT 70/24×4/200, shortly 3MNaVMT\*) was mixed together with CTAB in water solution. Ratio of individual compounds (VMT : CTAB : water) were *e.g.* 2 g : 2 g : 30 ml. Prepared solutions were stirred at 70 °C for 5 or 24 hours and subsequently centrifuged to separate solid fraction, which was again dispersed in water and centrifuged several times, as long as the absence of bromide ions was confirmed. Final product was dried at 100 °C for 24 hours.

Table 5.5: Condition of preparation organically modified sodium VMT.

<b>Sample</b>	<b>Weight ratio VMT : CTAB</b>	<b>Stirring temperature [°C]</b>	<b>Stirring time [hours]</b>	<b>Drying temperature [°C]</b>
o-NaVMT 1:0.5/5	1 : 0.5	70	5	100
o-NaVMT 1:0.75/5	1 : 0.75	70	5	100
o-NaVMT 1:1/5	1 : 1	70	5	100
o-NaVMT 1:0.5/24	1 : 0.5	70	24	100
o-NaVMT 1:0.75/24	1 : 0.75	70	24	100
o-NaVMT 1:1/24	1 : 1	70	24	100

The influence of CTAB concentration was compared for samples mixed five (Fig. 5.12) or 24 hours (Fig. 5.13).

Interlayer distance for sodium VMT is 1.23 nm, 1.13 nm and 1.0 nm corresponding to the peaks at 7.3, 7.8 and 8.7 °2 $\theta$ , respectively. During intercalation, interlayer distance rapidly increased (2.6 °2 $\theta$ , d-spacing 3.43 nm). Two new peaks at 5.1 °2 $\theta$  (d-spacing 1.70 nm) and 7.6 °2 $\theta$  (d-spacing 1.15 nm) appeared. Supposedly, these peaks moved from their initial positions at 7.8 °2 $\theta$  and 8.7 °2 $\theta$ , respectively. Initial ions were not fully replaced. Thus, organic ions reached only at the layer edges and only slightly increased their d-spacing. Obviously, shorter time of organophilization by various content of modifier did not show any significant effect on the interlayer distance. According to XRD, all three structures seemed to be similar from d-spacing point of view (initial peak at 3.40 nm, 3.45 and 3.50 nm), however they differed in amount of organic ions. Interlayer distances of next peaks were for all molar concentrations the same – 1.71 and 1.15 nm, respectively.

When the sodium VMT was stirred for 24 hours, structure change is slightly different. Generally, all CTAB concentrations increase interlayer distance more. For low content of CTAB, peak 2.6 °2 $\theta$  (3.43 nm) moved to 2.41 °2 $\theta$  (3.70 nm), the other peaks stayed at the same position. Higher concentrations

(namely 0.75 and 1.0) of modifying agent shifted all peaks to lower angles ( $2.19^{\circ}2\Theta$ , 4.01 nm). Other peaks moved to  $4.5^{\circ}2\Theta$  (1.95 nm),  $6.8^{\circ}2\Theta$  (1.30 nm) and  $9.1^{\circ}2\Theta$  (0.91nm), respectively. However, all peaks differed in their shape. While peaks of sample with 0.75 content of modifier presented irregular right side, (probably incomplete intercalation of VMT layers), thin and regular peaks showed the sample with the highest modifier content, what was reflected in high level of intercalation VMT structures. Therefore, this sample was selected as a proper one for preparation of composite.

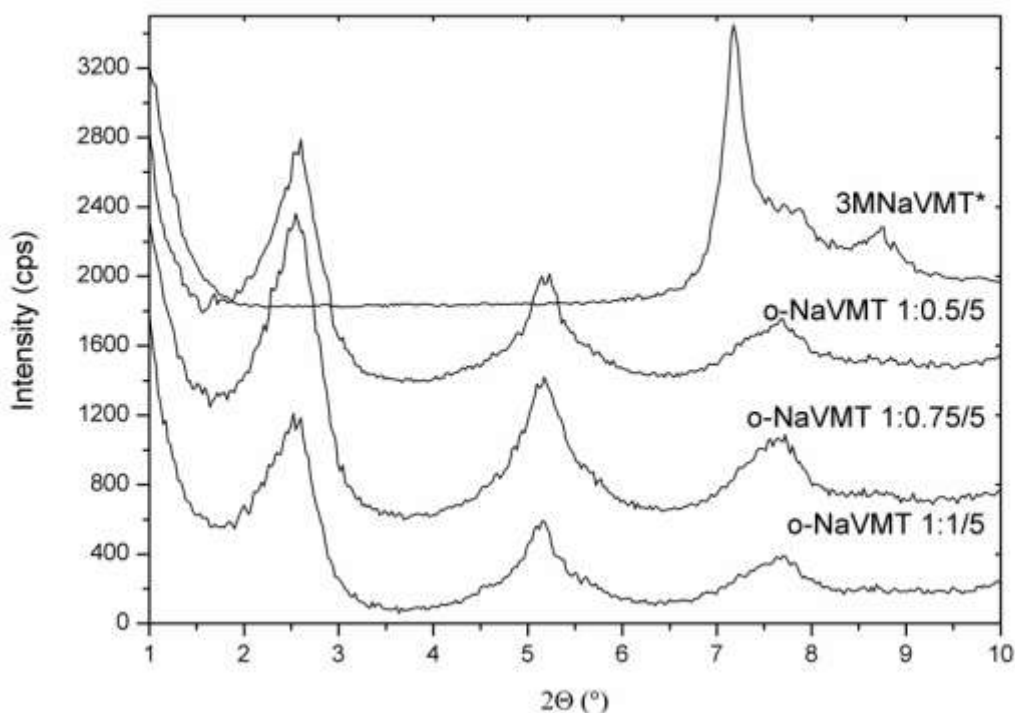


*Fig. 5.12: SAXS of intercalated sodium VMT by CTAB for 5 hours. Sample codes denoted in Table 5.5.*

The presence of CTAB in VMT structure was confirmed (Fig. 5.14) by peaks at  $1450$  and  $2800\text{--}3000\text{ cm}^{-1}$ . With higher amount of modifying agent, Si–O peak as well as durability of modification, the intensity decreases. However, CTAB inside VMT structure increased as confirmed by higher intensity of the peaks around  $2850\text{ cm}^{-1}$ , what is in agreement with XRD.



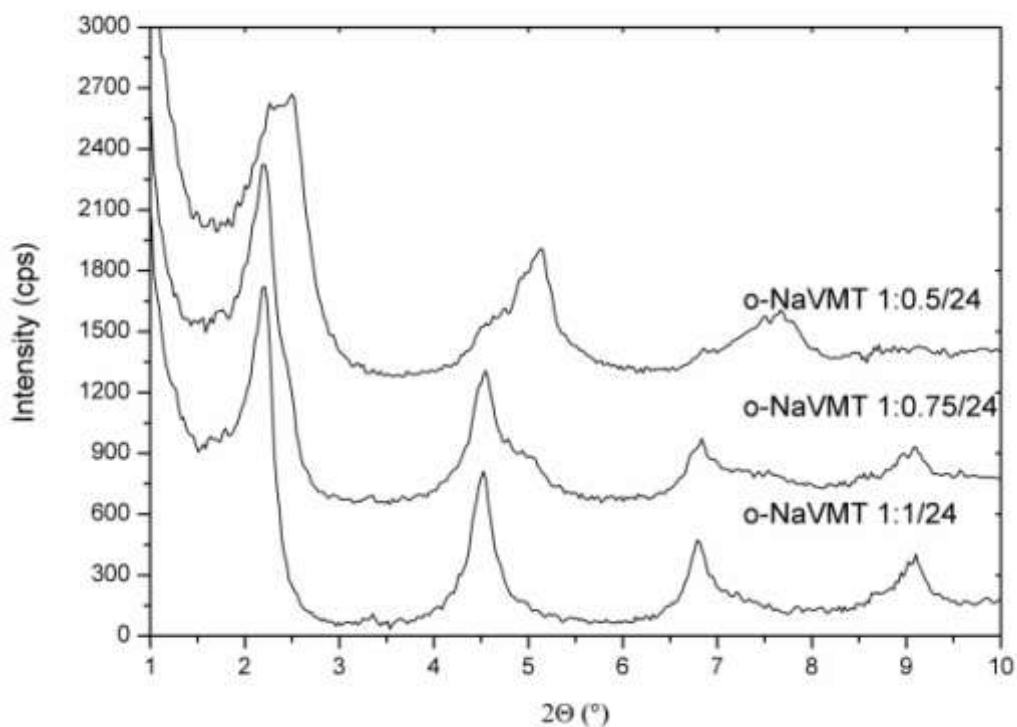


Fig. 5.13: SAXS of intercalated sodium VMT by CTAB for 24 hours. Sample codes denoted in Table 5.5.

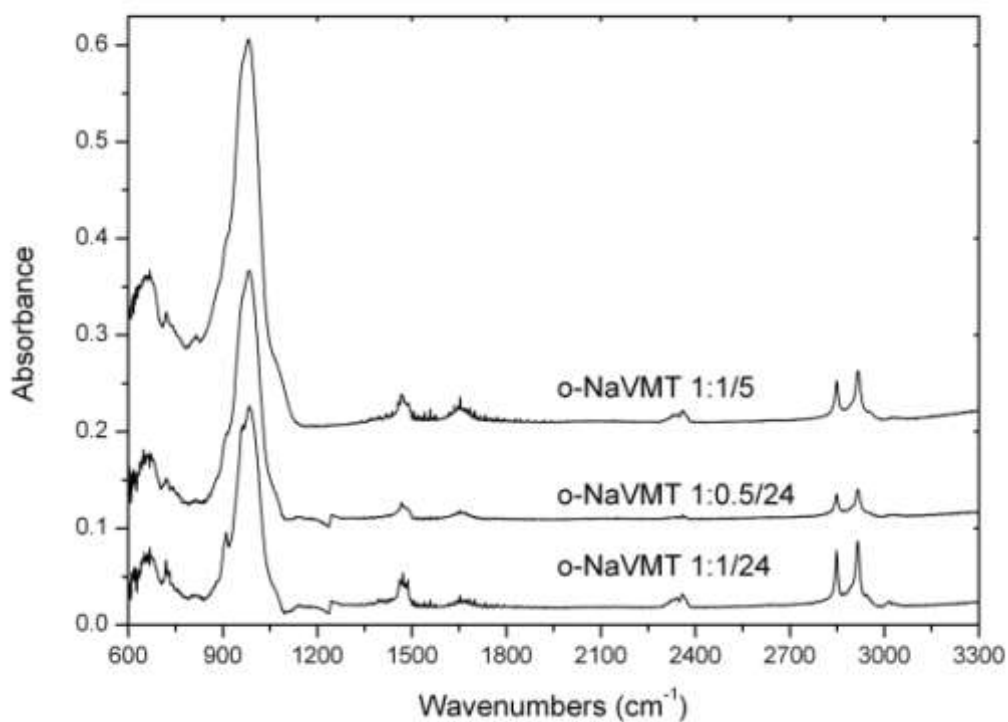


Fig. 5.14: FTIR spectra of organically modified sodium vermiculite. Sample codes denoted in Table 5.5.

## *Intercalation of HCl modified vermiculite by Maleic acid*

Two samples of VMT modified by HCl were chosen. VMT pre-modified by 2M hydrochloric acid at room temperature for 7 hours and the next at 60 °C stirred for 24 hours. Both of them were consequently modified by maleic anhydride together with acetic acid.

HCl form of VMT was magnetically mixed together with maleic anhydride and acetic acid in ratio 1 : 1 : 2 at room temperature for 24 hours. Consequently, acetic acid was evaporated and solid phase was dried at 80 °C for another 24 hours. Solid phase was milled by laboratory knife mill. Samples are termed as o-HClVMT 7/MA+AA and o-HClVMT 24/MA+AA.

The result of the intercalation is presented in Fig. 5.15. The structure of HCl modified VMT for 7 hours was dramatically changed during intercalation by maleic anhydride. HCl-VMT has two peaks at 7.1 and 8.7 °2 $\theta$  but they almost disappeared after organophilization which means partial exfoliation of vermiculite layers. These changes are also confirmed elsewhere [92, 96]. The structure of fully delaminated VMT (2MHClVMT 60/24/200) shows small changes at 8.8 °2 $\theta$  where the peak of small intensity appeared.

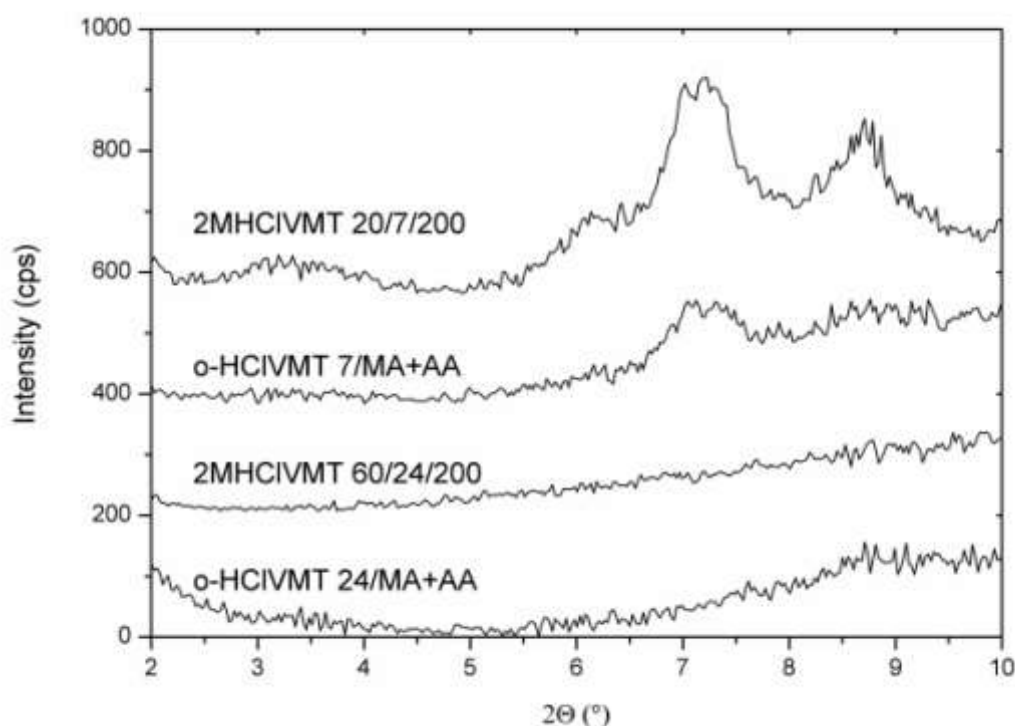


*Fig. 5.15: SAXS of HCl treated and maleic anhydride modified VMT. Sample codes denoted in Table 5.4.*

The presence of intercalation agent in HCl modified VMT is distinguishable in Fig.5.16. Higher amount of agent is contained in not fully delaminated structure (o-HClVMT 7/MA+AA) as can be seen in area from 1200 to 1700  $\text{cm}^{-1}$ . It means that more delaminated structure is less organophilized, which can have an important role for its dispersion in polymer matrix.

### ***Intercalation of sodium montmorillonite***

To compare influence of the same modifying agent, on the properties of filler in polymer matrix, sodium type of MMT (Cloisite  $\text{Na}^+$ ) were also intercalated by CTAB at identical conditions as for VMT. Ratio of modifying agent and MMT was chosen 1 : 1 and the sample was termed as o-NaMMT 1:1/24. Fig. 5.17 shows XRD spectra of pure sodium and organically modified MMT. The peak representing sodium ions in MMT structure ( $7.3^\circ 2\theta$ , 1.19 nm) shifts to lower angles at  $4.5^\circ 2\theta$  (d-spacing 1.96 nm) which indicate successful intercalation, but the interlayer distance was not improved as well as in vermiculite. Nevertheless, the peak indication at  $2^\circ 2\theta$  is observable, and MMT interlayer can be intercalated more, but this peak was not detected by XRD.

Organically modified VMT, as well as MMT are compared with commercially available MMT products, namely Cloisite 20A and Cloisite 15A in Fig. 5.18. Cloisite 20A (interlayer distance 2.42 nm) contain less amount of intercalation agent than Cloisite 15A, thus d-spacing of Cloisite 15A is 3.15 nm. However, both include small percentage of unmodified layers (peak at  $7.2^\circ 2\theta$ ).

In next Fig. 5.19 both laboratory and commercially modified clays are compared. It is clearly seen that commercially modified MMTs reached higher d-spacing than laboratory prepared MMT sample. MA treated HCl-VMT indicates exfoliated structure and CTAB intercalated sodium VMT is characterized by more peaks with various interlayer distances.

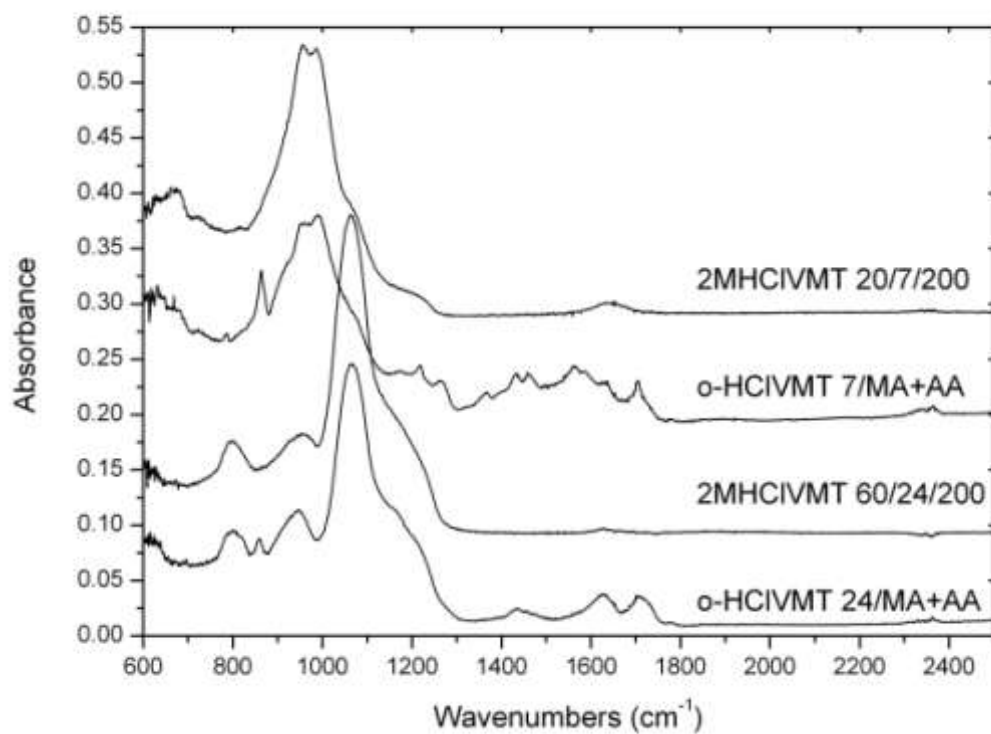


Fig. 5.16: FTIR spectra of HCl treated and MA modified VMT. Sample codes denoted in Table 5.4.

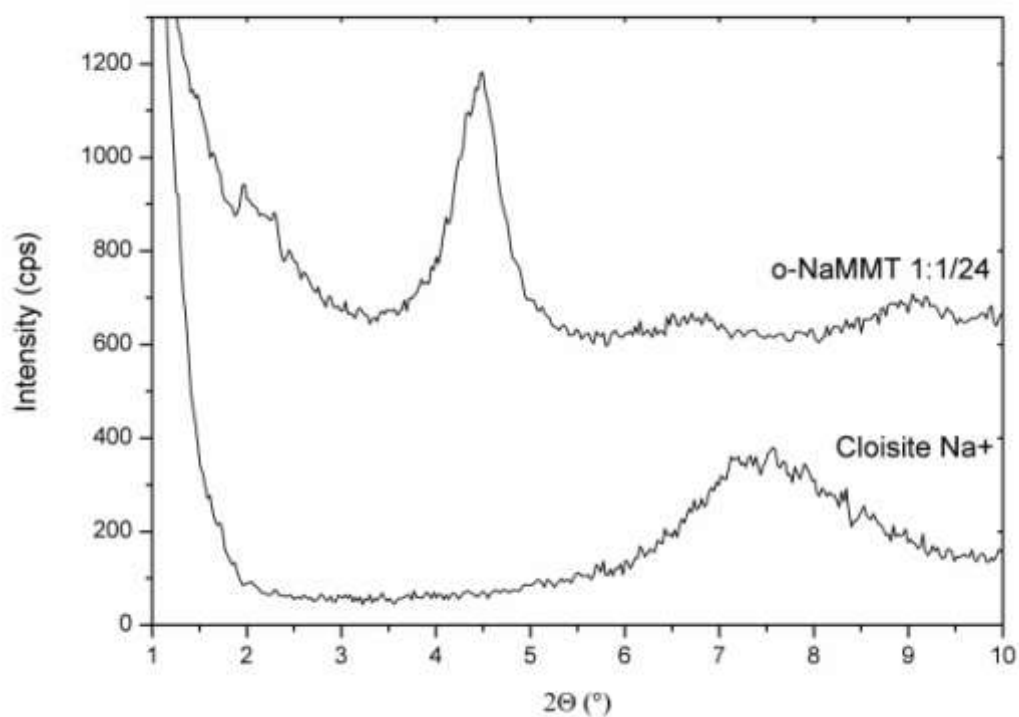


Fig. 5.17: SAXS of sodium MMT and its CTAB modified form.

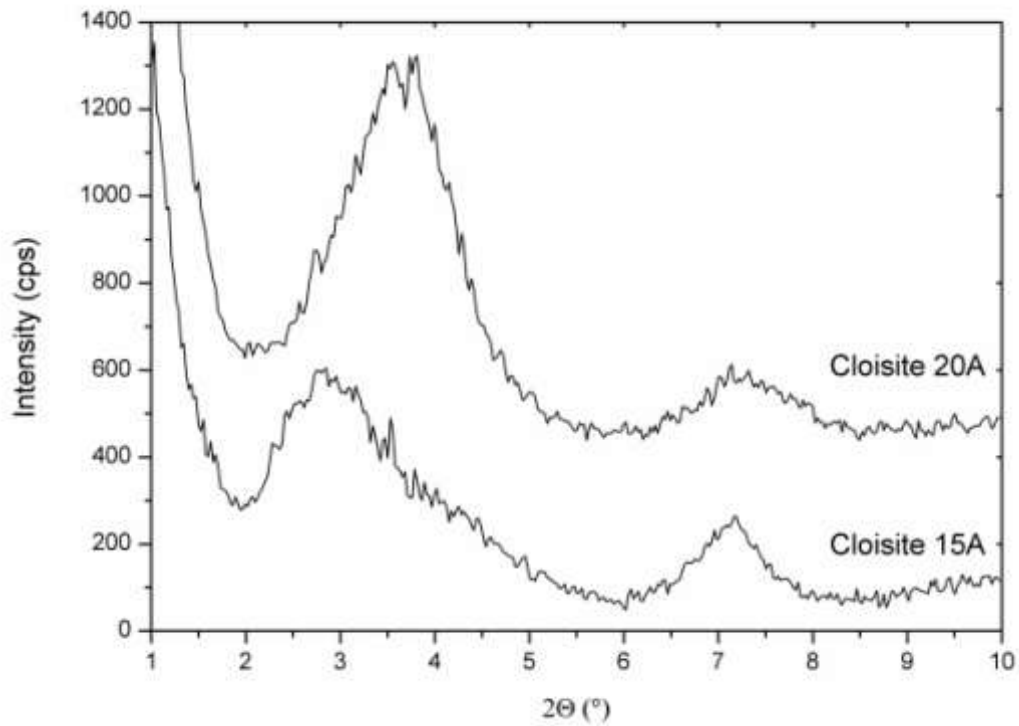


Fig. 5.18: Interlayer distances for Cloisite 15A and Cloisite 20A.

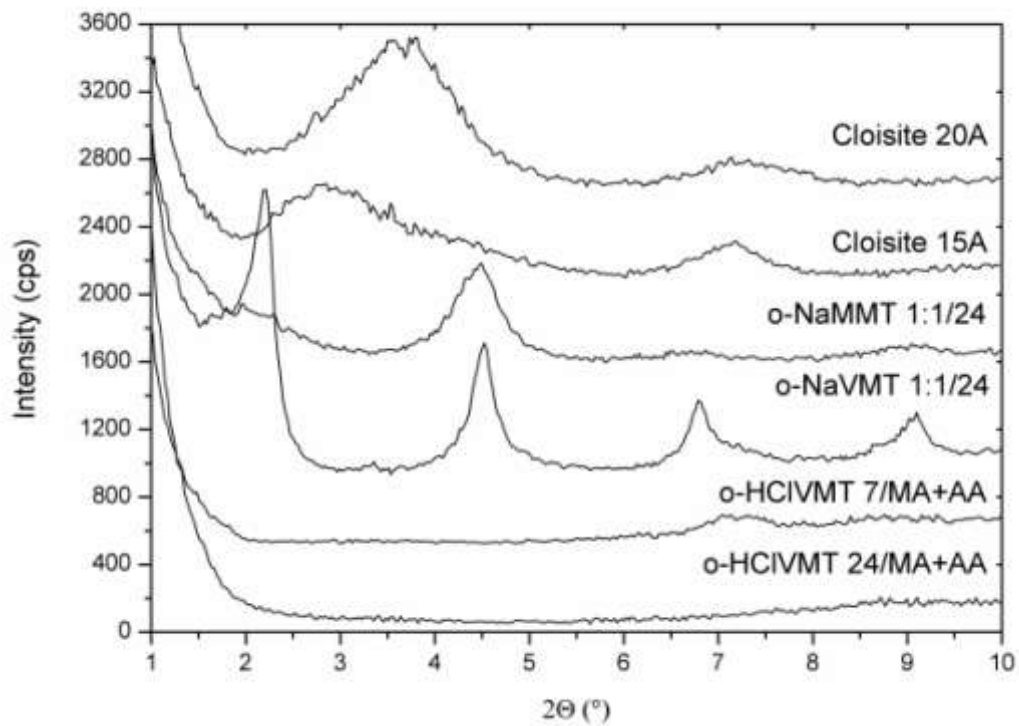


Fig. 5.19: Comparison of filler intercalated by organic cations.

### 5.1.4 Thermo gravimetric analysis of fillers

TGA was carried out on VMT, as well as MMT samples to obtain information about water and intercalation agent content. Temperature stability of organically modified clay was also measured. Temperature dependence is plotted in Figs. 5.20–5.22 and water and organic content is presented in Table 5.6.

Fig. 5.20 shows mass loss for fillers without organic modifier. These samples contain only water molecules which are evaporated during heating. Expanded VMT contains less than 2 %, which evaporated at temperature 100 °C [97]. However, clays contain also chemically bonded water, which evaporation starts at 190 °C, where next 1 % of water was removed and continues to 800 °C. Similar trend is for 7 hours HCl modified VMT, but water content was 4 % and 1 % of bonded water respectively. Other three samples do not contain bonded water at this temperature range. The content of free water for these samples is around 3.4 % for sodium VMT, 5.2 % for Cloisite Na<sup>+</sup> 5.2 % and 7.1 % for 24 hours modified HCl VMT.

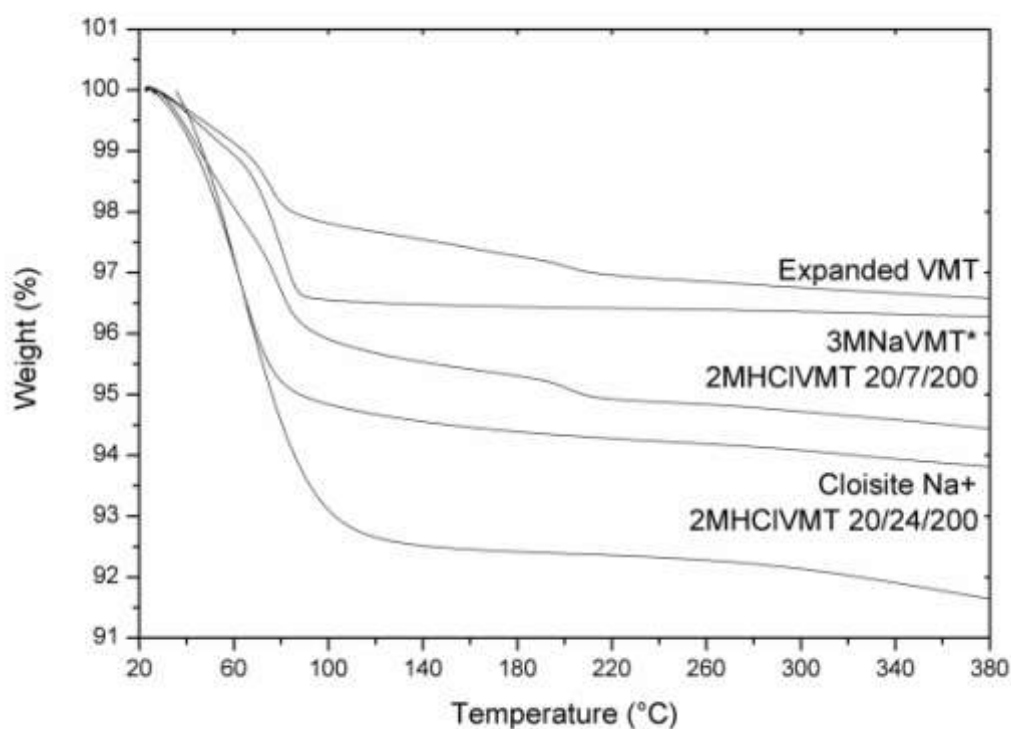


Fig. 5.20: TGA curves for inorganic fillers.

TGA curves for organically modified VMTs are in Fig. 5.21. All curves have similar course as their original unmodified samples to 100 °C. Growing temperature of the sample causes evaporation of organic modifier. Behind 100 °C MA begins to degrade. In both cases of HCl modified samples MA was

removed when before 230 °C reached. But they differ in the amount of modifier contained in their structure. While the sample treated by HCl for 24 hours contain only 10.8 % of MA, the sample treated for 7 hours contain 46.5 % of MA. This variance is caused by structural changes during treating. In contrast to MA, CTAB has higher temperature resistance. CTAB degradation in filler is in range 200–300 °C. Organic content in o-NaVMT 1:1/24 is 37.7 %.

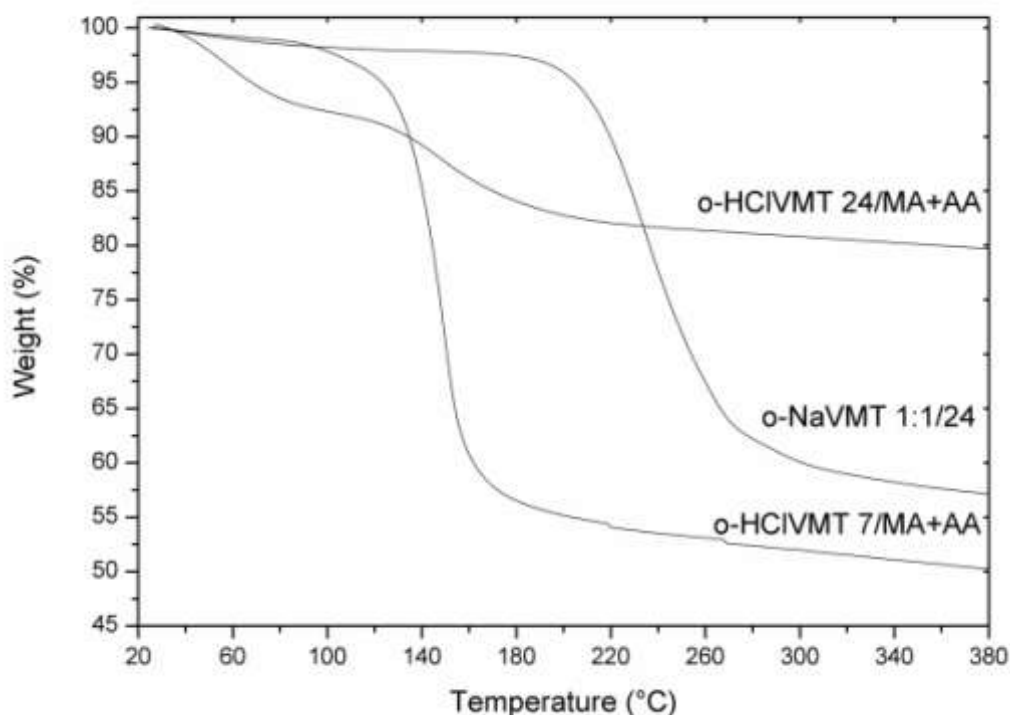


Fig. 5.21: TGA curves for organically modified VMT.

Commercial fillers and sodium MMT intercalated by CTAB are compared in Fig 5.22. This sample starts to lose its weight also at 200 °C like o-NaVMT. Contrary to organic VMT where the degradation finished at 300 °C, the degradation is quite fast till 290 °C but it slowly continue to 440 °C. Total amount of organic fraction is 34.2 %. Commercially prepared fillers are thermally more stable. Their degradation starts at 240 °C and degradation depend on the amount of organic fraction. Cloisite 20A contains 24.7 % of organic part and it is totally evaporated at 415 °C. Cloisite 15A with the content of 38.7 % loses its entire modifier at 490 °C.

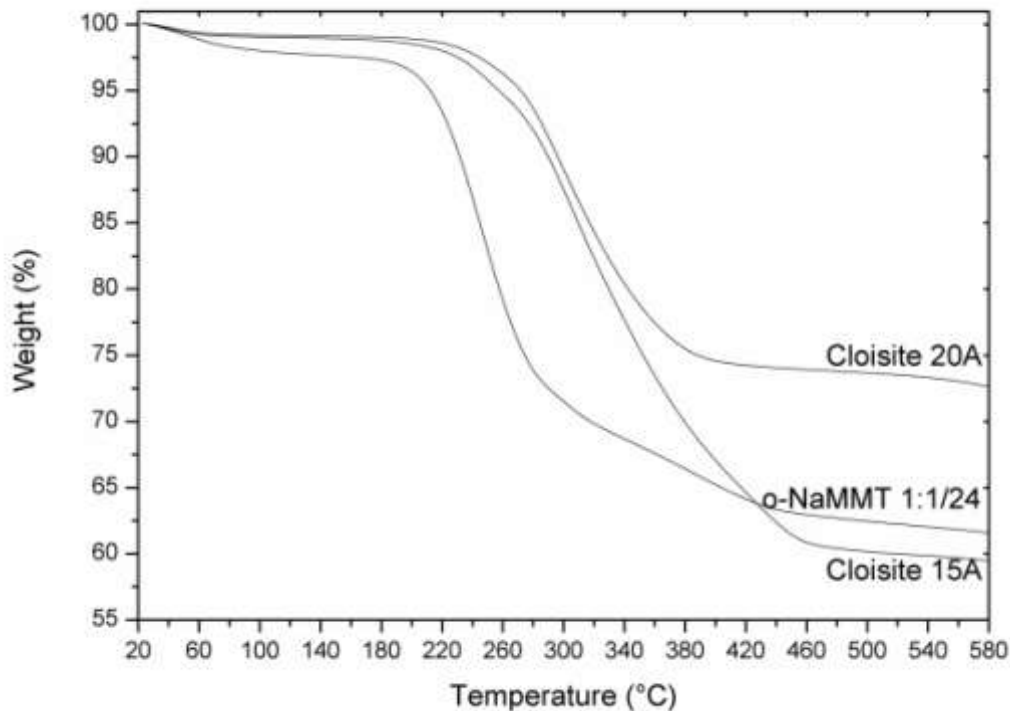


Fig. 5.22: TGA curves organically intercalated MMTs.

The content of the volatile components in filler structure was also characterized by ignition test. Small amount of filler was placed to ceramic dish, weighed and heated to 1000 °C. After 1 hour, it was cooled and weighed again. It was done for organic as well as inorganic fillers. Subsequently, content of water and organic parts was calculated. Results are given in Table 5.6 and compared with TGA.

As it is evident from the table, the content of volatile fraction during burning test is mostly higher in comparison with TGA. It is probably caused by higher temperature and longer duration of the test which leads to better volatilization. Content of water in inorganic VMTs were around 8 % and for montmorillonite 12 %. Water contained in pure fillers was deducted from total amount of volatile fraction and percentage of organic content was obtained. Organically modified VMTs contain more intercalating agent than MMT.



Table 5.6: Content of water and organic component, calculated from TGA and burning test.

Sample	TG analysis		Burning test		
	Water [%]	Org. cont. [%]	Water [%]	Org. cont. + water [%]	Org. cont. [%]
Expanded VMT	3.0	–	8.3	–	–
3MNaVMT*	3.4	–	5.3	–	–
2MHClVMT 20/7/200	5.0	–	8.6	–	–
2MHClVMT 20/24/200	7.1	–	8.9	–	–
Cloisite Na+	5.2	–	11.9	–	–
o-NaVMT 1:1/24	2.0	37,7	*	47.3	42.0
o-HClVMT 7/MA+AA	1.0	46.5	*	55.6	47.0
o-HClVMT 24/MA+AA	7.1	10.8	*	24.3	15.4
o-NaMMT 1:1/24	2.4	34.2	*	43.7	31.8
Cloisite 15A	1.0	38.7	*	43.3	31,4
Cloisite 20A	0.8	24.7	*	38.9	27.0

\* Water content is taken from the pure fillers

## 5.2 Polymer/clay composite preparation

### 5.2.1 Evaluation of the best compounding condition

Prepared clays as well as commercially available ones were compounded with polymer matrix. To find the optimal compounding conditions to reach high level of filler dispersion in polymer matrix ranks to the main goals of thesis. In the following chapter, three methods available at our laboratories and their effect on clay dispersion in polymer are compared. Applied testing devices were Brabender, twin screw extruder, Brabender, mixing chamber and Collin, double roll mill for plastics.

In Table 5.7 are summarized conditions of composite preparation. As can be seen, compounding on twin screw and mixing chamber, have to be done at temperature higher than forming temperature (190 °C), while mixing on double roll mill was done at lower temperature – 125 °C.

Surlyn® 9020 was chosen as polymer matrix. The level of exfoliation was tested using commercially available filler, Cloisite 20A, which exhibits high level of dispersion in matrix. The amount of clay was calculated to be 5 wt % of pure montmorillonite for all compounds.

Surlyn® is polymer, which can melts in wide processing window 185–285 °C. However, organically modified fillers easily degrade at temperature over 200 °C and higher. Thus the maximal temperature used for compounding by twin screw extruder and mixing chamber was 210 °C. Nevertheless, set up compounding condition on double roll mill is complicated. Surlyn® exhibits high tenacity to metal. Therefore, if temperature is too high, polymer is not possible to remove from the roll. On the other hand, at too low temperature, polymer is not melted. Each type of polymer (in this case Surlyn®), there is narrow window (5–10 °C), where it can be processed. If some additives, like fillers are used, it changes processing temperature, of course.

Filler dispersion in polymer matrix was investigated by the help of optical microscopy and scanning electron microscopy.

Optical microscopy pictures of the samples compounded via a) twin screw extruder, b) mixing chamber or c) double roll mill are compared in Fig. 5.23. This method was used as a first view to the structure of composites. The most numerous and the biggest filler particles are contained in the compound prepared inside mixing chamber. Their size is mostly 5–25 µm, but particles with 40 µm dimension are also included. Both devices, twin screw extruder and double roll mill, disperse clay particles to similar degree. Size of particles is predominantly less than 10–15 µm but agglomerates in larger size up to 25 µm can also be found.

Table 5.7: Compounding conditions for three methods.

	<b>Twin screw extr.</b>	<b>Mixing chamber</b>	<b>Double roll mill</b>
Temperature [°C]	170, 200, 210	210	125
Rotation [rpm]	15	30	10
Time [min]	1 pass	10	10

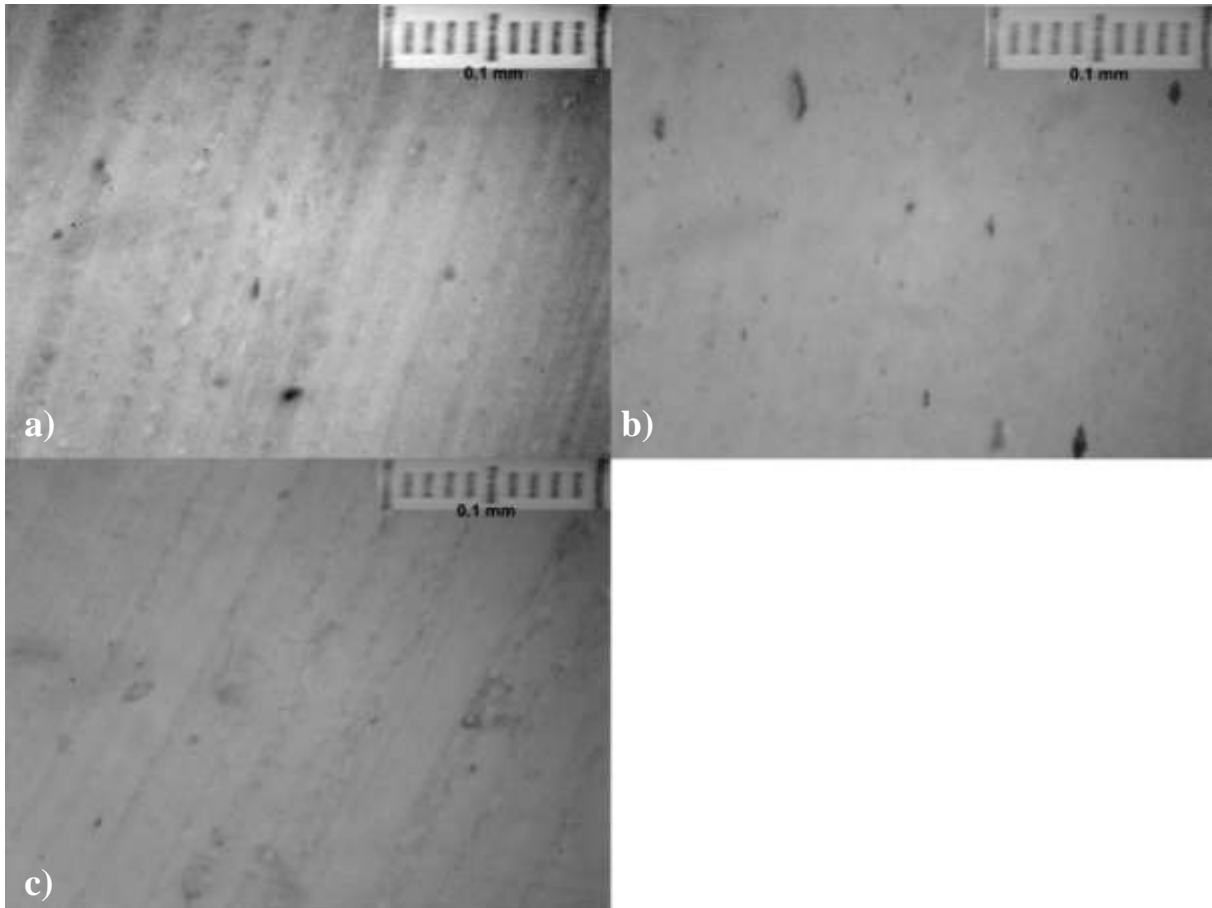
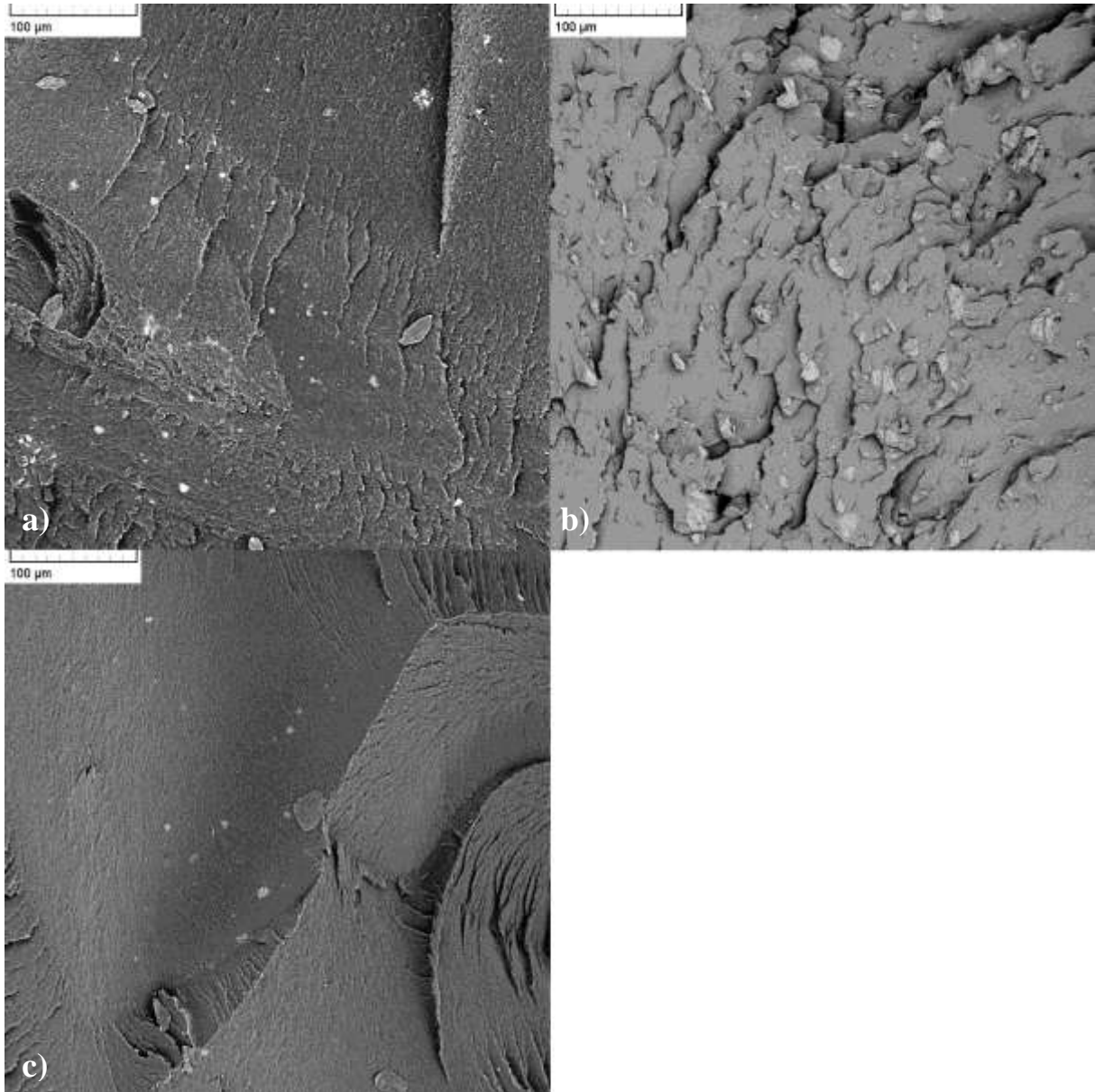


Fig. 5.23: Optical microscopy pictures (first approach to morphology) of Surlyn® 9020/Cloisite 20A compounds prepared on a) twin screw extruder, b) mixing chamber and c) double roll mill.

Differences in the dispersion level are more distinguishable on the SEM pictures (Fig. 5.24). Obviously, the worse clay dispersion in polymer was achieved when the mixing chamber was used (Fig. 5.24 b). Clay particles and aggregates 20–35  $\mu\text{m}$  in diameter are evident in the structure and their amount is high. When the composite on twin screw extruder was compounded, the number of aggregates and their size rapidly decreases. Their size is about 5–10  $\mu\text{m}$  and few about 20  $\mu\text{m}$ . Similar particle dimension are for compounding on double roll mill. Moreover, the amount of clay domains is smaller than for compounding on twin screw extruder.

Another important parameter for the preparation of polymer-filler compounds in this work was the amount of materials processed on each device. Optimal quantity of materials is up to 50 g in mixing chamber and 20–100 g on double roll mill, respectively. At least 400 g of materials is necessary to process in twin screw extruder. In laboratory conditions, only few grams of modified filler were prepared. From this reason, approximately 50 g of final compound is adequate to prepare for testing. Based on the results from microscopy and in dependence on the amount of material, the optimal compounding method, double roll mill, was selected.



*Fig. 5.24: SEM pictures of Surlyn® 9020/Cloisite 20A compounds prepared on a) twin screw extruder, b) mixing chamber and c) double roll mill.*

## 5.2.2 Materials

The influence of laboratory modified and commercial fillers on the final properties of polymer composites are compared in this study. Surlyn® 9020, Surlyn® 9910 and Surlyn® 8920 were used as polymer matrixes. Surlyn® 9020 was compounded with whole raw of fillers; however, the other polymers were mixed only with fillers presenting the most promising results with Surlyn® 9020.

In Table 5.8 are given all fillers compounded with polymers.

Table 5.8: Fillers compounded with polymers. Fillers short cuts are in brackets.

Fillers based on VMT		Fillers based on MMT	
Inorganic	Organic	Inorganic	Organic
Expanded VMT (ExpVMT)	–	Cloisite Na+	Cloisite 20A
3MNaVMT* (NaVMT)	o-NaVMT 1:1/24 (o-NaVMT)	–	o-NaMMT 1:1/24 (o-NaMMT)
2MHCI VMT 20/7/200 (HCIVMT 7)	o-HCI VMT 7/MA+AA (o-HCI VMT 7)		
2MHCI VMT 20/24/200 (HCIVMT 24)	o-HCI VMT 24/MA+AA (o-HCI VMT 24)		

## 5.2.3 Preparation of tested compounds

Based on the previous experiences, Collin, double roll mill was used for compounding. Mixing conditions are given in Table 5.9. As can be seen, sodium ions used for methacrylic acid neutralization significantly reduces compounding temperature. On the other hand, addition of some fillers (namely o-NaVMT and o-HCI VMT) caused rising in melting strength. Thus, the processing temperature had to be increased about approximately 10 °C.

Percentage of filler in matrix was set 3 and 5 wt % of VMT or MMT without modifier.

Table 5.9: Compounding conditions for various types of Surlyn®

	<b>Surlyn® 9020</b>	<b>Surlyn® 9910</b>	<b>Surlyn® 8920</b>
Temperature [°C]	125	125	95
Rotation [rpm]	10	10	10
Time [min]	10	10	10

Sheets 2 mm in thickness were press moulded from prepared compounds under temperature  $T = 210\text{ }^{\circ}\text{C}$  for  $t = 5\text{ min}$  and subsequently pressed during cooling by water. From these sheets specimens for each test were cut.

## 5.3 Characterization of structure and properties

### 5.3.1 X-Ray diffraction

X-ray diffraction was used as a suitable tool for analysis of filler dispersion.

Spectra for inorganic fillers are shown in Fig. 5.25. Interlayer distance of composites filled by inorganic fillers based on VMT does not change in comparison with pure fillers, while for MMT composite it reduces from 1.19 nm to 0.99 nm. Compound with sodium VMT show three peaks. The peak at  $7.1\text{ }^{\circ}2\Theta$  is for sodium ions, while the other two correspond to origin ions which were not successfully exchanged.

These two peaks ( $7.1$  and  $8.6\text{ }^{\circ}2\Theta$ ) are also visible for compound with organically modified VMT (Fig. 5.26). Although these layers are contained there, main part of VMT was markedly dispersed in matrix as is confirmed by the peak at  $1.72\text{ }^{\circ}2\Theta$  (5.14 nm). This interlayer distance is higher than for compound with commercial available Cloisite 20A ( $2.50\text{ }^{\circ}2\Theta$ , 3.49 nm). However, particles of Cloisite 20A are not dispersed at the same level, as well. Partially they have interlayer only 1.62 nm. Next curve in the same figure belongs to compound of Surlyn® with sodium MMT modified by CTAB. As is evident also from next Fig. 5.27 where curves of fillers and compounds are together, interlayer distance probably decreases to 1.41 nm. However, as can be supposed from the next tests, the first peak can be hid in small angles and not visible.

CTAB intercalated fillers and Cloisite 20A are compared with their polymer composites. Peaks movements described above.

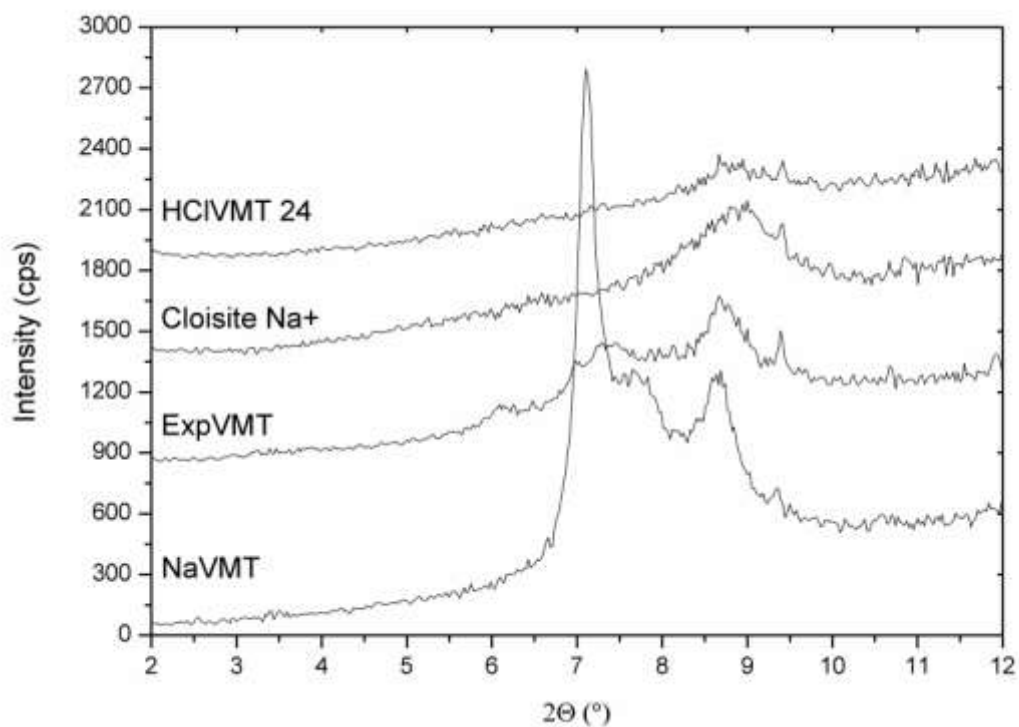


Fig. 5.25: X-ray diffraction of Surlyn® 9020 compounds with inorganic fillers.

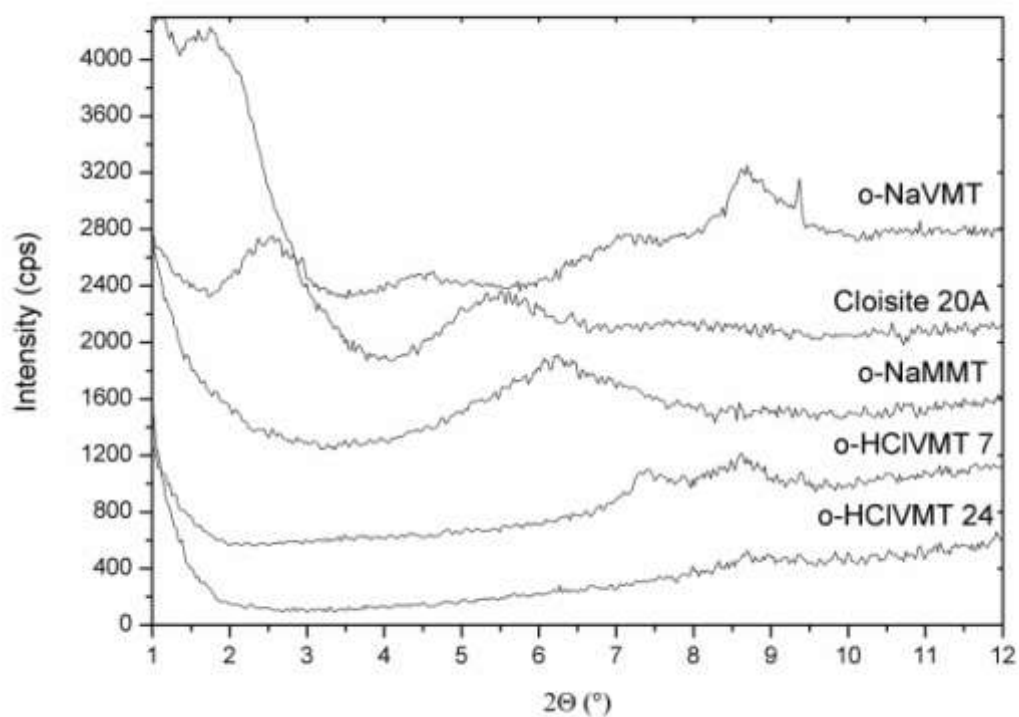


Fig. 5.26: X-ray diffraction of Surlyn® 9020 compounds with organically modified clays.

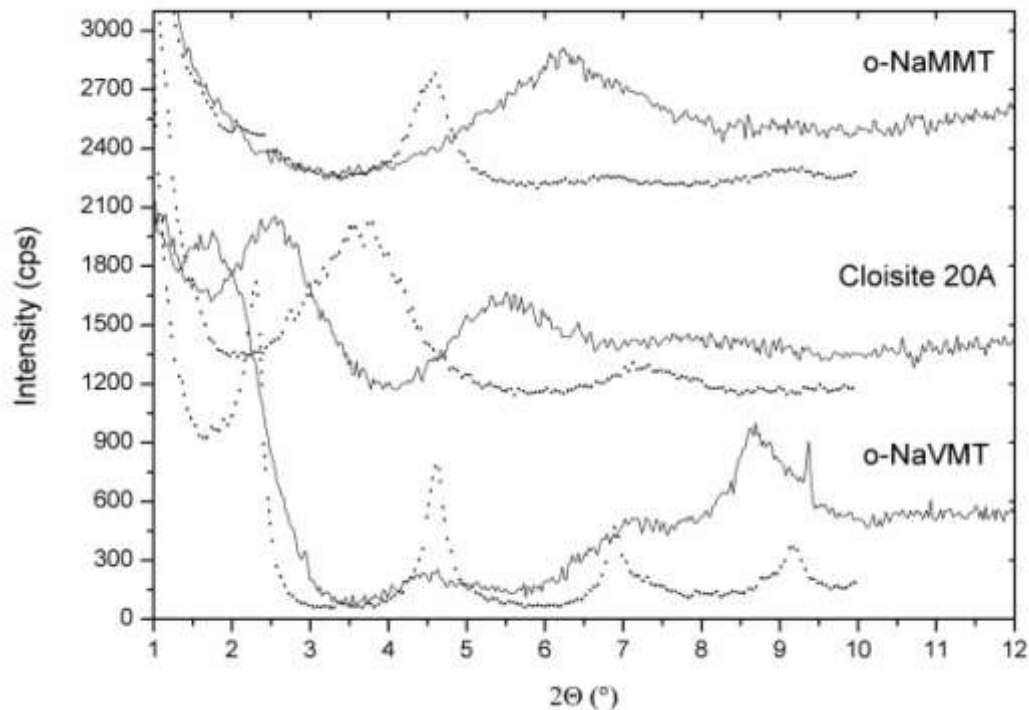


Fig. 5.27: Comparison of interlayer spacing between polymer–clay compound (full line) and filler (dot line).

### 5.3.2 Optical microscopy

Optical microscopy was carried out on Jena NU-2 microscopy with the magnification of 32 $\times$ . The magnification was elevated 10 $\times$  via photo camera and final magnification 320 $\times$  was reached.

In Fig. 5.28 and 5.29 are presented the dispersion levels of both inorganic and organic fillers in polymer matrix. Inorganic fillers were quite large particles of non-dispersed clay. The particle size is in range from few micrometers to 50  $\mu\text{m}$ . The largest particles are for expanded and HCl modified VMT, while the sodium VMT form and MMT make majority particles up to 30  $\mu\text{m}$ .



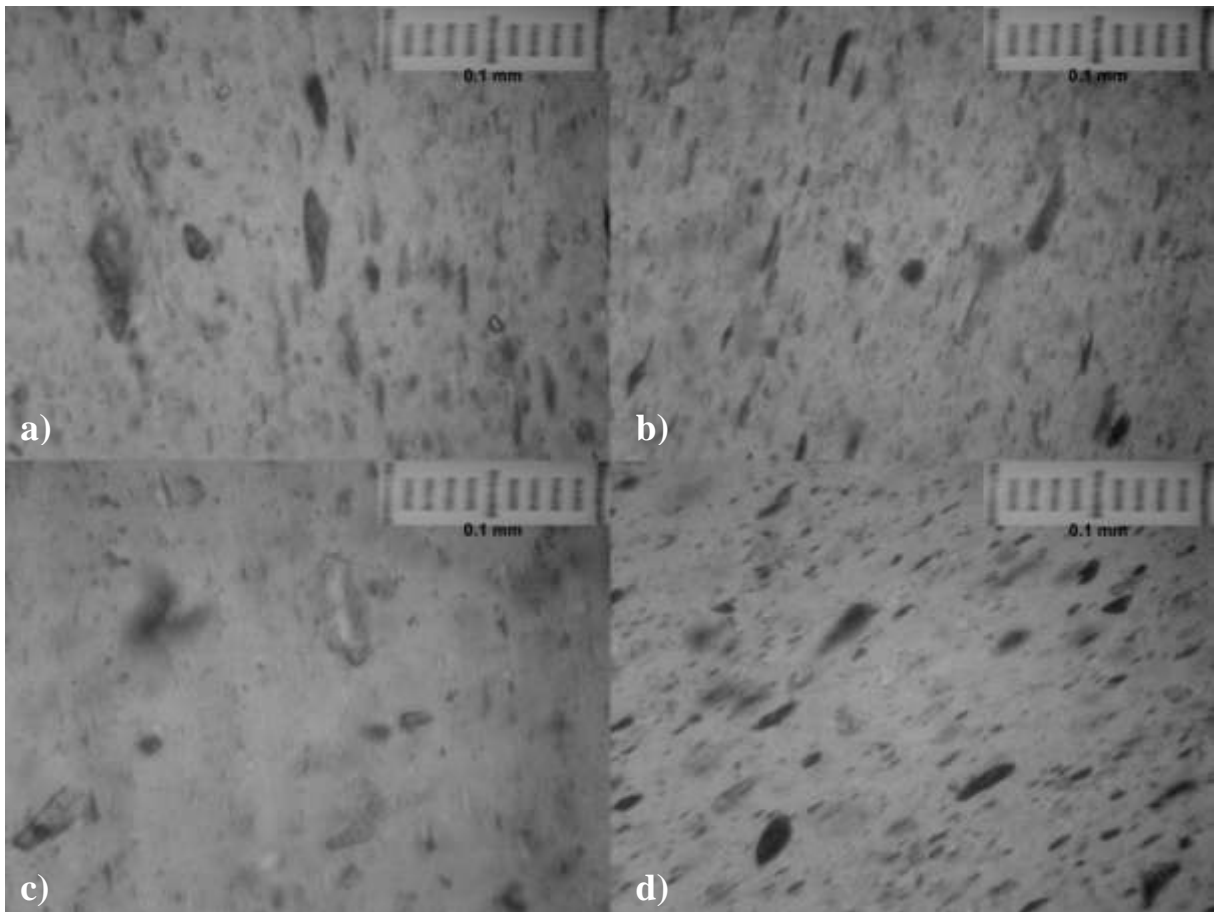


*Fig. 5.28: Optical microscopy (first approach to morphology) of Surlyn® 9020 compounds filled by inorganic fillers, namely a) expanded VMT, b) NaVMT, c) HCIVMT 24 and d) Cloisite Na<sup>+</sup>*

Organically modified clays by MA in polymer (Fig. 5.29 a, b) produce filler particles in similar size as inorganic ones. On the other hand, VMT modified by CTAB and Cloisite 20A (Fig. 5.29 c, d) reach quite high level of dispersion in size up to 5–10  $\mu\text{m}$ . High amount of these particles is contained in o-NaVMT compound, while aggregates in organically MMTs filled samples are infrequent.

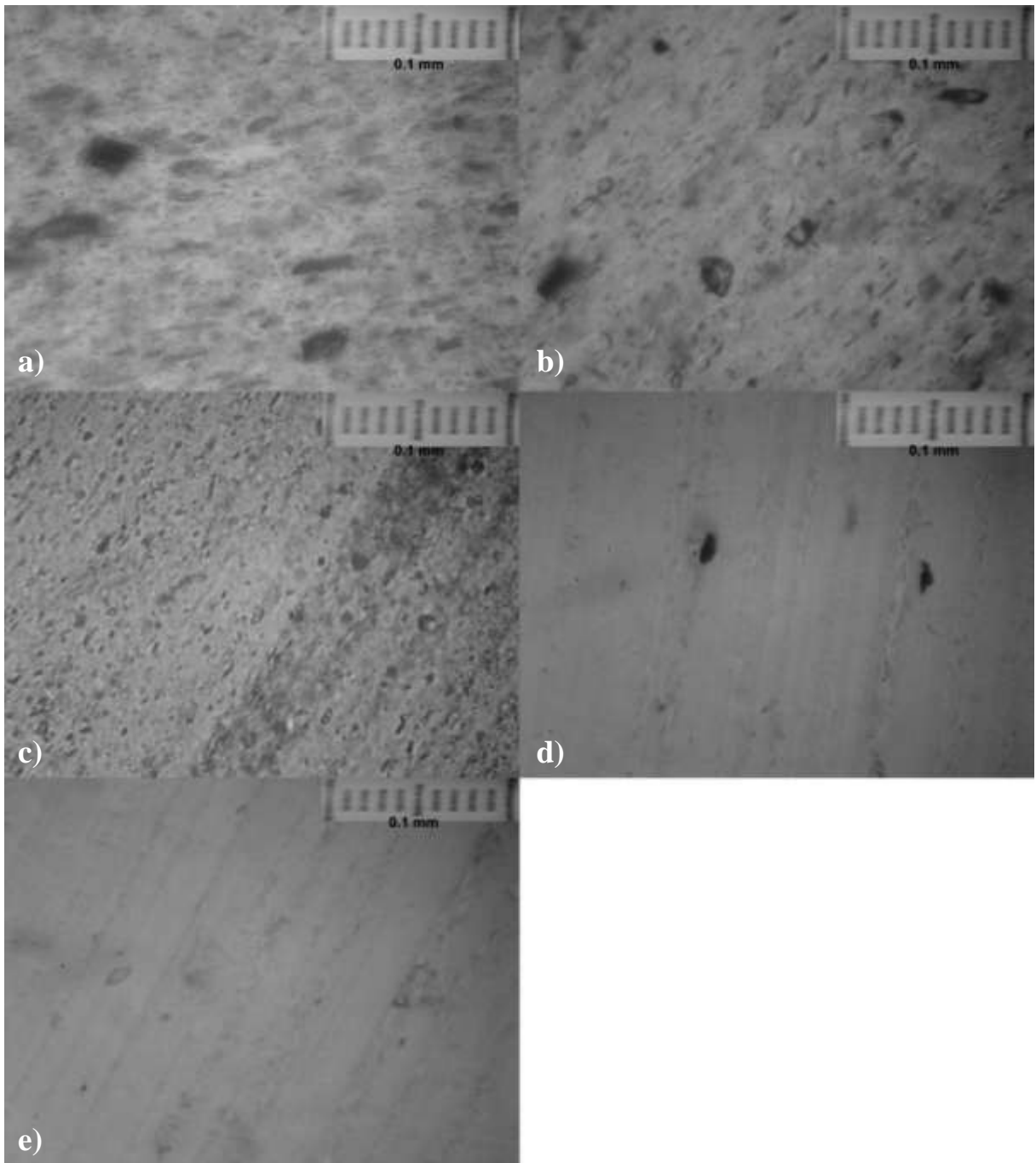


*Fig. 5.29: Optical microscopy (first approach to morphology) of Surlyn® 9020 compounds with organic fillers a) HCIVMT 7, b) HCIVMT 24, c) o-NaVMT, d) o-NaMMT and e) Cloisite 20A.*

Evidently, the morphology of polymer-clay compounds is not possible to examine via optical microscopy precisely. Therefore, detailed morphology was achieved by the help of electron microscopy.

### 5.3.3 Scanning electron microscopy

The polymer–clay composite structure was verified by scanning electron microscopy. Dispersion level for inorganic clays is compared in Fig. 5.30. All compounds contained undispersed particles as already confirmed via optical microscopy. Plate-like shape in thickness of few microns and width to 40  $\mu\text{m}$  is clearly seen for NaVMT compound. Aggregates of HCIVMT 24 filled sample are larger, nearly 50 microns. Size of MMT particles mainly differ from 5–25  $\mu\text{m}$ . Evidently, natural clays are not well dispersed in matrix what will be reflected in mechanical properties of compounds.

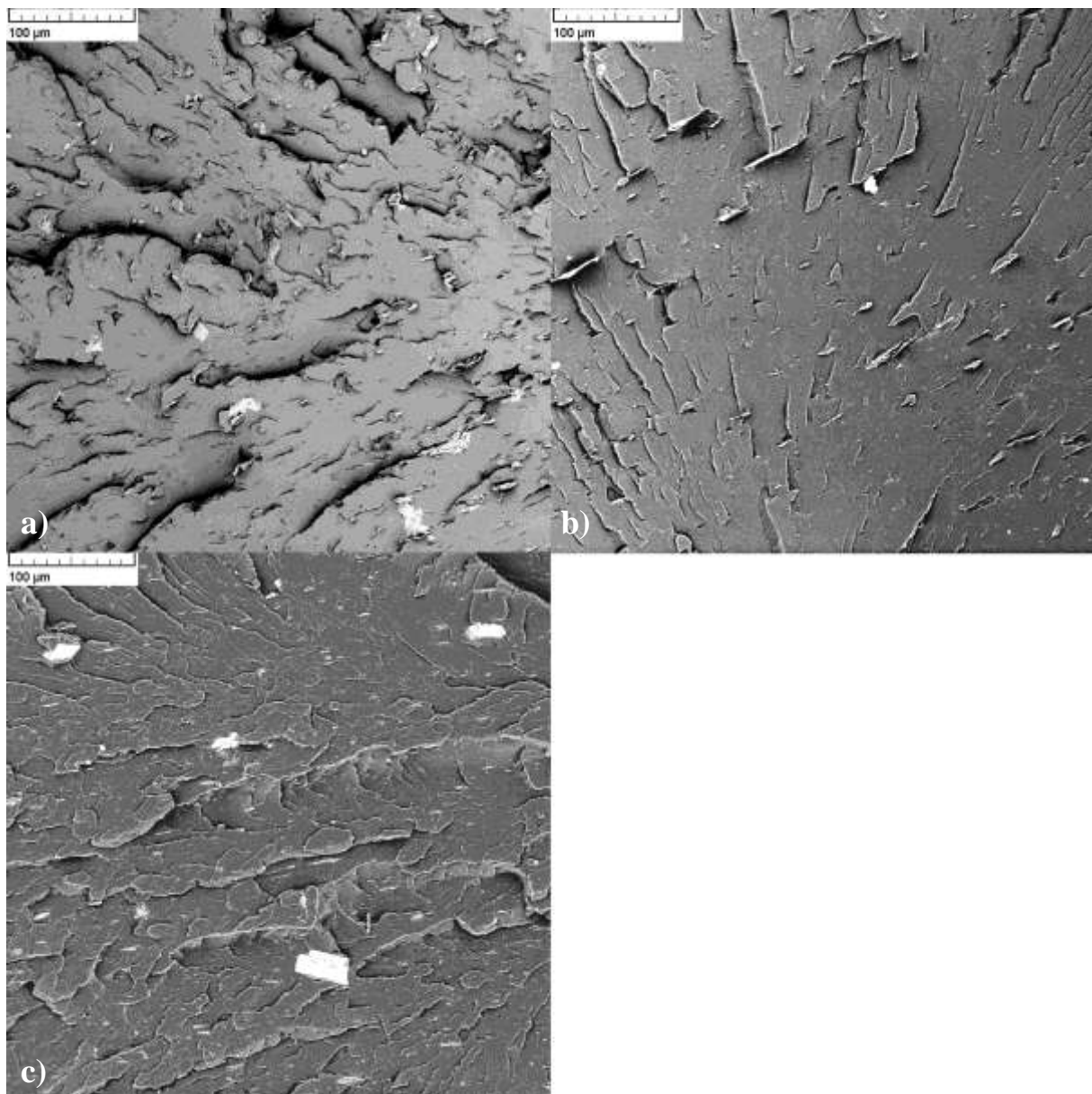


*Fig. 5.30: SEM photos of Surlyn® 9020 compounded with inorganic fillers  
a) Cloisite Na<sup>+</sup>, b) NaVMT and c) HCIVMT 24*

Dispersion of organically modified fillers in Surlyn® 9020 is in Fig. 5.31 and Fig. 5.32 respectively. Evidently, dispersion differs from inorganic clays. Aggregate size and their amount are significantly lower. Both VMT based fillers have similar dimension up to 20 microns but for o-HClVMT are aggregates more frequent. Moreover, the compatibility between clay and filler is not very high, as proved from Fig. 5.31 a). Some larger clay particles miss or its adhesion with polymer is low. On the other hand organic sodium VMT seems to be in good adhesion to polymer; however, particles are not well intercalated in matrix (Fig. 5.31 b and 5.32 a) or in more details in Fig. 5.33 b) and 5.34 a). The reason can be incomplete saturation by sodium ions during modification. Consequently, interlayers were not organophilized, which led to creation of agglomerates. MMT modified in the same way is better dispersed in the same polymer. No clay particles are visible on cryogenically fractured samples (Fig. 5.31 c) and more detail in 5.33 c) but on the etched samples are small particles in size up to 3  $\mu\text{m}$  (Fig. 5.32 and Fig. 5.34). It is a significant improvement also in contrast to commercially available Cloisite 20A where few agglomerates are presented (in size up to 10  $\mu\text{m}$ ).

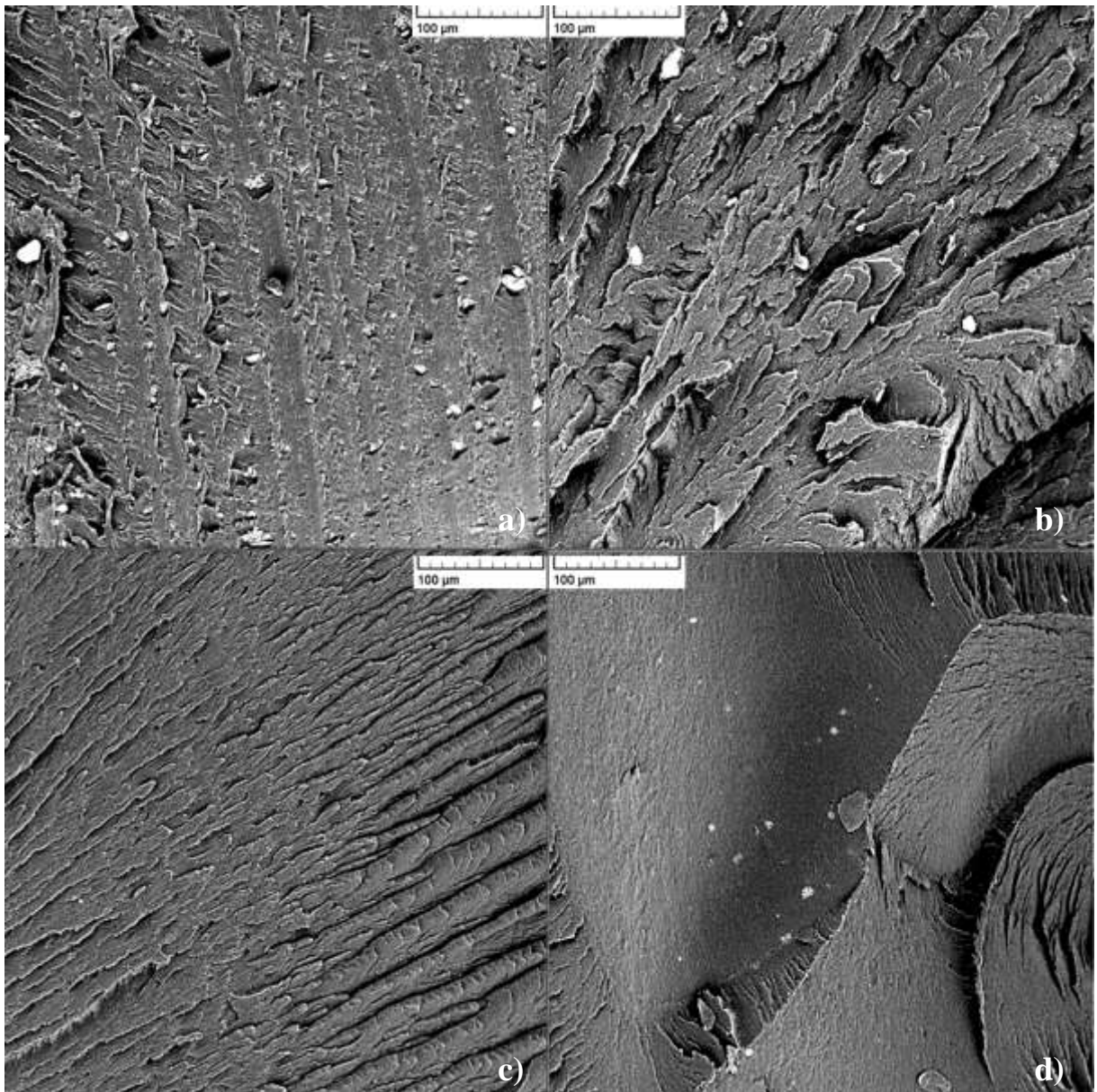


*Fig. 5.31: SEM photos of cryogenically fractured Surlyn® 9020 compounded with organic fillers a) o-HClVMT 24, b) o-NaVMT, c) o-NaMMT, and d) Cloisite 20A.*

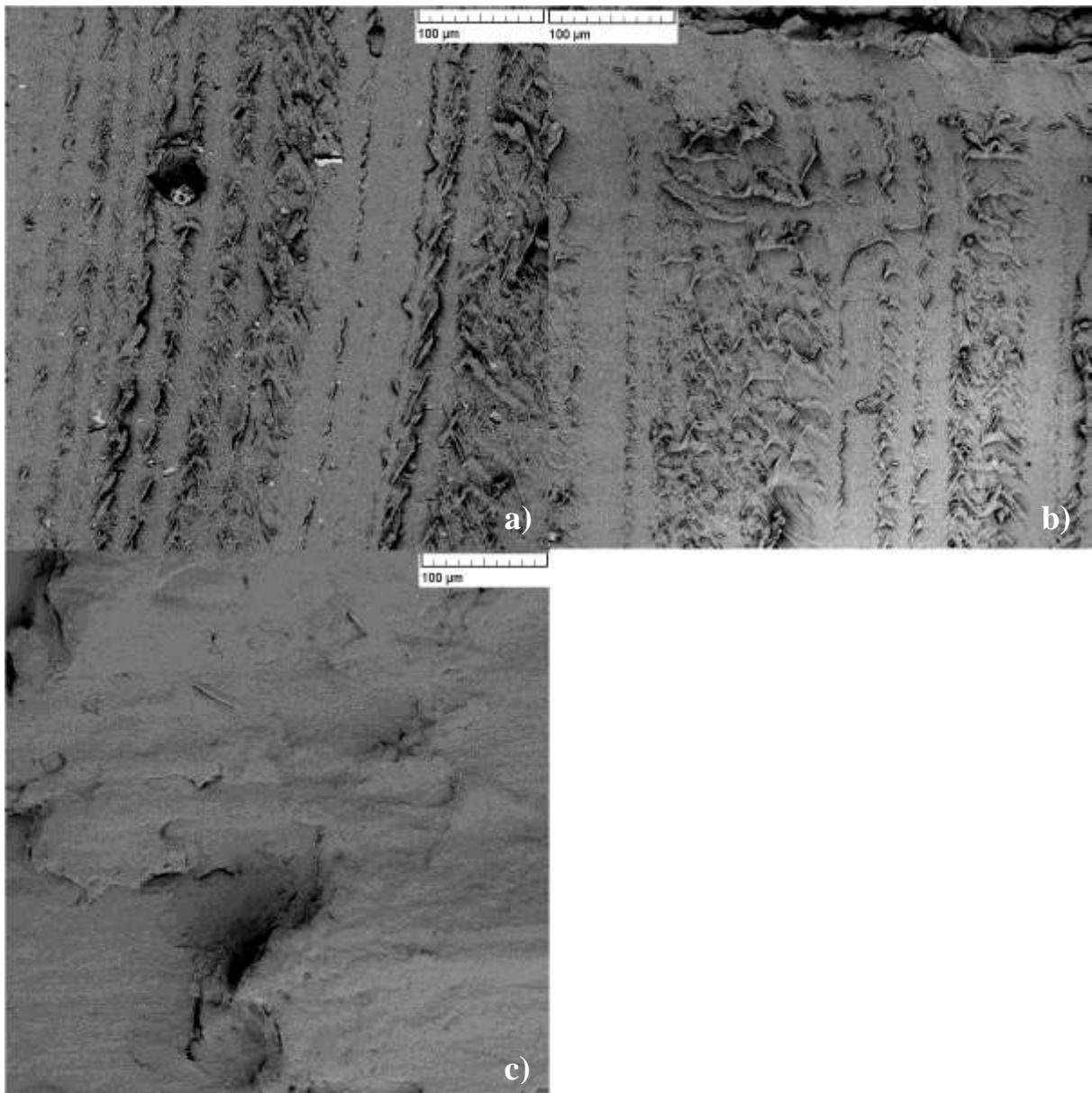


*Fig. 5.32: SEM photos of selectively etched Surlyn® 9020 compounded with organic fillers a) o-NaVMT, b) o-NaMMT, and c) Cloisite 20A.*

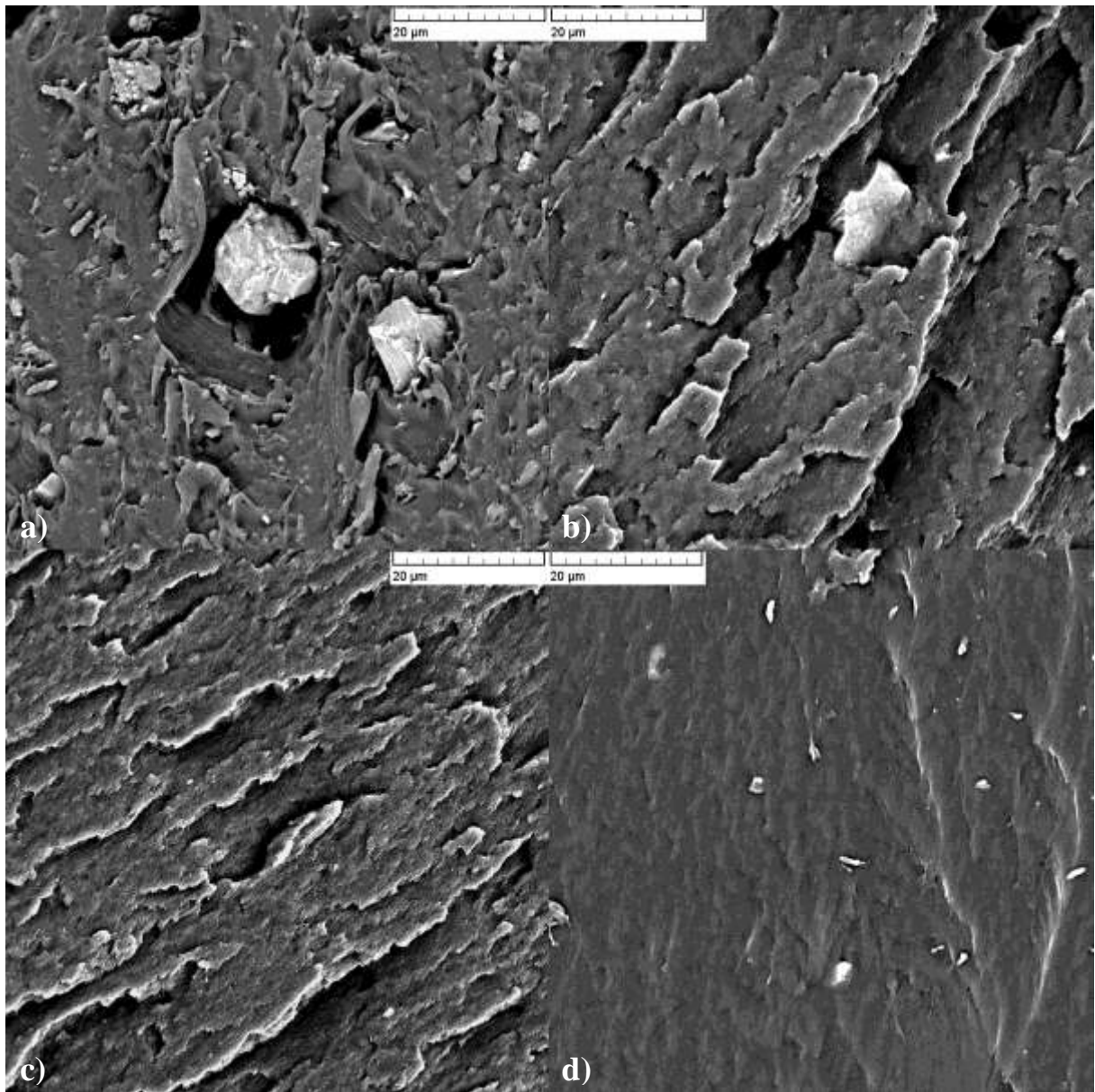


*Fig. 5.33: Detailed study of clay particles in cryogenically fractured polymer composites, a) o-HClVMT, b) o-NaVMT, c) o-MMT and d) Cloisite 20A*

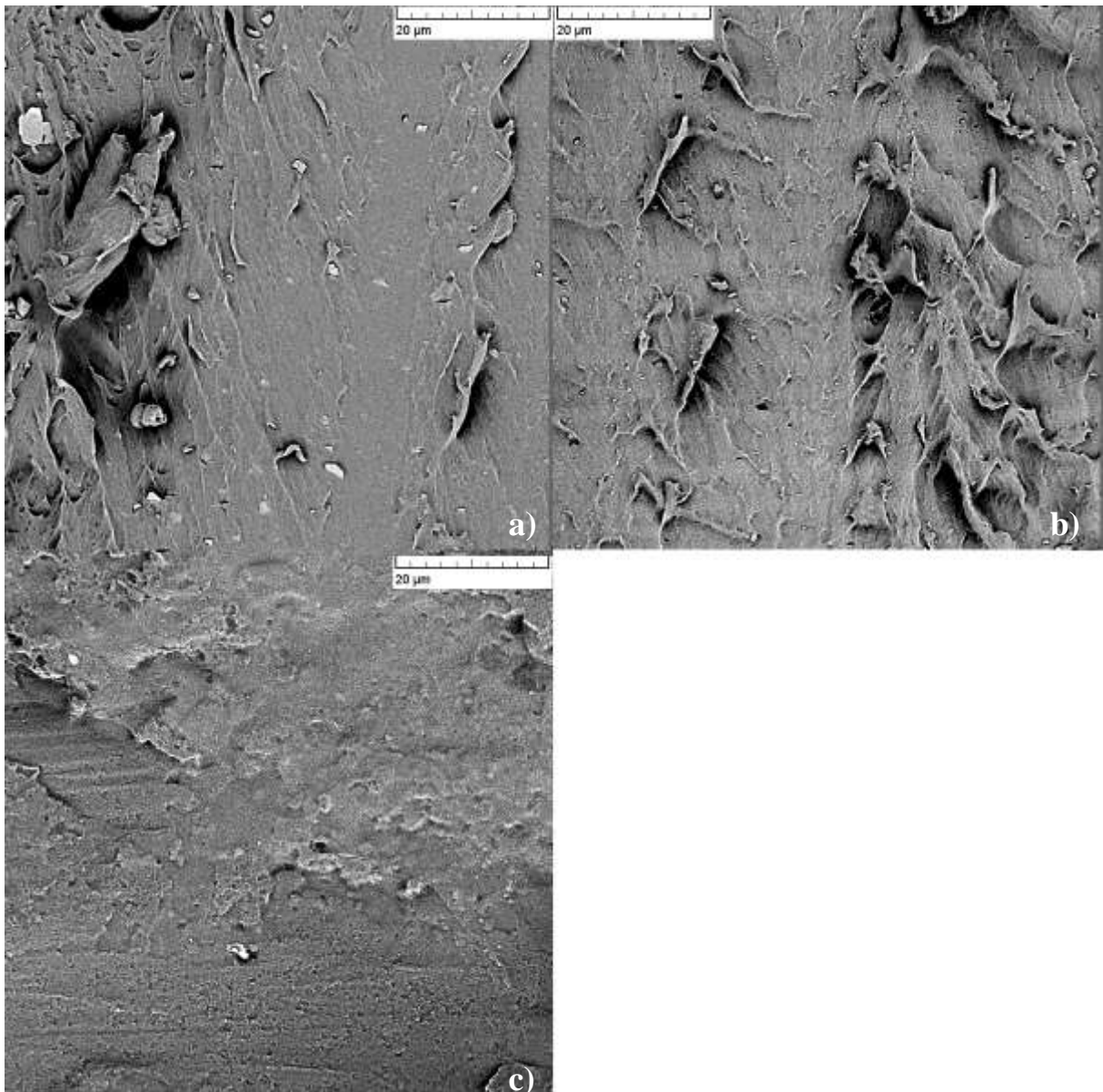


*Fig. 5.34: Detailed study of clay particles in selectively etched polymer composites, a) o-NaVMT, b) o-MMT and c) Cloisite 20A*

### **5.3.4. Transmission electron microscopy**

The detailed dispersion of clay particles in polymer matrix is observed by TEM microscopy. In Figs. 5.35–5.37 clay dispersion in compounds of three various fillers, namely Cloisite 20A, MMT and VMT modified by CTAB is compared. The surface of press moulded sheets and cut across the sheet thickness was scanned for each compound.

In Figure 5.35 a) surface of compound with Cloisite 20A is presented. Its particles are oriented parallel with the sheet surface as a result of melt flow. Agglomerates reached size up to several microns; however larger particles were



also presented. Particle distribution seems to be quite regular (Fig. 5.33 b), layers are intercalated and exfoliation was not observed.

Surlyn® with MMT intercalated by CTAB is presented in Fig. 5.36. As shown from the surface, clay particles are larger in contrast to Cloisite 20A. On the other hand no clay layers were found on the cross section. This fact can be a result of higher filler dispersion, which was also confirmed by SEM.

In the last Fig. 5.37 TEM of organically modified VMT compound are demonstrated. The particles seem to be the largest, indicating high aspect ratio of VMT. Clay layer are clearly seen, however their distribution is rather in contrast to MMT and layers are oriented in more directions.

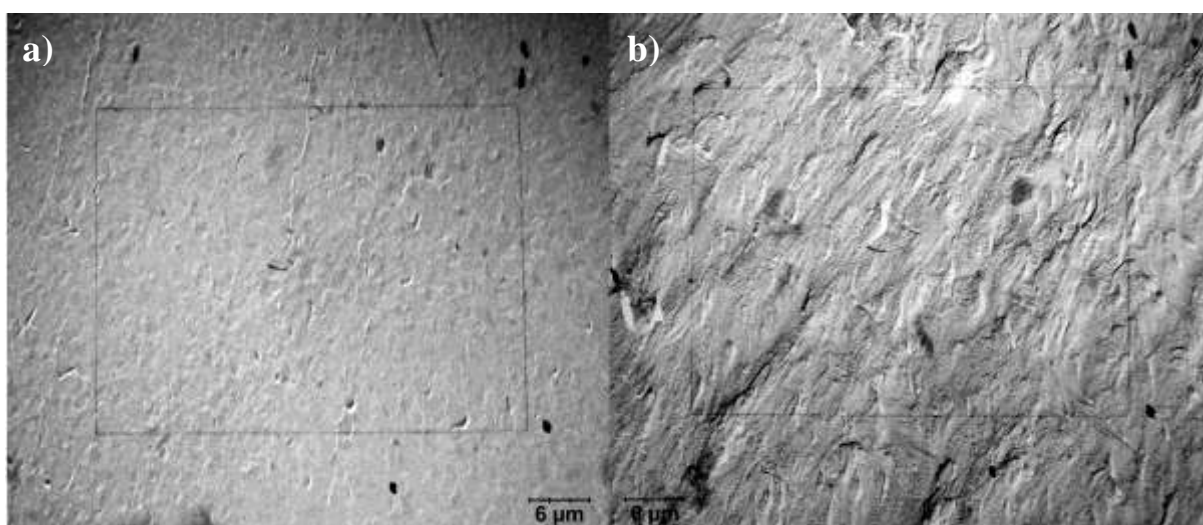


*Fig. 5.35: TEM photos of Surlyn® 9020 compounded with Cloisite 20A, a) surface of press moulded sheet and b) cut across the thickness of the sheet.*

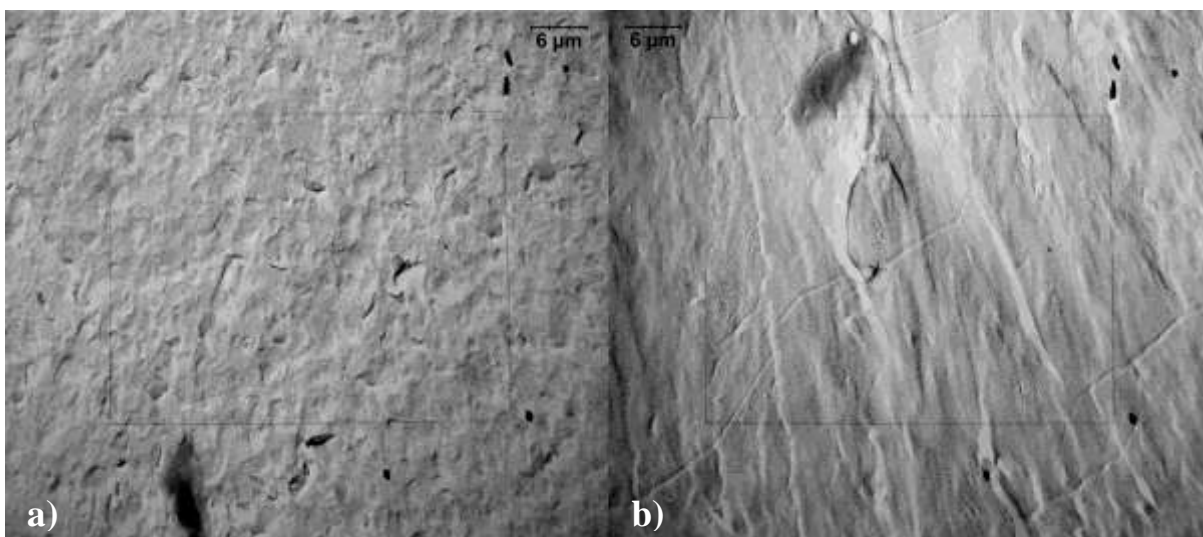


*Fig. 5.36: TEM photos of Surlyn® 9020 compounded with MMT modified by CTAB, a) surface of press moulded sheet and b) cut across the thickness of the sheet.*

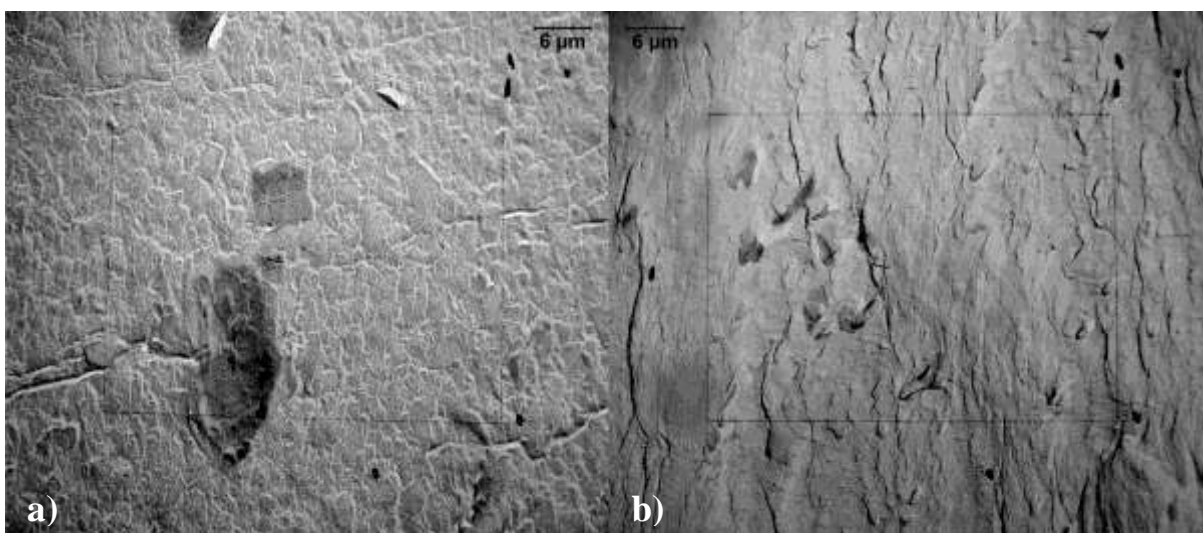


Fig. 5.37: TEM photos of Surlyn® 9020 compounded with VMT modified by CTAB, a) surface of press moulded sheet and b) cut across the thickness of the sheet.

### 5.3.5 Tensile test

Enhancement of mechanical properties of prepared compounds belongs to main goals of presented study. Obviously, compounding conditions and level of filler dispersion in polymer matrix significantly affect the final properties. Tensile properties were tested for both 3 and 5 wt % of filler concentration in polymer matrix. In Tables 5.10 and 5.11, tensile properties for variously filled compounds differing in the amount of clay content are written.

All results are compared to pure Surlyn® 9020 and improvement or downgrade is plotted in Fig. 5.38–5.40.

Table 5.10: Tensile properties for the compounds containing 3 wt % of filler

Compound	<i>E</i> -modulus [MPa]	Tensile stress at yield [MPa]	Tensile stress at break [MPa]	Elongation at break [%]
Surlyn® 9020	220 ± 14	6.8 ± 0.1	26.9 ± 0.6	449 ± 11
Cloisite Na+	264 ± 6	8.2 ± 0.4	26.7 ± 0.9	442 ± 18
Expanded VMT	253 ± 11	7.6 ± 0.3	25.7 ± 0.6	412 ± 10
NaVMT	265 ± 8	7.1 ± 0.3	27.0 ± 0.9	432 ± 13
HClVMT 24	266 ± 10	7.9 ± 0.2	26.6 ± 0.8	421 ± 7
o-HClVMT 7	255 ± 9	7.9 ± 0.2	26.2 ± 1.3	455 ± 5
o-HClVMT 24	270 ± 14	8.1 ± 0.2	28.4 ± 0.9	431 ± 13
o-NaVMT	336 ± 5	9.1 ± 0.3	28.9 ± 0.3	444 ± 14
o-NaMMT	357 ± 1	10.5 ± 0.4	28.2 ± 0.4	426 ± 10
Cloisite 20A	360 ± 17	9.6 ± 0.6	28.1 ± 0.9	445 ± 9

Table 5.11: Tensile properties for the compounds containing 5 wt % of filler

Compound	<i>E</i> -modulus [MPa]	Tensile stress at yield [MPa]	Tensile stress at break [MPa]	Elongation at break [%]
Surlyn® 9020	220 ± 14	6.8 ± 0.1	26.9 ± 0.6	449 ± 11
Cloisite Na <sup>+</sup>	269 ± 7	8.3 ± 0.1	25.9 ± 0.7	438 ± 17
Expanded VMT	267 ± 13	8.6 ± 0.2	28.6 ± 0.3	402 ± 3
NaVMT	282 ± 14	7.4 ± 0.1	27.2 ± 0.9	410 ± 18
HCIVMT 24	293 ± 14	7.7 ± 0.1	29.6 ± 0.4	421 ± 8
o-HCIVMT 7	239 ± 10	7.2 ± 0.3	24.2 ± 0.4	483 ± 5
o-HCIVMT 24	295 ± 6	8.7 ± 0.1	27.2 ± 0.7	415 ± 4
o-NaVMT	408 ± 16	9.3 ± 0.1	27.8 ± 0.6	419 ± 12
o-NaMMT	437 ± 3	12.2 ± 0.3	29.5 ± 0.3	371 ± 20
Cloisite 20A	439 ± 10	9.9 ± 0.1	27.9 ± 0.5	438 ± 17

Pure Surlyn® 9020 gain modulus 220 MPa. Filler addition leads to polymer reinforcement and resulting in higher modulus. It is also dependent on the polymer–filler interaction. This effect is clearly seen in Fig. 5.38. Although, modulus for inorganic fillers rises from 15 to 35 % (in dependence on wt % of filling), modulus of organically modified clays increases nearly 100%.

Compounds with both concentrations of inorganic fillers gain similar modulus level, as well both MA modified VMTs.

Modulus of sample filled by CTAB modified VMT (5 wt. %) reached 408 MPa. Compounds with the same way intercalated MMT gain modulus (437 MPa) similarly as with commercial Cloisite 20A (439 MPa). Modulus of compounds with 3 wt. % of fillers was lower about 35 %. Lower level of o-NaVMT dispersion in matrix (caused by incomplete structure modification) should lead to worse properties of its composites, in comparison with o-MMT composites.

Presence of filler in polymer also affected the yield stress positively. Whereas, sodium and HCl VMT improve modulus more than Cloisite Na<sup>+</sup> and expanded VMT, the effect on yield stress was opposite. The former mentioned samples increase yield stress about 10–15 %, while the later over 20 %. Organically modified HCl VMT influences yield similarly like inorganic filler. The highest yield stress, nearly 80 % (5 wt % of filler), present MMT modified by CTAB (even higher than for commercial clay with 45% accrual).

Break stress strongly depends on the amount of inhomogenities in composite and interaction between clay and polymer. Evidently, samples with inorganic fillers contain more inhomogenities, which is confirmed by break stress decrease (Fig. 5.40). For organically modified fillers, stress at break mainly rises, but only about few percents.

Presence of filler is reflected also in elongation, which decreases for all clay compounds in dependence in filler reinforcing effect.

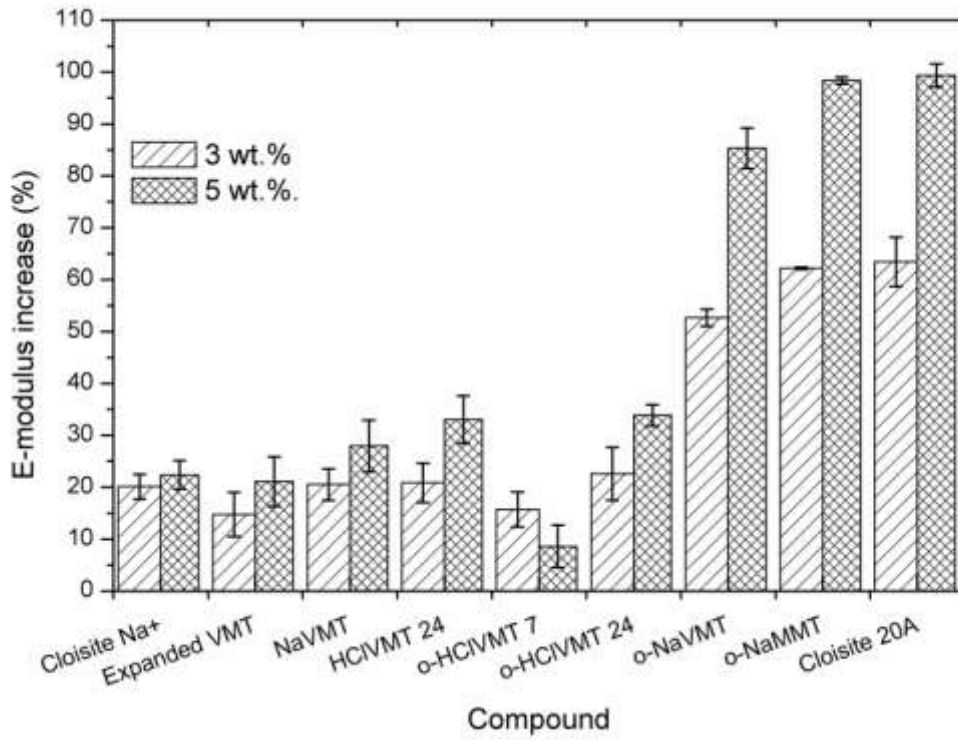


Fig. 5.38: E-modulus increase in comparison to pure Surlyn® 9020 in %.

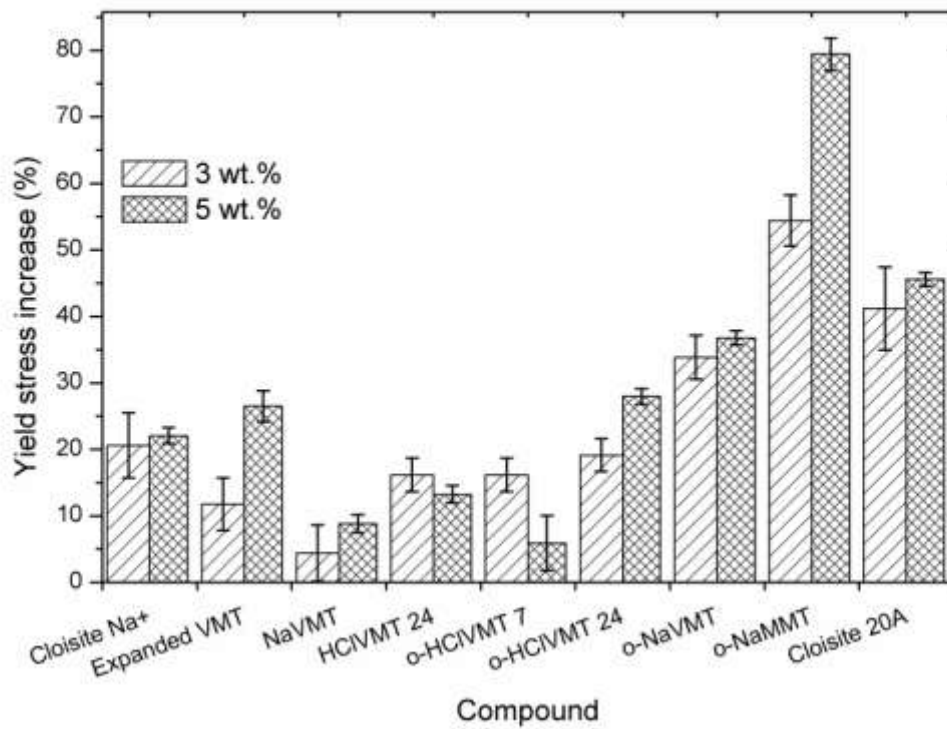


Fig. 5.39: Yield stress increase in comparison to pure Surlyn® 9020 in %.

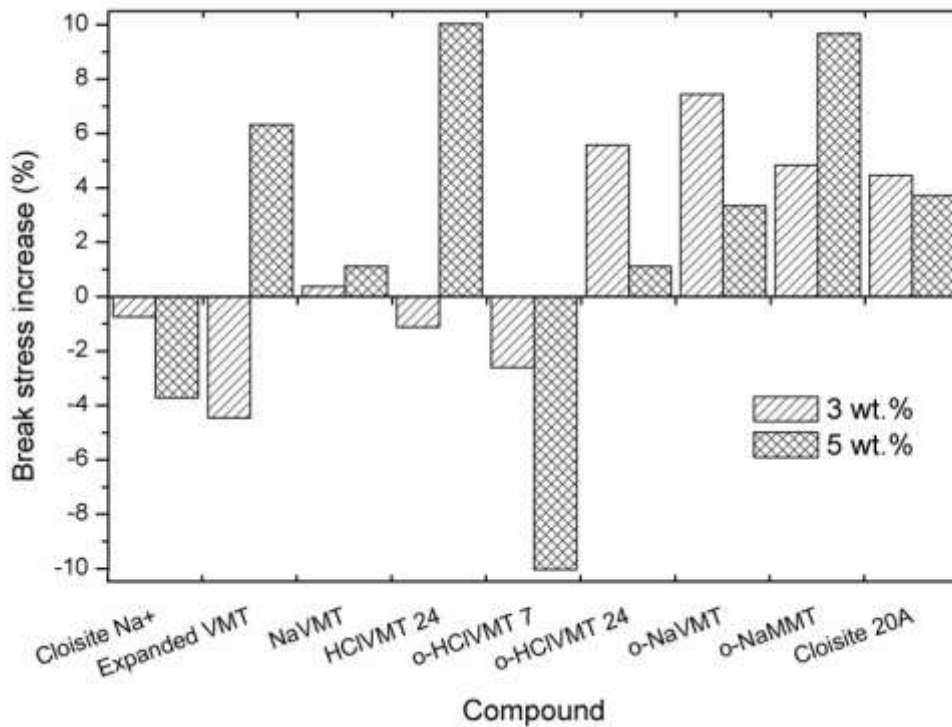


Fig. 5.40: Break stress increase in comparison with pure Surlyn® 9020 in %.

As expected, inorganic fillers improve tensile properties negligible in comparison to pure Surlyn®. However, it should be interesting that milled expanded VMT presents similar mechanical properties as sodium MMT despite the fact of larger particle size ( $25\text{--}40\ \mu\text{m} > 10\ \mu\text{m}$  for Cloisite Na<sup>+</sup>). Moreover, sodium and HCl VMT form increase modulus approximately 10 % more. Organically intercalated fillers markedly improve modulus and yield. Although compounds with sodium VMT presented better properties than with MMT, the same trend was not observed for organic clays, probably because of presence of another ions leading to worse dispersion and lower mechanical properties.

### 5.3.6 Gas permeability

The permeability of gas through a material is a crucial factor affecting lifetime of packages, especially food products. Every polymeric material is permeant for gasses; however, time of permeation depends on the thickness of sample, its density and composition. Surlyn® indicates quite low permeability coefficient in comparison to polyolefins. Generally compounding of layered fillers into polymer structure strongly reduces permeability. Crucially in dependence on the level on filler dispersion level in polymer matrix. When the

aggregates are presented in compound, permeability should be higher than for original polymer.

In this work, permeability was measured according standard CSN 64 0115. Conditions of the test were described in chapter 4.2.7 in details. Samples were press moulded in thickness of 0.2–0.3 mm and contained 5 wt % of the filler.

Test results are given in Table 5.12. Permeability of pure Surlyn® for nitrogen and technical gas was similar  $6.6 \times 10^{-16}$  and  $10.5 \times 10^{-16}$ , and for CO<sub>2</sub> was higher  $85.9 \times 10^{-16}$ . Filler addition into polymer matrix drops the permeability, but not for all fillers. Sodium VMT samples increases permeability in respect to unfilled matrix. On the other hand, expanded VMT as well as sodium MMT reduced permeance up to 20 % for all gasses (see Fig. 5.41). Laboratory prepared organic clays dropped permeability about 20 % and 30 % for o-NaVMT and o-NaMMT, respectively. The highest decline in permeability presents Cloisite 20A (nearly 45 %), which is strong reduction of this property.

Table 5.12: Permeability results for Surlyn® 9020 compounds.

Compounds	Permeability coefficient [ $\times 10^{-16}$ mol/m.s.Pa]		
	N <sub>2</sub>	CO <sub>2</sub>	Gas
Surlyn® 9020	6.57 ± 0.1	85.9 ± 2	10.5 ± 0.3
Cloisite Na+	5.43 ± 0.3	74.1 ± 3	8.88 ± 0.2
Expanded VMT	5.89 ± 0.3	75.4 ± 4	8.81 ± 0.4
NaVMT	7.04 ± 0.4	84.4 ± 5	11.7 ± 0.5
o-NaVMT	5.22 ± 0.2	68.0 ± 3	7.80 ± 0.3
o-NaMMT	4.86 ± 0.1	52.0 ± 2	7.57 ± 0.2
Cloisite 20A	3.68 ± 0.2	48.9 ± 3	5.67 ± 0.3

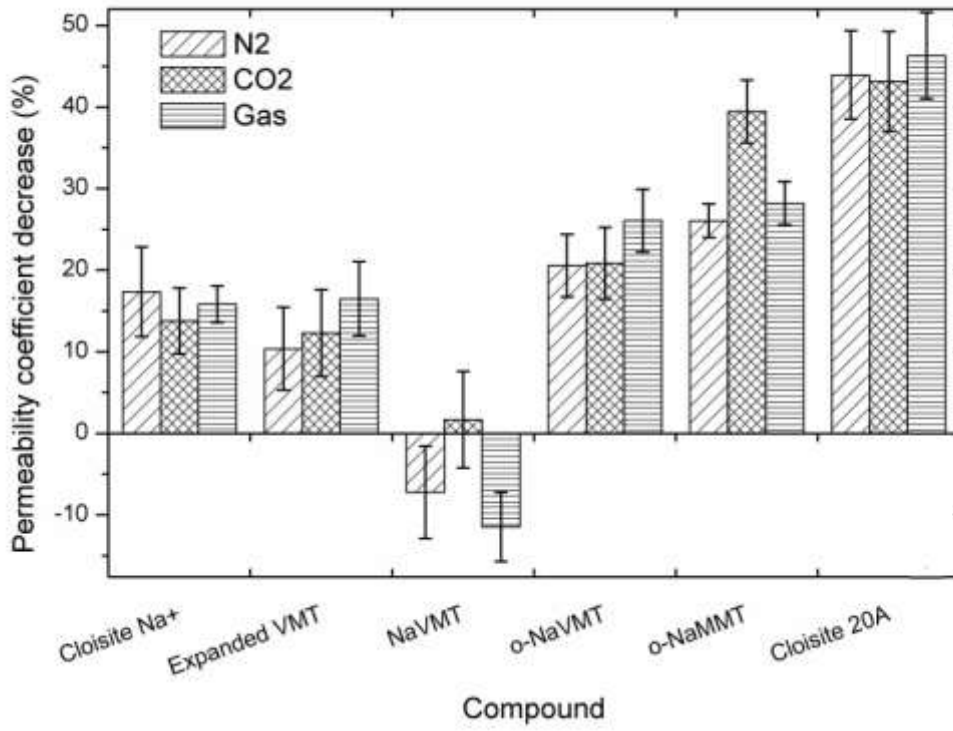


Fig. 5.41: Permeability decrease in %, in comparison to pure polymer Surlyn® 9020.

## 5.4 Ion effect on filler dispersion in matrix

Surlyn® polymers contain wide product grade differing in amount of methacrylic acid, its degree of neutralization and ion used for neutralization. Current data for Surlyn® 9020 do not characterize behaviour of zinc neutralized polymers absolutely, because Surlyn® 9020 is terpolymer and contain three components. To evaluate the effect of modified VMT on properties for only zinc and moreover sodium type of Surlyn®, Surlyn® 9910 and Surlyn® 8920, respectively were compounded. Both contained the same amount of methacrylic acid and were neutralized to the same level. In the following chapter, effect of ion on the resulting properties of composite is compared. As fillers, Cloisite 20A and organically modified sodium VMT – o-NaVMT were employed.

### *Morphology observation*

Firstly, the level of filler intercalation was studied via X-ray diffraction and microscopy. Tensile tests and gas permeability were chosen as suitable for characterization of compounds.

The level of filler exfoliation is compared in Fig. 5.42. Organic VMT presents nonintercalated layers in area of  $8.5^\circ 2\theta$  (1.0 nm) for both polymers. O-NaVMT compounded with Surlyn® 9010 does not exhibit any other significant peak, while in sample with Surlyn® 8920 peaks at  $6.5^\circ 2\theta$ ,  $4.2^\circ 2\theta$  and  $1.9^\circ 2\theta$  (d-spacing 1.3, 2.0 and 4.7 nm) are contained. It corresponds with peaks of used filler. Thus, organic VMT particles which were successfully organophilized by CTAB are better dispersed or exfoliated in zinc based matrix.

In the case of Cloisite 20A, higher level of exfoliation was achieved for sodium matrix with small peak at  $6.0^\circ 2\theta$  typical for sodium MMT. On the other hand, zinc matrix presents significant peaks at  $2.6^\circ 2\theta$  (3.4 nm, intercalated layers) and  $5.6^\circ 2\theta$  (sodium ion contained in interlayer). Both peaks are shifted to higher interlayer distances in comparison with Cloisite 20A. According XRD MMT was more exfoliated in sodium type of Surlyn®.



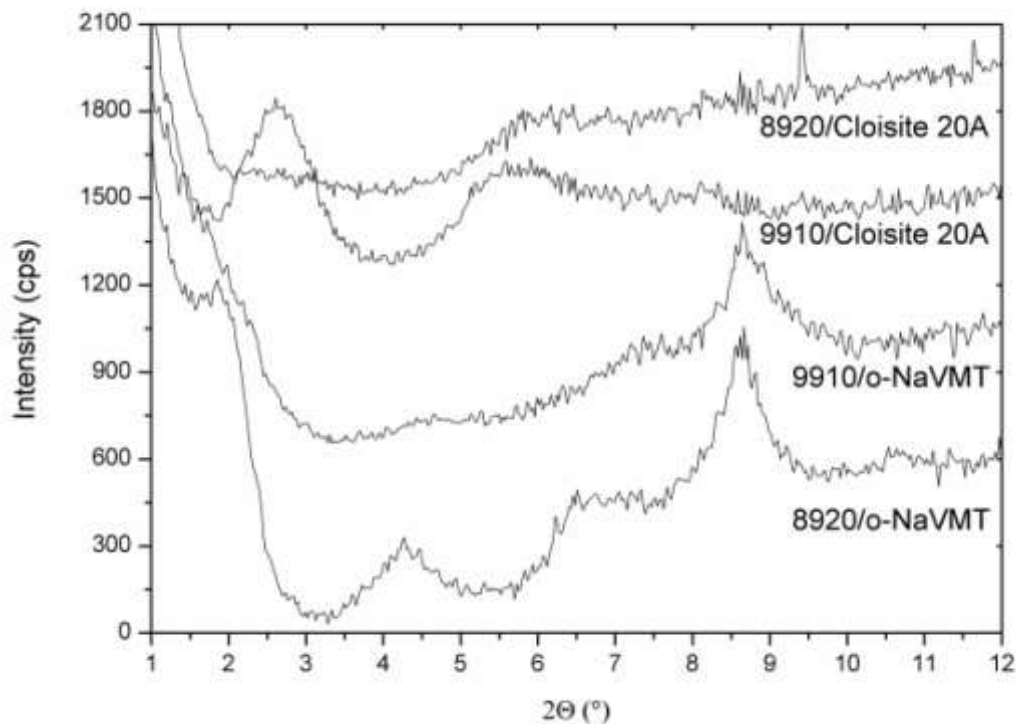
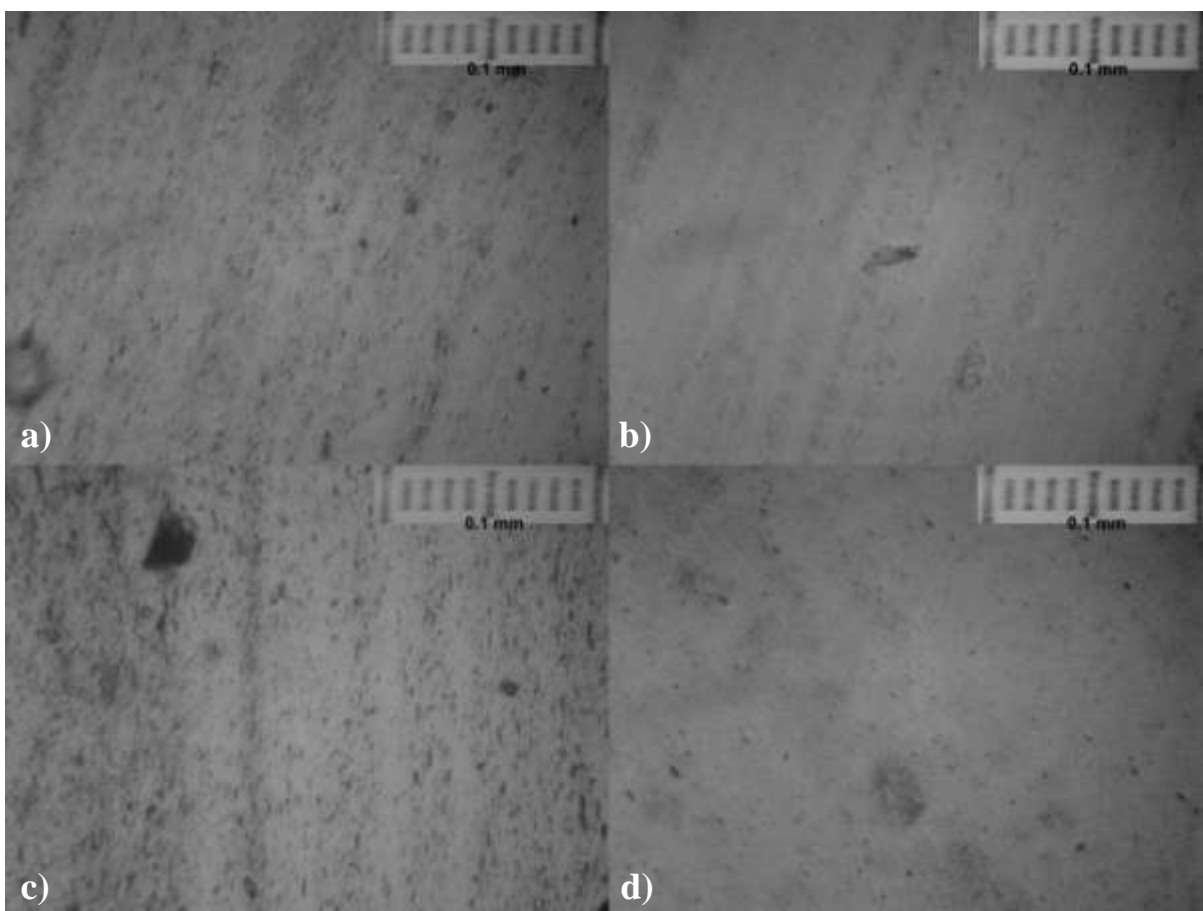


Fig. 5.42: X-ray diffraction spectra of zinc and sodium Surlyn® filled by *o*-NaVMT and Cloisite 20A.

X-ray diffraction also shows higher exfoliation of VMT in zinc neutralized ionomer, while MMT in sodium ionomer. Level of filler dispersion by optical microscopy is compared in Fig. 5.43. Figures a) and c) compare organic VMT in various matrixes. Majority of particles in Surlyn® 9910 are in dimension around 5  $\mu\text{m}$  but larger are also included (10 or 15  $\mu\text{m}$ ). Less often are particles up to 40  $\mu\text{m}$  in diameter. It looks similarly for Surlyn® 8920 however contained particles seem to be slightly larger than in case of zinc Surlyn®. The same trend should be observed for filler Cloisite 20A although XRD results indicate opposite trend. The amount of particles visible on pictures is lower than in case of VMT and their dimensions are mostly up to 5  $\mu\text{m}$ . The presence of bigger particles (up to 20  $\mu\text{m}$ ) is rather rare case and indicates poorer compounding.



*Fig. 5.43: Optical microscopy (first approach to morphology) of zinc and sodium ionomer compounds. Surlyn® 9910 filled by a) o-NaVMT, b) Cloisite 20A and Surlyn® 8920 compounded with c) o-NaVM and d) Cloisite 20A.*

SEM pictures confirmed the previous results obtained from optical microscopy (Fig. 5.44). In case of VMT filled polymers, particles up to 25 microns are presented, similarly to Surlyn® 9020. However, the compatibility of organically modified VMT with Surlyn® 8920 is lower. Missing clay particles in the structure indicate imperfect adhesion.

The particle content in both Surlyn® composites with Cloisite 20A is low. More aggregates seem to be in sodium ionomer, although XRD pattern do not exhibit any marked peaks. As a result from SEM, zinc based ionomer have higher compatibility to clay particles, reflecting in better dispersion.

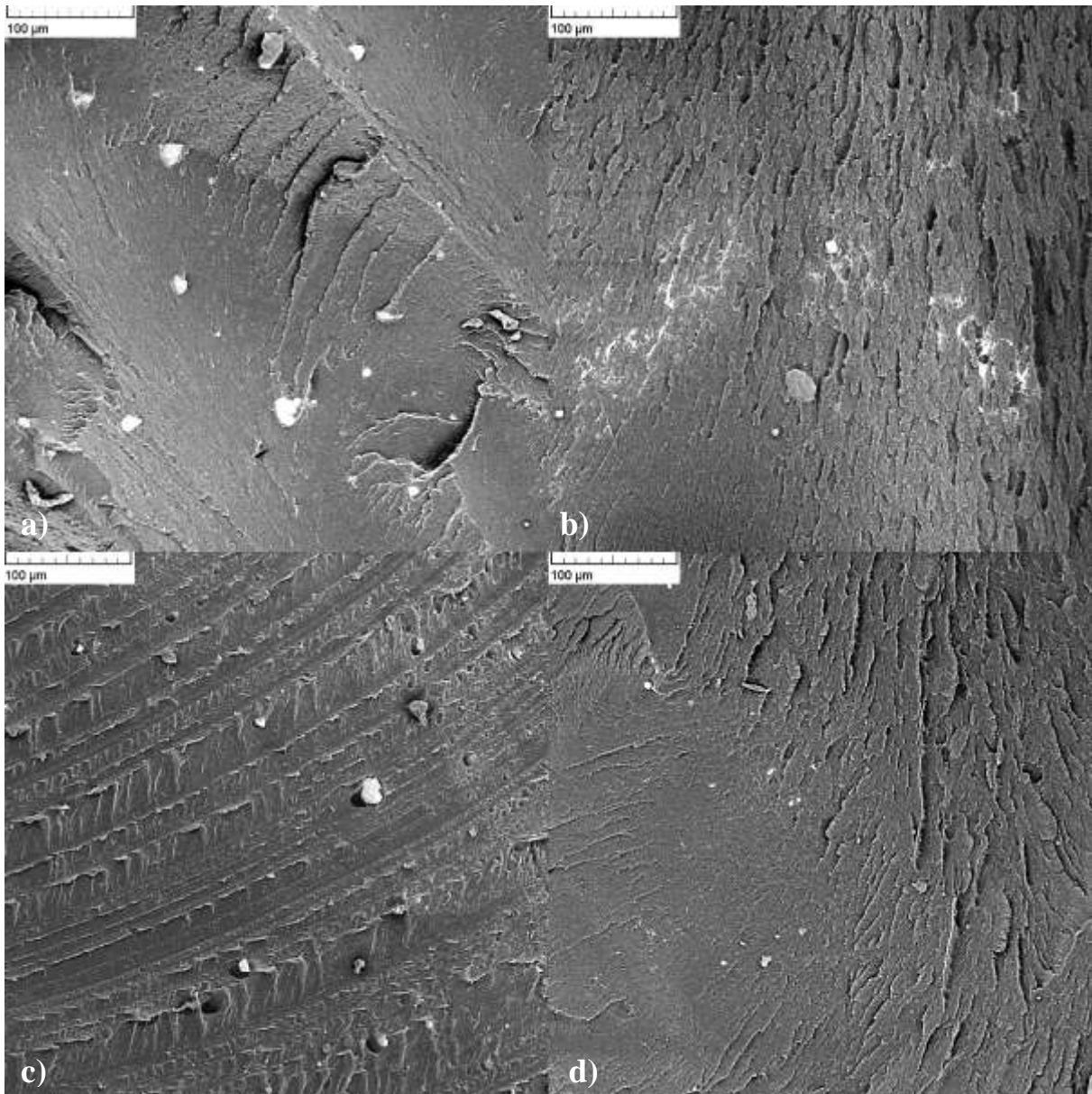


*Fig. 5.44: SEM pictures of Surlyn® 9910 filled by a) o-NaVMT and b) Cloisite 20A and Surlyn® 8920 filled by c) o-NaVMT and d) Cloisite 20A*

### ***Tensile properties***

The effect of various ions on the composites behaviour was also investigated by mechanical tests. The results of tensile properties are given in Tables 5.13 and 5.14 for Surlyn® 8920 and Surlyn® 9910, respectively. Evidently, Surlyn® 8920 presents higher E modulus (about 100 MPa) than Surlyn® 9910.

It is known, that the higher modulus of polymer is, the lower modulus improvement can be reached [98, 99]. This work will suppose that difference of 100 MPa is not so high and the results are comparable. The filler amount (3 and 5 wt %) was compared similarly to Surlyn® 9020, again.

Table 5.13: Tensile properties of Surlyn® 8920

Compound	<i>E</i> -Modulus [MPa]	Tensile stress at yield [MPa]	Tensile stress at break [MPa]	Elongation at break [%]
<b>Weight content of filler 3 %</b>				
Surlyn® 8920	654 ± 31	17.3 ± 0.2	34.7 ± 0.8	493 ± 13
Cloisite Na+	686 ± 11	16.3 ± 0.1	30.2 ± 2.5	456 ± 34
NaVMT	673 ± 20	14.9 ± 0.2	32.7 ± 2.0	497 ± 45
o-NaVMT	741 ± 17	14.7 ± 0.3	33.2 ± 1.6	519 ± 40
Cloisite 20A	841 ± 16	17.5 ± 0.3	27.6 ± 1.7	422 ± 24
<b>Weight content of filler 5 %</b>				
Cloisite Na+	746 ± 9	16.6 ± 0.2	29.8 ± 2.5	449 ± 29
NaVMT	751 ± 26	14.8 ± 0.1	29.4 ± 1.8	452 ± 24
o-NaVMT	769 ± 17	14.7 ± 0.2	30.3 ± 1.2	502 ± 22
Cloisite 20A	1025 ± 45	18.4 ± 0.5	28.2 ± 2.0	443 ± 35

Table 5.14: Tensile properties of Surlyn® 9910

Compound	<i>E</i> -modulus [MPa]	Tensile stress at yield [MPa]	Tensile stress at break [MPa]	Elongation at break [%]
<b>Weight content of filler 3 %</b>				
Surlyn® 9910	557 ± 25	15.7 ± 0.1	32.5 ± 0.4	467 ± 14
Cloisite Na+	654 ± 10	16.4 ± 0.5	29.3 ± 0.6	458 ± 12
NaVMT	630 ± 19	14.1 ± 0.2	30.5 ± 2.3	450 ± 36
o-NaVMT	677 ± 14	14.6 ± 0.2	32.8 ± 1.6	479 ± 24
Cloisite 20A	841 ± 16	17.9 ± 0.3	27.7 ± 2.1	426 ± 32
<b>Weight content of filler 5 %</b>				
Cloisite Na+	665 ± 23	16.8 ± 0.2	28.8 ± 1.3	444 ± 18
NaVMT	678 ± 19	14.4 ± 0.2	31.3 ± 1.7	462 ± 16
o-NaVMT	767 ± 25	15.0 ± 0.5	32.4 ± 0.6	489 ± 6
Cloisite 20A	961 ± 21	18.7 ± 0.4	28.2 ± 2.1	430 ± 42

*E*-modulus changes are given in Fig 5.45. Addition of 3 wt % of inorganic filler is reflected in significant variation for both polymers. *E*-modulus of sodium polymer increases approximately up to 5 %, for zinc one up to 15 % for Cloisite Na<sup>+</sup> and NaVMT. At higher clay content, differences between both polymers are negligible. When organic fillers were used, the modulus grows markedly mainly, for Cloisite 20A. Better properties of MMT compounds, depends on MMT higher dispersion level in the matrix. *E*-modulus of both fillers Cloisite 20A and o-NaVMT raises more for Surlyn® 9910. It seems, that presence of zinc ions have more positive effect on the modulus than sodium ones.

Clay presence in polymer matrix decreases yield stress for all fillers expect of Cloisite 20A (Fig.5.46). Both yield stress and stress at break are reduced more for sodium type of polymer.

Although, Surlyn® 8920 and Surlyn® 9910 contain the same amount of methacrylic acid and are neutralized to the same level, they exhibit different properties with fillers caused by presence of various ions. Unfilled sodium polymer reach higher tensile modulus than zinc one, however, addition of organic clay to matrix increases modulus of zinc ionomer to the same level. When the improvement is compared in percentages, zinc polymer achieves better properties. Similar results for another pair of zinc and sodium ionomer was obtained by Shah and Paul [28].

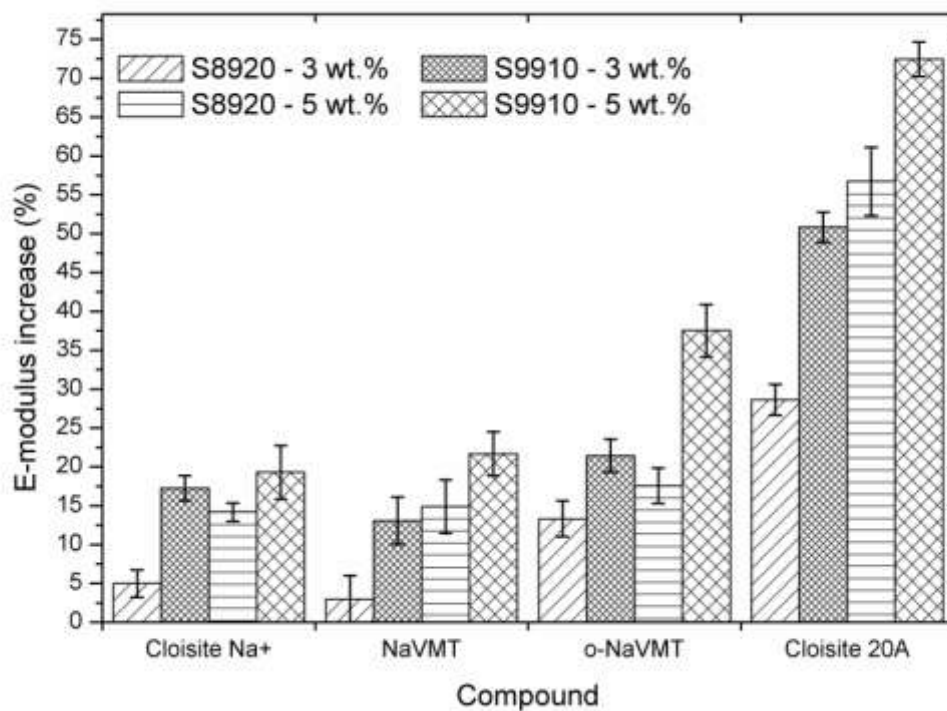


Fig. 5.45: Effect of filler addition on the E-modulus of Surlyn® 8920 and Surlyn® 9910

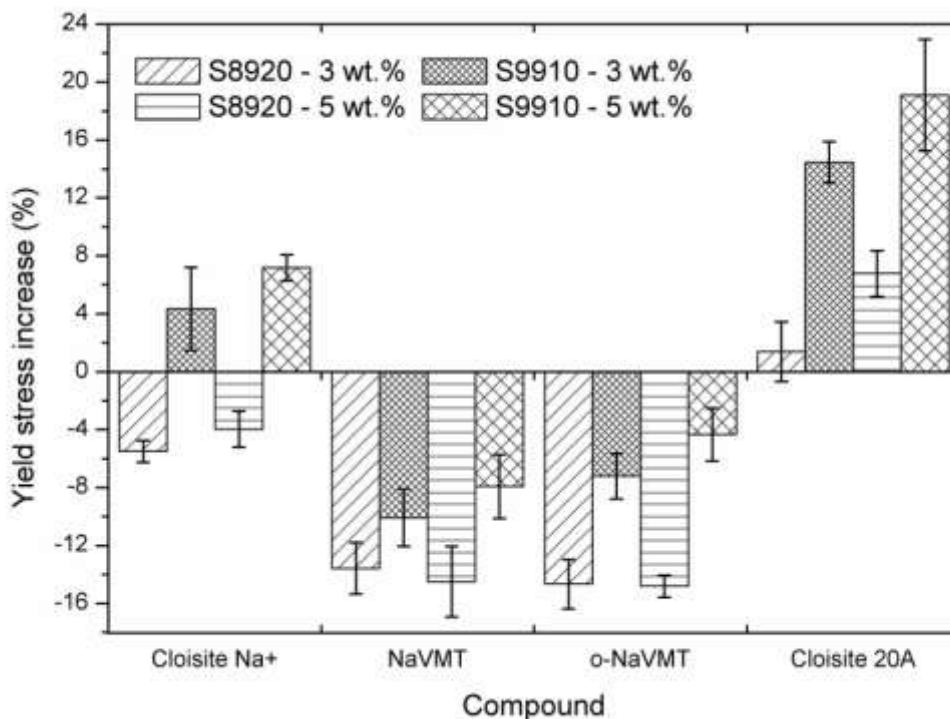


Fig. 5.46: Effect of filler addition on the yield stress of Surlyn® 8920 and Surlyn® 9910

During the tensile measurement of Surlyn® compounds, interesting phenomenon appeared. Samples were tested three days and one month after press moulding and significant changes of  $E$ -modulus were pointed out (Table 5.15).  $E$ -modulus of pure matrixes after one month increases about 25 % and 40 % for sodium and zinc Surlyn®, respectively. Similarly  $E$ -modulus grows for their compounds. As a result,  $E$ -modules for both pure polymers and their compounds reached comparable values. Similar trend was found out for Surlyn® 9020 as well.

These changes of  $E$ -modulus can be connected with the ion aggregate evolution, whose presence in ionomer structure was recorded in several papers [100–102]. Unfortunately, the effect of time dependency on mechanical properties was not studied in details so far. However, this dependence seems to be very interesting and its study is going to continue.

Table 5.15: Time dependence of *E*-modulus for samples filled by 5 wt %.

Compound	<i>E</i> -modulus [MPa]		<i>E</i> -modulus [MPa]	
	Surlyn® 8920		Surlyn® 9910	
	3 days	30 days	3 days	30 days
Pure matrix	654 ± 31	824 ± 10	558 ± 26	819 ± 19
Cloisite Na+	747 ± 9	848 ± 12	666 ± 23	951 ± 16
Cloisite 20A	1025 ± 45	1226 ± 28	962 ± 21	1259 ± 28

### *Gas permeability*

Permeability measurement also belongs to suitable procedure comparing ion effect on behaviour of filled samples. Permeability of both pure ionomers is similar for all gasses. Fillers insertion to the matrixes decreases permeance for all gasses (Table 5.16 and Fig.5.47). The most significant permeability decrease is for both sodium and zinc compounds with Cloisite 20A, 35 % (N<sub>2</sub>), 45 % (CO<sub>2</sub>) and 30–40 % (Technical gas). Comparable decrease to Cloisite is achieved for organic VMT in sodium Surlyn®. Except Cloisite 20A, stronger permeability decrease (from 10–20 %) was gained for sodium composites, although SEM microscopy showed the presence of bigger agglomerates in Surlyn® 8920.

Table 5.16: Permeability coefficient for Surlyn® 8920 and Surlyn® 9910 and their compounds with 5 wt % of fillers.

Compound	Surlyn® 8920			Surlyn® 9910		
	Permeability coefficient [ $\times 10^{-16}$ mol/m.s.Pa]					
	N <sub>2</sub>	CO <sub>2</sub>	Gas	N <sub>2</sub>	CO <sub>2</sub>	Gas
Pure	5.23±0.2	55.8±2	7.27±0.3	4.48±0.1	57.7±2	7.34±0.3
Cloisite Na+	4.27±0.3	49.9±3	6.51±0.3	4.30±0.2	53.0±1	6.21±0.2
NaVMT	3.76±0.3	40.9±5	5.83±0.4	3.92±0.1	47.6±3	6.32±0.1
o-NaVMT	3.50±0.2	29.9±2	5.27±0.3	3.65±0.2	40.6±3	5.60±0.2
Cloisite 20A	3.40±0.3	33.1±1	5.12±0.1	2.98±0.2	32.3±2	4.07±0.2

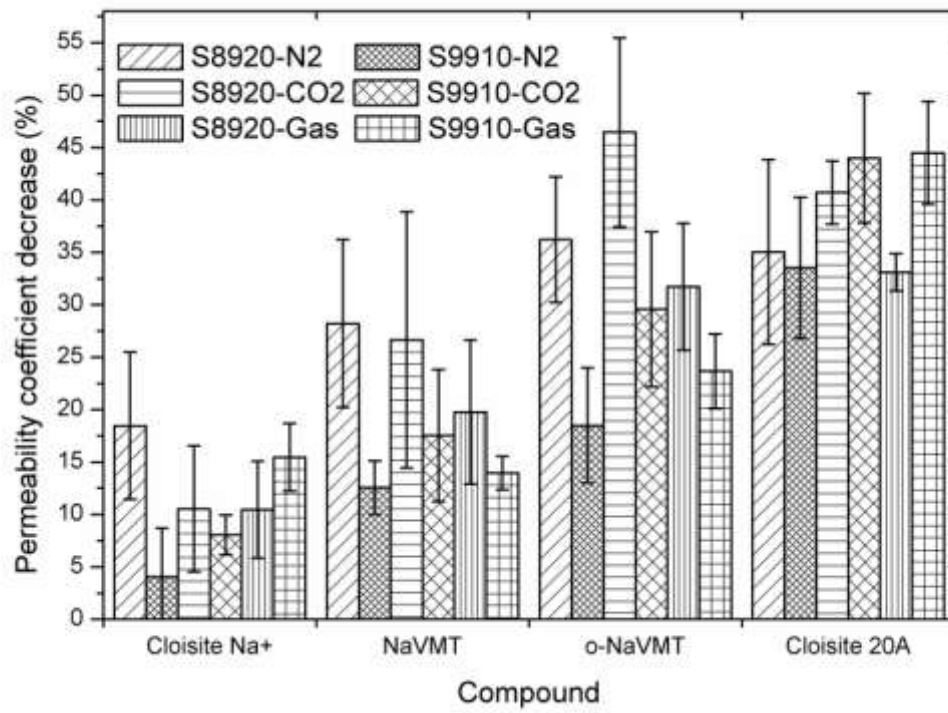


Fig. 5.47: Permeability decrease in % for Cloisite 20A compounded with Surlyn® 9910 and Surlyn® 8920.



## 5.5 Effect of degree of MAA group neutralization on resulting polymer/clay properties

As already mentioned Surlyn® is produced in various grades differing in MAA content and neutralization level. The influence of both factors on final properties of selected types of Surlyn® (Fig. 5.48) was carried out. Cloisite 20A was employed in amount of 5 wt % for this purpose (MMT based filler).

Testing compounds of clay with Surlyn® 9020, Surlyn® 9910 and Surlyn® 8920 were prepared as described in chapter 5.2.3 and the compounds of Surlyn® 1605, Surlyn® 1705 and Surlyn® 9721 were prepared by compounding in twin screw extruder (chapter 5.2.1). Nevertheless, the level of filler dispersion is for both methods comparable.

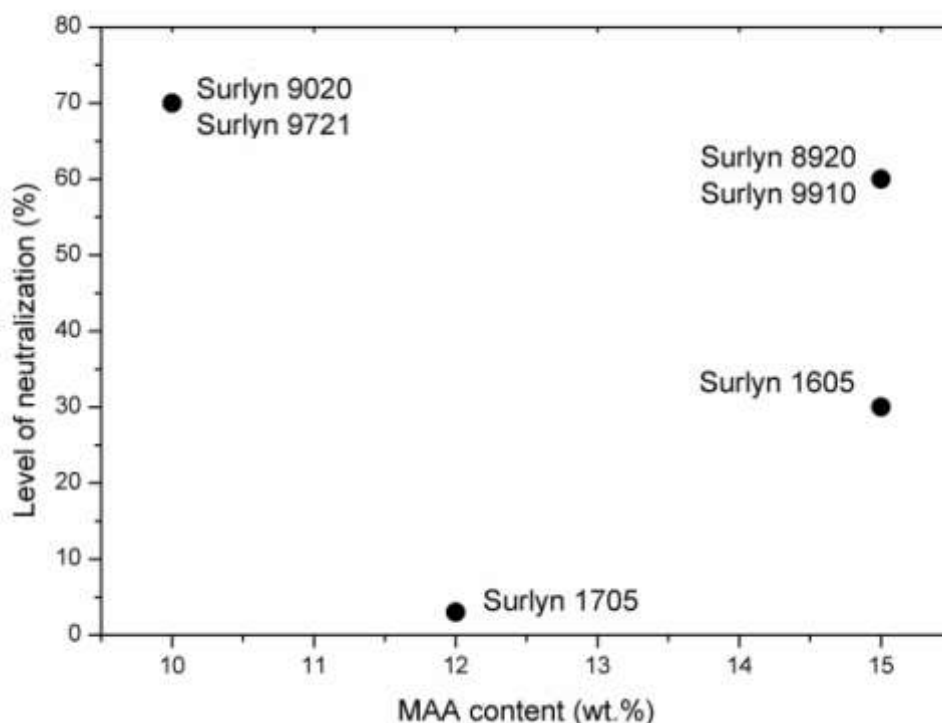
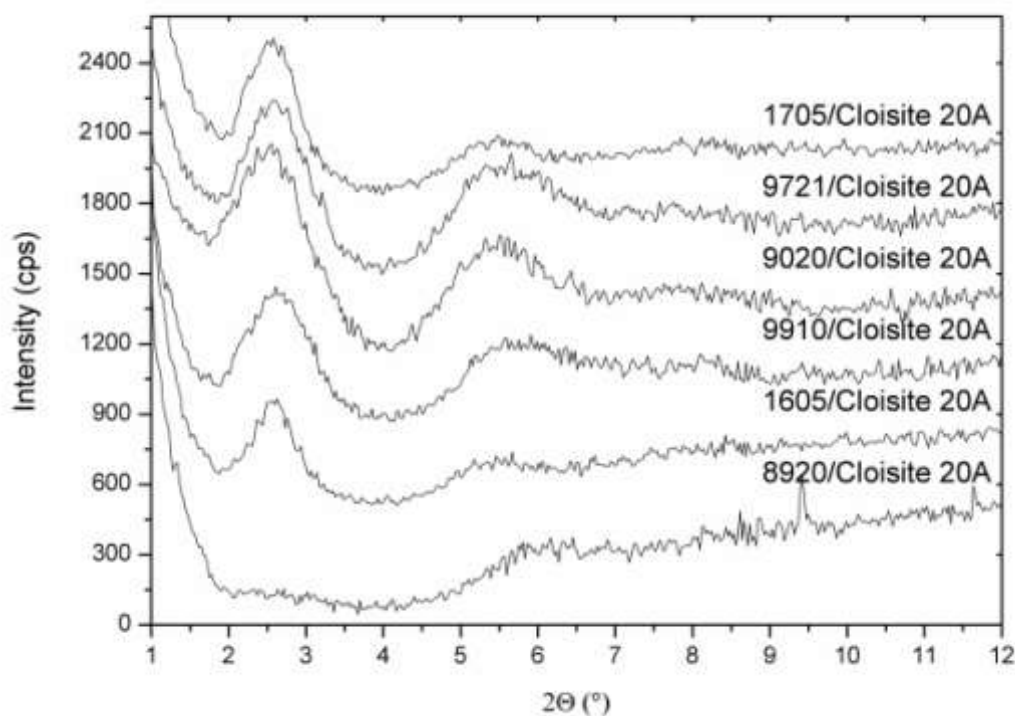


Fig. 5.48: Classification of Surlyn® in dependence on MAA content and level of its neutralization.

To compare the level of filler dispersion in matrix, XRD and microscopy were employed. The level of filler intercalation in various types of matrixes is compared in Fig. 5.49. Sodium based Surlyn® 8920 does not exhibit any typical peak for MMT. Surlyn® 1605 presents also low peak intensity ( $d$ -spacing 3.42 nm) in comparison with zinc polymers. Supposedly, higher amount of neutralized acid groups slightly reduce the interlayer distance for zinc based matrixes. Another types of Surlyn®, namely Surlyn® 1705, Surlyn® 9910 and Surlyn® 9721 presents  $d$ -spacing 3.46 nm, 3.40 nm 3.38 nm,

respectively. The interlayer distance for Surlyn® 9020 is 3.49 and does not support this theory; however, it contains the third comonomer which can influence its behaviour.



*Fig. 5.49: Diffraction patterns of Surlyn® compounds with MMT based filler Cloisite 20A.*

Dispersion level of Cloisite 20A in various matrixes by optical microscopy was compared in Fig. 5.50. Surlyn® 1605 contain particles with dimension in order of tens of microns (Fig. 5.50 a), while Surlyn® 8920 particles are smaller up to 5  $\mu\text{m}$  (Fig. 5.50 b). Bigger aggregates contain also Surlyn® 1705 (Fig. 5.50 d), which was as well as 1605 prepared on twin screw extruder. On the other hand, Surlyn® 9721 (Fig. 5.50 e) was compounded on extruder too, and larger particles are not included. The reason should be the lower level of MAA group neutralization of Surlyn® 1605 and 1705. The theory of the higher filler dispersion in more neutralized polymers is also supported by the presence of small filler aggregates in Surlyn® 9910 (Fig. 5.50 f). Theory is not confirmed by Surlyn® 9020 (Fig. 5.50 c), which is highly neutralized, but contain larger particles. The reason is probably caused by the presence of the third comonomer in its structure.

More detailed study is in Fig. 5.51, where the SEM pictures of etched surface are visualised. As a result of SEM microscopy, the theory about better filler dispersion in more neutralized polymers is supported.

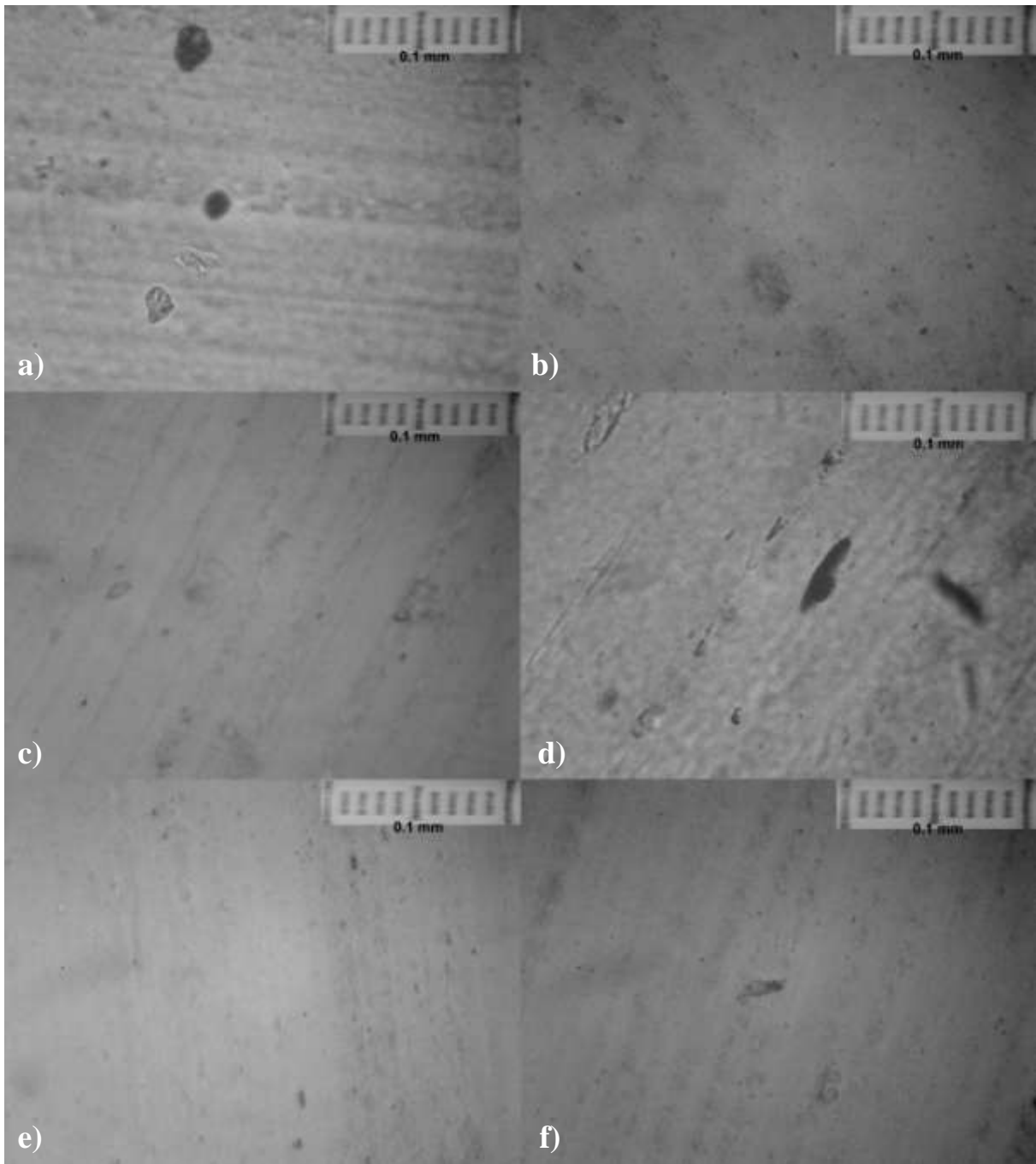


*Fig. 5.50: Microscopy of Cloisite 20A compounds with a) Surlyn® 1605, b) Surlyn® 8920, c) Surlyn® 9020, d) Surlyn® 1705, e) Surlyn® 9721 and f) Surlyn® 9910.*

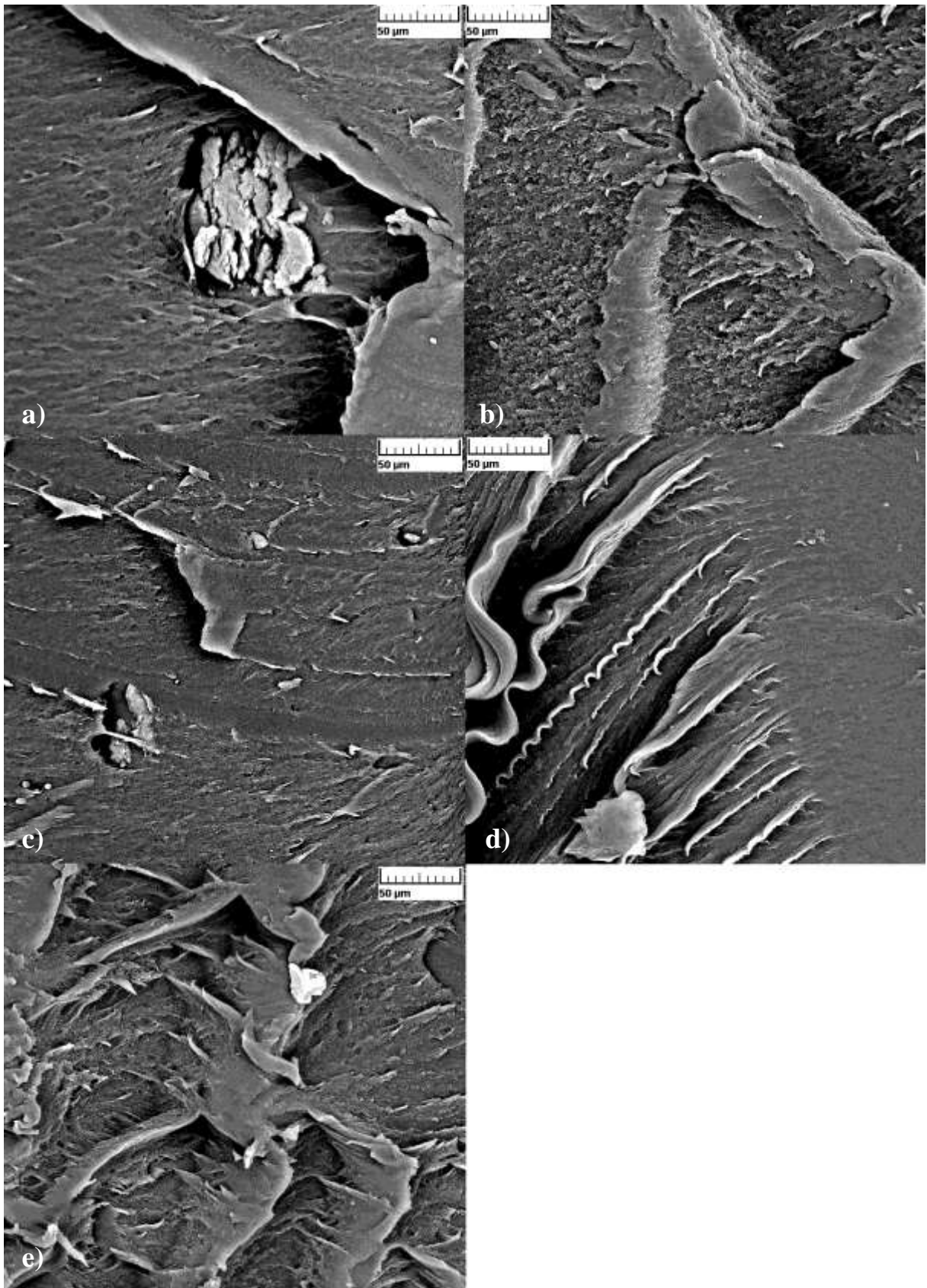


*Fig. 5.51: SEM photos of selectively etched compounds with Cloisite 20A in a) Surlyn® 1605, b) Surlyn® 8920, c) Surlyn® 1705, d) Surlyn® 9721 and e) Surlyn® 9910.*

The tensile modulus for pure matrix and compound with Cloisite 20A are presented in Table 5.17. Evidently, modulus depends on the amount of MAA and its neutralization level. Tensile properties increase with the amount of MAA or neutralization level, what was confirmed by current results; however, presence of the third comonomer supposedly decline mechanical properties. Compounding with filler improves the properties in tens of percent as shown in Fig. 5.52. Improvement is related to pure matrix of each compound. Clearly, if the acid group neutralization decreases, relative modulus increases only about 35 %, what contrast to other ones (60 %). Difference in modulus by the presence of various ions was pointed out. Nevertheless, modulus is markedly influenced by the presence of third comonomer as pointed before. Then, the modulus increases twofold compared with pure matrix, although the microscopy showed imperfectly dispersed particles.

Table 5.17: Modulus of pure polymer and filled by Cloisite 20A

<b>Polymer matrix</b>	<b><i>E</i>-modulus [MPa]</b>	
	<b>Pure polymer</b>	<b>Cloisite 20A</b>
Surlyn® 1705	391 ± 21	535 ± 24
Surlyn® 1605	287 ± 17	380 ± 25
Surlyn® 8920	654 ± 31	1025 ± 45
Surlyn® 9910	558 ± 26	962 ± 21
Surlyn® 9721	629 ± 30	1025 ± 20
Surlyn® 9020	220 ± 14	439 ± 10

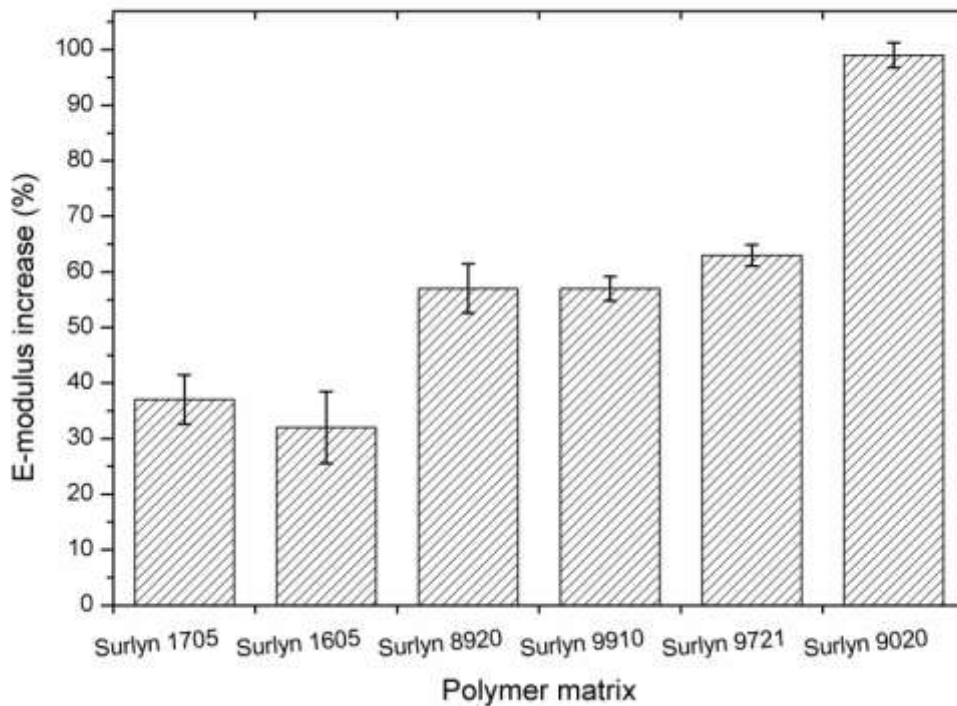


*Fig. 5.52: Modulus improvement of Surlyn® compounds with Cloisite 20A.*

Similar to tensile properties, the effect of MAA content and neutralization can be evaluated from gas permeability and results of gas permeability for nitrogen, carbon dioxide and technical gas for all tested polymers and their compounds with Cloisite 20A are shown in Table 5.18 and Fig. 5.53. Generally, unfilled zinc polymers present lower permeability than sodium ionomers, mainly for nitrogen. The lowest values of permeability showed the less neutralized polymer Surlyn® 1705. It seems that gas diffusion is faster with higher level of neutralization. On the other hand, presence of third comonomer dramatically increases the permeability. Nevertheless as can be found in graph the worse permeability was, the lower permeability of filled sample was achieved.

Table 5.18: Permeability coefficient of unfilled and filled Surlyn® compounds.

Polymer	Permeability coefficient [ $\times 10^{-16}$ mol/m.s.Pa]					
	N <sub>2</sub>		CO <sub>2</sub>		Gas	
	Pure	Cloisite 20A	Pure	Cloisite 20A	Pure	Cloisite 20A
Surlyn 1705	3.85±0.1	3.51±0.1	45.5±1	33.7±2	5.84±0.2	5.45±0.2
Surlyn 1605	5.13±0.3	3.32±0.2	63.6±1	43.2±2	7.48±0.2	4.96±0.2
Surlyn 8920	5.23±0.2	3.40±0.3	55.8±2	33.1±1	7.27±0.3	5.06±0.1
Surlyn 9910	4.48±0.1	2.98±0.2	57.7±2	32.3±2	7.34±0.3	4.07±0.2
Surlyn 9721	4.71±0.2	3.13±0.3	50.3±3	37.1±2	6.94±0.2	5.00±0.2
Surlyn 9020	6.57±0.1	3.68±0.2	85.9±2	48.8±3	10.6±0.3	5.66±0.3

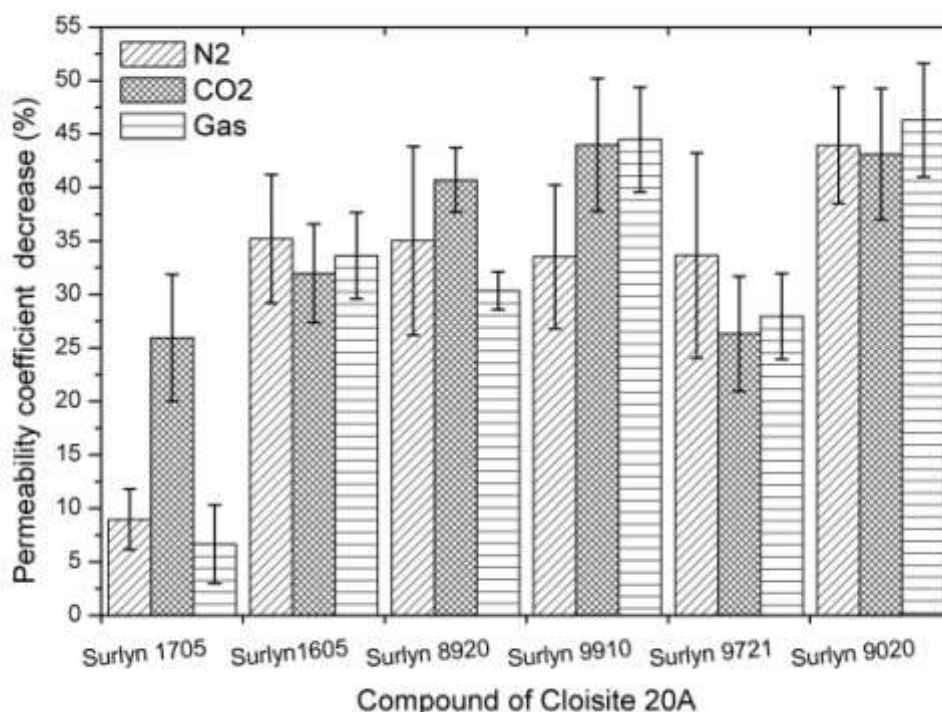


Fig. 5.53: Comparison of permeability decrease in % of filled compounds.

Evidently, the modulus with increasing neutralization was raising and gas permeability decreased. In presented study was in more details studied Zn<sup>2+</sup> neutralized polymer. However, similar results were obtained for sodium neutralized ones in study of Cui et al. [103]. The opposite tendency was observed for the content of MAA in ionomer when the Surlyn® 9721 and 9910 were compared. Lower methacrylic acid amount in composite is reflected in higher modulus increase; on the other hand, the permeability was decline.

## CONCLUSION

In the theoretical part of the presented thesis, the poly (ethylene-co-methacrylic acid) copolymer is introduced and its behaviour is discussed. Furthermore, inorganic fillers, mainly layered clays, are summarized and their ability to modify polymer matrix is studied.

Following experimental part deals with the clay based fillers, which were modified by several methods and consequently examined. Moreover, these fillers were subsequently compounded with polymer matrix, and their effect on final properties of the compound was investigated.

Clay fillers employed for the purpose were vermiculite (VMT) and montmorillonite (MMT), from silicate group. Both types contain layered structure which consists on octahedral and tetrahedral sheets where the individual layers are separated by exchangeable cations. These cations can be replaced by organics which increase interlayer distance and improve clay compatibility to polymer matrix. MMT contains one type of cation in the structure, while VMT interlayer was created by several ions, which had to be uniformed by NaCl or treated by acid (HCl). Dependence on solution concentration, temperature and time was pointed out. The amount of Na<sup>+</sup> ions in VMT structure rises with higher NaCl concentration in solution and enhanced temperature. The most positive effect was caused by repeated stirring in renewed solution. When VMT was hydrated by HCl, its structure was partially or fully delaminated with higher temperature and time of reaction. VMT samples which indicate the highest level of saturation and MMT were consequently modified with organic modifier cetyltrimethylammonium bromide (CTAB) and VMT treated by HCl by maleic anhydride (MA). Various concentrations of VMT : CTAB were again employed. Prepared fillers were tested by X-ray diffraction to obtain interlayer distance and TGA for the detection of organic content amount. Both fillers indicate increasing of interlayer distance; however, VMT was not fully modified because of incomplete exchange of ions in the structure.

Modified fillers and commercials Cloisite 20A were compounded with Surlyn®, commercially available copolymer of ethylene and methacrylic acid (MAA) which acid groups are partially neutralized by metal ions. Used matrixes differed in amount of methacrylic acid, neutralization level and also by type of neutralizing ions (sodium or zinc). In dependence on Surlyn® composition following behaviour was studied: comparison of laboratory modified fillers with commercial one, influence of the neutralizing ion (sodium or zinc) and neutralization level of MAA on the final composite properties.

Firstly, the effect of various filler compounded with Surlyn® 9020 on the resulting properties was studied. The modification method played an important role on the filler dispersion in matrix. VMT sample treated by HCl and modified



by MA indicated low compatibility reflected on poor dispersion and thus physical properties which were similar to composites with unmodified clays. Both VMT and MMT intercalated by CTAB and Cloisite 20A reached higher dispersion and relative high increase in modulus and strong permeability decrease.

The investigation of ion effect on the composite properties showed higher dispersion of filler particles in zinc neutralized matrix than in sodium. This fact leads to higher reinforcement of zinc composite. Time was also found out as crucial factor for mechanical properties. The tensile properties were measured 3 days and one month after press moulding. As discovered, the modulus of the same sample significantly increased nearly about 20 %. Supposedly this change is caused by evolution in the polymer structure in ionic regions. The attention to this phenomenon is going to be paid in future study.

The final goal of the presented work was the influence of MAA neutralization level on the composites properties. The results showed that with higher level of MAA group neutralization modulus increased more, while gas permeability decreased strongly nearly for all samples.

# CONTRIBUTION TO THE SCIENCE AND PRACTICE

Current investigation shows the possibility how to improve mechanical, thermal or rheological properties of polymers by addition of chemically modified filler. Many types of filler, like MMT, are widely studied and employed. However, clays consist from many groups with variable behaviour. Investigation of their effect on the final properties of composite leads to the interesting improvements and unexpected behaviour.

Surlyn® belongs to rather expensive polymers, widely used in packaging and sporting goods. Surlyn® itself presents high ability against the gas permeation; however its permeability is significantly reduced, when is compounded with layered fillers, as confirmed in present work. On the other hand, improved mechanical properties can be useful for the next field of application.

Henceforth, many questions remain whether the benefit of improved properties is sufficient enough to cost reduction and improve stability to satisfy industry requirements.

## REFERENCES

- [1.] LÉBR, T. *Před sto lety odstartoval bakelit éru umělé hmoty* [Online]. Technet.cz. 6. 2 2009. [quot. 5. 6 2009]. <[http://technet.idnes.cz/pred-sto-lety-odstartoval-bakelit-eru-umele-hmoty-fsi-/tec\\_technika.asp?c=A090205\\_101730\\_tec\\_technika\\_vse](http://technet.idnes.cz/pred-sto-lety-odstartoval-bakelit-eru-umele-hmoty-fsi-/tec_technika.asp?c=A090205_101730_tec_technika_vse)>.
- [2.] *Před 100 lety se světu poprvé představil bakelit* [Online]. České noviny.cz. 5. 2. 2009. [quot. 5. 6. 2009]. <[http://www.ceskenoviny.cz/tema/index\\_view.php?id=358575&id\\_seznam=8](http://www.ceskenoviny.cz/tema/index_view.php?id=358575&id_seznam=8)>.
- [3.] RAAB, M., KOTEK, J. *Quo vadete, polymery?* Vesmír. 2009, vol. 88, p. 186-189.
- [4.] *Polyethylene* [Online]. SRI Consulting, 1. 2011 [quot. 7. 6. 2009]. <<http://www.sriconsulting.com/WP/Public/Reports/polyethylene/>>
- [5.] DuPont [Online]. [quot. 4. 6. 2009]. <<http://www.dupont.com>>.
- [6.] EINSENBURG, A., KIM, J. S. *Introduction to Ionomers*. New York : Wiley-Interscience, 1998. 327 p. ISBN 0-471-24678-6.
- [7.] MAURITZ, K. *Surlyn®* [Online]. [quot. 4. 6. 2009]. <<http://www.psrc.usm.edu/mauritz/index.html>>.
- [8.] ARDANUY, M., VELASCO, J. I., MASPOCH, M. L., HAURIE, L., FERNANDEZ, A. I. *J. Appl. Pol. Sci.* 2009, 113, 2, p. 950-958.
- [9.] SANCHEZ-VALDES, S., LOPPEZ-QUINTANILLA, M. L., RAMIREZ-VARGAS, E., MEDELLIN-RODRIGUEZ, F. J., GUTIERREZ-RODRIGUEZ, J. M. *Macromol. Mater. Eng.* 2006, 291, 2, p. 128-136.
- [10.] REES, R. W., VAUGHAN, D. J. *Polym. Prepr. Am. Chem. Soc. Div. Polym. Chem.* 1965, 6, p. 287-295.
- [11.] EINSENBURG, A., RINAUDO, M. *Polym. Bull.* 1990, 24, 6, p. 671.
- [12.] FALL, R. A. *Puncture Reversal of Ethylene Ionomers – Mechanistic Studies*. [Online] Blacksburg : Virginia Polytechnic Institute and State University, 2001. Ph.D. Thesis.
- [13.] CUI, L., TROELTZSCH, CH., YOON, P. J., PAUL, D. R. *Macromolecules*. 2009, 42, 7, p. 2599-2608.
- [14.] SOVA, M., KREBS, J. *Termoplasty v praxi: Praktická příručka pro konstruktéry, výrobce, zpracovatele a uživatele termoplastů*. Praha : Verlag Dashofer, 2001. ISBN: 80-86229-15-7.
- [15.] EISENBERG, A., HIRD, B., MOORE, R. B. *Macromolecules*. 1990, 23, p. 4098-4107.
- [16.] AL-ATI, T., HOTCHKISS, J. H. *J. Appl. Polym. Sci.* 2002, 86, p. 2811-2815.
- [17.] JIA, Y., KLEINHAMMES, A., WU, Y. *Macromolecules*. 2005, 38, p. 2781-2785.
- [18.] WAKABAYASHI, K., REGISTER, R. A. *Macromolecules*. 2006, 39, p. 1079 -1086.

- [19.] WILSON, A. D., PROSSER H. J. *Development in Ionic Polymers - 1.* Essex : Applied Science Publisher, 1983. 336 p.
- [20.] DeBOLT, M. A. a ROBERTSON, R. E. *Polym. Eng. Sci.* 2006, 46, 4, p. 385-398.
- [21.] JAKLEWICZ, M., LITAK, A., OSTOJA-STARZEWSKI, M. *J. Appl. Polym. Sci.* 2004, 91, 6, p. 3866-3870.
- [22.] MONTOYA, M., ABAD, M. J., BARRAL, L., BERNAL, C. *Eur. Polym. J.* 2006, 42, 2, p. 265-273.
- [23.] QU, G., LIU, J. *Yingyong Huaxue.* 1996, 13, 4, p. 71-73.
- [24.] YOO, Y., PARK, J. CH., WON, J. CH., CHOI, K.-Y., LEE, J. H. *Polymer (Korea).* 2004, 28, 6, p. 468-477.
- [25.] BAOUZ, T., FELLAHI, S. *J. Appl. Poly. Sci.* 2005, 98, 4, p. 1748-1760.
- [26.] LIU, H., LIM, H. T., AHN, K. H., LEE, S. J. *J. Appl. Polym. Sci.* 2007, 104, 6, p. 4024-4034.
- [27.] SHAH, R. K., KRISHNASWAMY, R. K., TAKAHASHI, S., PAUL, D. R. *Polymer.* 2006, 47, 17, p. 6187-6201.
- [28.] SHAH, R. K., PAUL, D. R. *Macromolecules.* 2006, 39, 9, p. 3327-3336.
- [29.] YOO, Y., SHAH, R. K., PAUL, D. R. *Polymer.* 2007, 48, 16, p. 4867-4873.
- [30.] START, P. R., MAURITZ, K. A. *J. Polym. Sci, Part B: Polym. Phys.* 2003, 41, 13, p. 1563-1571.
- [31.] START, P. R., SHARP, M. A., MAURITZ, K. A. *Polym. Prepr. Am. Chem. Soc. Div. Polym. Chem.* 2003, 44, 1, p. 1126-1127.
- [32.] Shah, Rhutesh K., Hunter, D. L. a Paul, D. R. *Polymer.* 2005, 46, 8, p. 2646-2662.
- [33.] Wypych, G. *Handbook of Fillers - A Definitive User's Guide and Databook. 2.* Toronto: ChemTec Publishing, 2000. p. 909. ISBN 978-1-884207-69-3.
- [34.] Rothon, R. N. *Particulate-Filled Polymer Composites. 2.* Shawbury: Smithers Rapra Technology, 2003. p. 571. ISBN: 978-1-85957-382-2.
- [35.] Kulshreshtha, A.K., Vasile, C. *Handbook of Polymer Blends and Composites.* Shawbury: Smithers Rapra Technology, 2002. p. 2536. Sv. 1. ISBN 978-1-85957-309-6 .
- [36.] USUKI, A., KOJIMA, Y., KAWASUMI, M., OKADA, A., FUKUSHIMA, Y., KURAUCHI, T., KAMIGAITO, O. *J. Mat. Res.* 1993, 8, 5, p. 1179-1184.
- [37.] LI, C., CHOU, T.-W. *Journal of Solids and Structures.* 2003, Sv. 10, 40, stránky 2487-2499 .
- [38.] LI, Y., QIU, X.M., YIN, Y., YANG, F., FAN, Q. *Phys. Lett. A.* 2009, 27-28, 373, p. 2368-2373 .
- [39.] FISCHER, H. *Mater. Sci. Eng.* 2003, 23, p. 763-772.

- [40.] ULTRACKI, L. A. *Clay-Containing Polymeric Nanocomposites*. Strawbury: Rapra Technology Limited, 2004. p. 434. v. 1. ISBN: 1-85957-437-8.
- [41.] SEYMOUR, R. B. *Polymeric Composites (New Concepts in Polymer Science) (Hardcover)*. VSP Books, 1990. p. 194. ISBN-10: 9067641219.
- [42.] PINNAVIA, T. J., BEALL, G. W. *Polymer-clay nanocomposites*. Chichester: John Wiley and Sons Ltd., 2000. p.350. ISBN: 0-471-63700-9.
- [43.] Ciullo, P.A. *Industrial Minerals and Their Uses - A Handbook and Formulary*. New Jersey: William Andrew Publishing/Noyes, 1996. p. 689. ISBN: 978-0-8155-1408-4.
- [44.] ZHANG, Y., GITTINS, D. I., SKUSE, D., COSGROVE, T., van DUIJNEVELDT, J. S. *Langmuir*. 2008, 20, 24, p. 12032-12039.
- [45.] ZHANG, Y., HAN, W., LIU, W., XU, S.-A., WU, C.-F. *J. Macromol. Sci. Part B Phys.* 2008, 47, 3, p. 532-543.
- [46.] POSPÍŠIL, M., KALEDOVÁ, A., ČAPKOVÁ, P., ŠIMONÍK, J., VALÁŠKOVÁ, M. *J. Colloid Interface Sci.* 2004, 277, p. 154-161.
- [47.] RATNAYAKE, U. N., HAWORTH, B., HOURSTON, D. J. *J. Appl. Pol. Sci.* 2009, 111, 1, p. 320-334.
- [48.] CHINELLATO, A. C., VIDOTTI, S. E., HU, G.-H., PESSAN, L. A. *J. Polym. Sci. Part B Polym. Phys.* 2008, 46, 17, p. 1811-1819.
- [49.] ZHANG, F.-A., CHEN, L., MA, J.-Q. *Polym. Adv. Tech.* 2009, 20, 6, p. 589-594.
- [50.] HWANG, S. Y., LEE, W. D., LIM, J. S., PARK, K. H., IM, S. S. *J. Polym. Sci. Part B Polym. Phys.* 2008, 46, 11, p. 1022-1035.
- [51.] BEYER, G. *Polym. Adv. Tech.* 2008, 19, 6, p. 485-488.
- [52.] Minerals by clas. [Online] [quot. 5. 6. 2009] <[http://www.galleries.com/minerals/by\\_class.htm](http://www.galleries.com/minerals/by_class.htm)>.
- [53.] BANSAL, A., MISHRA, K. K. *Paintindia*. 2009, 59, 3, p. 121-130.
- [54.] SOLAR, L., NAVARRO, R., GÓMEZ, C., REINECKE, H. *J. Nanosci. Nanotechnol.* 2007, 12, 7, p. 4546-4551.
- [55.] KELNARA, I., KHUNOVÁB, V., KOTEKA, J., KAPRÁLKOVÁ, L. *Polymer*. 2007, 48, 18, p. 5332-5339 .
- [56.] GINTERT, M.I J., JANA, S. C., MILLER, S. G. *Evaluation of nanoclay exfoliation strategies for thermoset polyimide nanocomposite systems*. Society for the Advancement of Material and Process Engineering, 2007. SAMPE Conference Proceedings.
- [57.] CHIU, C.-W., CHU, C.-C., CHENG, W.-T., LIN, J.-J. *Eur. Polym. Jl.* 2008, 44, 3, p. 628-636.
- [58.] LIN, J.J., CHENG, I.J., WANG, R.C., LEE, R.J. *Macromolecules*. 2001, 34, p. 8832–8834.
- [59.] NAYAK, S. K., MOHANTY, S. *J. App. Polym. Sci.* 2009, 112, p. 778-787.

- [60.] VAIA, R. A., TEUKOLSKY, R. K., GIANNELIS, E. P. *Chem. Mater.* 1994, 7, 6, p. 1017–1022.
- [61.] KLAPYTAA, Z., FUJITAB, T., IYI, N. *Appl. Clay Sci.* 2001, 19, 1-6, p.5-10.
- [62.] YANG, J.-H., HAN, Y.-S., CHOY, J.-H., TATEYAMA, H. *J. Mater. Chem.* 2001, 11, p. 1305 - 1312.
- [63.] IJDO, W. L., PINNAVAIA, T. J. *Chem. mater.* 1999, 11, 11, p.3227-3231.
- [64.] POSPÍŠIL, M., ČAPKOVÁ, P., MĚŘÍNSKÁ, D., MALÁČ, Z., ŠIMONÍK, J. *J. Colloid Interface Sci.* 2001, 236, p 127-131.
- [65.] MĚŘÍNSKÁ, D., CHMIELOVÁ, M., WEISS, Z., ČAPKOVÁ, P., ŠIMONÍK, J. *Intern. Polym. Proc.* 2003, 18, p. 133-137.
- [66.] MĚŘÍNSKÁ, D., VACULIK, J., KALEDOVÁ, A., WEISS, Z., CHMIELOVA, M., ŠIMONÍK, J. *J. polym. eng. 2003*, 23, 4, p. 241-257.
- [67.] GIANNELIS, E.P., KRISHNAMOORTI, R., MANIAS, E. *Adv. Polym. Sci.*, 118, p. 108-147, 1999.
- [68.] KOVÁŘOVÁ, L. *The study of multi-component Interactions in dispersive polymer environment.* Tomas Bata University in Zlín, 2005, Ph.D. Thesis.
- [69.] FORNES, T. D., HUNTER, D. L., PAUL, D. R. *Macromolecules.* 2004, 37, 5, p. 1793-1808.
- [70.] FORNES, T. D., YOON, P. J., HUNTER, D. L., KESKKULA, H., PAUL, D. R. *Polymer.* 2002, 43, 22, p. 5915-5933.
- [71.] HOTTA, S., PAUL, D. R. *Polymer.* 2004, 45, 22, p. 7639-7654.
- [72.] FITZER, R. C. patent: *PCT/US97/02506* US, 1997.
- [73.] MEYER, Jr., DOMBROSKI, M. F., EZRA, J. R. T. M. R. B. K. patent: *WO/1994/006864* 1994.
- [74.] SULLIVAN, J. M. patent: *CA Patent 2031904* US, 1991.
- [75.] SULLIVAN, M. J., NEALON, J., BINETTE, M. patent: *6667001* 2003.
- [76.] van den BROEK, A. T. J. patent: *6581359* 2003.
- [77.] Individul Clay Minerals. [Online] 2001. [quot. 28. 7. 2011] <<http://pubs.usgs.gov/of/2001/of01-041/htmldocs/clay.htm>>.
- [78.] Southern clay products, Inc. Product bulletin - Cloisite Na+. [Online] [quot. 15. 8. 2011] <[http://www.scprod.com/product\\_bulletins/PB%20Cloisite%20NA+.pdf](http://www.scprod.com/product_bulletins/PB%20Cloisite%20NA+.pdf)>
- [79.] Southern clay product, Inc. Product bulletins. [Online] [quot. 15. 8. 2011] <[http://www.scprod.com/product\\_bulletins.asp](http://www.scprod.com/product_bulletins.asp)>.
- [80.] RAHN, O., VAN ESELTINE, W.P. *Annual Rewiew of Microbiology.* 1947, 1, p. 173-192.
- [81.] Sigma-Aldrich. [Online] [quot. 10. 7. 2011.] <<http://www.sigmaaldrich.com/technical-service-home/product-catalog.html>>.
- [82.] WASEDA, Y., MATSUBARA, E., SHINODA, K. *X-Ray Diffraction Crystallography - Introduction, Examples and Solved Problems.* Springer-Verlag, 2011. ISBN: 978-3-642-16634-1.

- [83.] RAMACHANDRAN, V.S., BEAUDIN, J.J. *Handbook of analytical techniques in concrete science and technology, principles, techniques and applications*. New York: William Andrew Publishing/Noyes Publications, 2001. ISBN: 0-8155-1437-9.
- [84.] GUINEBRETIERE, R. *X-ray diffraction by polycrystalline materials*. Chippenham : ISTE Ltd, 2007. ISBN: 978-1-905209-21-7.
- [85.] Fourier transform infrared spectroscopy. [Online] Materials evaluation and engineering, Inc., 2009. [quot. 13. 8. 2011] <<http://mee-inc.com/ftir.html>>.
- [86.] CAMPBELL, D., WHITE, J.R. *Polymer characterization*. New York : Chapman and Hall, 1989. ISBN: 0-214-27160-5.
- [87.] MOORE, D.R., TURNER, S. *Mechanical evaluation strategies for plastics*. Cambridge : Woodhead Publishing Limited, 2001. ISBN: 1-85573-379-X.
- [88.] KONECNY, P. *Gas permeability in rubber matrix*. Faculty of technology, Tomas Bata University in Zlin. 2007. PhD Thesis.
- [89.] The crystal structure of VMT. [Online] Grena a.s. [quot. 15. 7. 2011] <[http://svt.pi.gin.cz/gre\\_en/c1007-en-the-crystal-structure-of-VMT.html](http://svt.pi.gin.cz/gre_en/c1007-en-the-crystal-structure-of-VMT.html)>.
- [90.] OSMAN, M.A. *J. Mater. Chem.* 2006, 16, p. 3007-3013.
- [91.] MARTYNKOVÁ, G.S., VALÁŠKOVÁ, M., ŠUPOVÁ, M. *Phys. Stat. Sol.* 2007, 204, 6, p. 1870-1875.
- [92.] LIU, B., DING, Q., ZHANG, J., HU, B. *Polymer Composites*. 2005, 26, 5, p. 706-712.
- [93.] RITTLER, H.R. *Method of treating phyllosilicates*. US4952388 USA, 1990.
- [94.] SLADE, P.G., RAUPACH, M. EMERSON, W.W. *Clays and Clay Minerals*. 1978, 26, 2, p. 125-134.
- [95.] PLACHÁ, D., MARTYNKOVÁ, G.S., RUMMELI, M.H. *J. Colloid Interface Sci.* 2008, 327, 1, p. 341-347.
- [96.] TJONG, S.C., MENG, Y.Z., HAY, A.S. *Chem. Mater.* 2002, 14, p. 44-51.
- [97.] WRITTING, A. The role of heat in ceramics. [Online] 2011. [quot. 1. 8. 2011] <[http://www.ehow.com/info\\_8670865\\_role-heat-ceramics.html](http://www.ehow.com/info_8670865_role-heat-ceramics.html)>.
- [98.] HALPIN, J.C., FINLAYSON, K.M., ASHTON, J.E. *Primer on composite materials analysis*. 2nd rev. Lancaster : Technomic Pub. Co., 1992. p. 227.
- [99.] HALPIN, J.C., KARDOS, J.L. *Polym. Eng. Sci.* 1976, 16, p. 344-352.
- [100.] GRADY, B.P. *Polymer*. 2000, 41, p. 2325-2328.
- [101.] WINEY, K.I., LAURER, J.H., KIRKMEYER, B.P. *Macromolecules*. 2000, 33, p. 507-513.
- [102.] WALTERS, R.M., SOHN, K.E., WINEY, K.I., COMPOSTO, R.J. *J. Polym. Sci.* 2002, 41, p. 2833-2841.
- [103.] CUI, L., TROELTZSCH, CH., YOON, P. J. PAUL, D. R. *Macromolecules*, 2009, 42, p. 2599-2608

# AUTHOR'S PUBLICATIONS

## Research Papers

1. ZÁDRAPA, P.; MALÁČ, J.; KONEČNÝ, P. Filler and mobility of rubber matrix molecules. *Polym. Bull.* 2011, 67, 5, 927-936.
2. ZÁDRAPA, P., ZÝKOVÁ, J., TRIPSKÁ, E., MALÁČ, J., KOVÁŘOVÁ, L. Preparation of (ethylene-methacrylic acid) copolymer/VMT composites, *SENSIG'10/MATERIALS'10 Proceedings of the 3<sup>rd</sup> WSEAS international conference of Advances in sensors, signals and materials*. WSEAS Stevens Point, Wisconsin, USA 2010, p. 75-78. ISBN: 978-960-474-248-6.
3. ZÝKOVÁ, J., KALEDOVÁ, A., MATĚJKA, V., ZÁDRAPA, P., MALÁČ, J., Influence of kaolinite modification on the PVC composite properties. *SENSIG'10/MATERIALS'10 Proceedings of the 3<sup>rd</sup> WSEAS international conference of Advances in sensors, signals and materials*. WSEAS Stevens Point, Wisconsin, USA 2010, p. 30-34. ISBN: 978-960-474-248-6.

## Conference contributions

1. ZÁDRAPA, P.; KOVÁŘOVÁ, L.; MALÁČ, J. Composite and nanocomposite materials base on Surlyn®/clay. In Šandera, P., *Proceedingst of the International Conference NANO'06*. Brno: Vysoké učení technické, Fakulta strojního inženýrství, 2006. p. 87 - 92. ISBN 80-214-3331-0.
2. KOVÁŘOVÁ, L.; KALEDOVÁ, A.; ZÁDRAPA, P.; MALÁČ, J. Thermo-mechanical and rheological properties of PVC/MMT nanocomposites. In Šandera, P., *Proceedingst of the International Conference NANO'06*. Brno: Vysoké učení technické, Fakulta strojního inženýrství, 2006. p. 287 - 92. ISBN 80-214-3331-0.
3. KOVÁŘOVÁ, L.; ZÁDRAPA, P.; MALÁČ, J. Comparison of different types of clay modification in PVC/clay nanocomposite. In *Nanostructured polymers and polymer nanocomposites*. Praha : Ústav Makromolekulární Chemie AV ČR, v.v.i, 2007. p. 142. ISBN 978-80-85009-55-2.
4. ZÁDRAPA, P.; KOVÁŘOVÁ, L.; MALÁČ, J. Nanocomposite materials based on Surlyn®/clay. In *Nanostructured polymers and polymer nanocomposites*. Praha : Ústav Makromolekulární Chemie AV ČR, v.v.i, 2007. p. 143. ISBN 978-80-85009-55-2.
5. ZÁDRAPA, P.; KOVÁŘOVÁ, L.; MALÁČ, J. Thermal properties and flow behaviour of Surlyn®/clay nanocomposites. In Šandera, P.,



- JUNIORMAT '07 International Conference*. Brno: Vysoké učení technické, Fakulta strojního inženýrství, 2007. p. 35 - 38. ISBN 978-80-214-3459-2.
6. KOVÁŘOVÁ, L.; ZÁDRAPA, P.; MALÁČ, J. The effect of clay agglomerate size on final properties of PVC/clay nanocomposites. In Šandera, P., *JUNIORMAT '07 International Conference*. Brno: Vysoké učení technické, Fakulta strojního inženýrství, 2007. p. 149 -152. ISBN 978-80-214-3459-2.
  7. KOVÁŘOVÁ, L.; ZÝKOVÁ, J.; ZÁDRAPA, P.; MALÁČ, J. Thermal properties of PVC/clay nanocomposites. In Šandera, P., *JUNIORMAT '07 International Conference*. Brno: Vysoké učení technické, Fakulta strojního inženýrství, 2007. p. 129 - 132. ISBN 978-80-214-3459-2.
  8. ZÁDRAPA, P.; KOVÁŘOVÁ, L.; MALÁČ, J. Effect of methacrylic acid neutralization degree on Surlyn®/filler composite properties. In *Program and Proceedings PPS-24 CD*, Dipartimento di Ingegneria Chimica e Alimentace dell Università degli Studi di Salerno, 2008. p. 431. ISBN 88-7897-025-5.
  9. ZÝKOVÁ, J.; KOVÁŘOVÁ, L.; ZÁDRAPA, P.; MALÁČ, J. Thermal properties of PVC/clay nanocomposites and composites. In *Program and Proceedings PPS-24 CD*, Dipartimento di Ingegneria Chimica e Alimentace dell Università degli Studi di Salerno, 2008. p. 441. ISBN 88-7897-025-5.
  10. ZÝKOVÁ, J., KOVÁŘOVÁ, L., ZÁDRAPA, P., MALÁČ, J. Effect of Different Clay Treatment on Thermal Behaviour of PVC/Clay Nanocomposites and Composites. *5<sup>th</sup> International Conference on Polymer Modification, Degradation and Stabilization*, Liège, Belgium, 2008.
  11. ZÁDRAPA, P., ZÝKOVÁ, J., KOVÁŘOVÁ, L., MALÁČ, J. Mechanical and Rheological Properties of Surlyn®/Clay Composites. *5<sup>th</sup> International Conference on Polymer Modification, Degradation and Stabilization*, Liège, Belgium, 2008.
  12. ZÁDRAPA, P., KOVÁŘOVÁ, L., MALÁČ, J., ZÝKOVÁ J., MONSO B. E. Surlyn®/Clay Composites: morphological study and mechanical properties. In *Proceedings PPS-25 CD*, Indian Institute of Technology, Goa, India, 2009, p.41.
  13. ZÝKOVÁ, J., ZÁDRAPA, P., KOVÁŘOVÁ, L., ČERNOCHOVÁ, J. Mechanical and thermal properties of PVC/Clay composites. In *Proceedings PPS-25 CD*, Indian Institute of Technology, Goa, India, 2009, p.54.
  14. ZÁDRAPA, P., ZÝKOVÁ, J., KOVÁŘOVÁ, L., MALÁČ, J. Ion effect on the properties of Surlyn®/clay nanocomposites. In *Proceedings of the*

*Polymer Processing Society Europe/Africa Regional Meeting PPS-2009 CD*, Larnaca, Cyprus, 2009, p. 179.

15. ZÝKOVÁ, J., VAŠÁK, R., KOVÁŘOVÁ, L., PASTOREK, M., MALÁČ, J., ZÁDRAPA, P. PVC-paste organoclays composites: Effect on the mechanical and thermal properties. In *Proceedings of the Polymer Processing Society Europe/Africa Regional Meeting PPS-2009 CD*, Larnaca, Cyprus, 2009, p. 180.
16. ZÁDRAPA, P., HNIDÁKOVÁ, D., KOVÁŘOVÁ, L., MALÁČ, J. Properties study of Surlyn®/clay composites. In *EPF (European Polymer Congress)*, Graz University of Technology, Institute of Chemistry and Technology of Materials, 2009, p. 261.
17. ZÁDRAPA, P., ZÝKOVÁ, J., KOVÁŘOVÁ, L., MALÁČ, J. Kompozity ionomer-jíl. Sborník konference Plastko 2010 CD. Zlín, Czech Republic, 2010.
18. ZÝKOVÁ, J., KOVÁŘOVÁ, L., KALEDOVÁ, A., ZÁDRAPA, P., MALÁČ, J. Effect of the modification on the thermal properties PVC-paste organoclay composites. Sborník konference Plastko 2010 CD. Zlín, Czech Republic, 2010.

# CURRICULUM VITAE

## **Personal data:**

*Name:* Petr Zádrapa

*Date of Birth:* 1981, October 21

*Present Address:* Tomas Bata University in Zlín, Faculty of Technology,  
Department of Polymer Engineering, TGM 275 Zlín,  
Czech Republic

*Nationality:* Czech

*E-mail:* zadrapa@ft.utb.cz

## **Employment:**

2009 – present Assistant at Tomas Bata University in Zlín, Faculty of  
Technology, Department of Polymer Engineering

## **Education:**

2006 – present Tomas Bata University in Zlín, Faculty of Technology,  
Department of Polymer Engineering; Ph.D. Degree  
Programme – Chemistry and Technology of Materials  
Course – Technology of Macromolecular Materials

2001 – 2006 Tomas Bata University in Zlín, Faculty of Technology,  
Master's degree programme – Polymeric materials and  
technologies, Course – Polymeric Engineering

## **Work on projects:**

Collaborator Grant FI-IM3/085, Polyolefinic based nanocomposites with  
extraordinary applicable properties.  
Grant KAN100400701, Nanotechnology for public, project  
Hybrid nanocomposite materials.

## **Membership in conference committees and scientific bodies:**

2006 – present Member, Society of Plastic Engineers

# LIST OF FIGURES

Fig. 1:	The discovery of new polymer in time [3].	9
Fig. 1.1:	Theoretical structure of poly(ethylene-CO-methacrylic acid) ionomer [5].	11
Fig. 1.2:	WAXS profile for a) branched polyethylene, b) ethylene/methacrylic acid copolymer and c) ethylene/methacrylic acid copolymer neutralized with Na ions [7].	11
Fig. 1.3:	Copolymerization of ethylene and methacrylic acid (step 1).	12
Fig. 1.4:	Structure of Surlyn® neutralized by NaOH (step 2).	12
Fig. 1.5:	Various grades of Surlyn® are influenced by MAA content and MAA degree neutralization [5].	14
Fig. 2.1:	The platelets of layered silicate, a) exchangeable ions between layers, and b) organic cations intercalated between layers [39].	16
Fig. 2.2:	Structure of a) tetrahedron, and b) octahedron [43].	17
Fig. 2.3:	Schematically visualized layers of a) kaolin and b) MMT [43].	18
Fig. 2.4:	Comparison of a) sodium MMT and b) MMT intercalated by organic cation [59].	19
Fig. 2.5:	Clay/polymer compound with a) intercalated structure, and b) exfoliated structure [59].	20
Fig. 2.6:	Scheme of the a) conventional composite, b) intercalated composite, and c) exfoliated composite.	21
Fig. 2.7:	X-ray diffraction pattern of a) conventional clay composite, b) intercalated clay nanocomposite, and c) exfoliated (delaminated) clay nanocomposite [68] [67].	21
Fig. 2.8:	TEM micrographs of nanocomposite prepared from a) lithium, b) sodium and c) zinc neutralized Surlyn® [28].	22
Fig. 4.1:	Structure of a) VMT, and b) MMT [43].	27
Fig. 4.2:	Intercalating agent of commercially available fillers. HT is Hydrogenated Tallow (~65 % C18; ~30 % C16; ~5 % C14) [74].	28
Fig. 4.3:	Modifying agent a) Cetyltrimethylammonium bromide and b) malein anhydride [76].	29
Fig. 4.4:	Bragg's law	30
Fig. 4.5:	Measuring cell for gas permeability	34
Fig. 5.1:	Comparison of VMT and MMT structures.	35
Fig. 5.2:	The effect of the solution temperature on the VMT structure. Sample codes denoted in Table 5.1.	38
Fig. 5.3:	The effect of the drying temperature on vermiculite structure. Sample codes denoted in Table 5.1 and 5.3.	39

Fig. 5.4:	The effect of the solution molarity on the structure changes of vermiculite. Sample codes denoted in Table 5.1–5.3.....	40
Fig. 5.5:	The effect of the mixing time on the level of Na <sup>+</sup> saturation during room temperature. Sample codes denoted in Table 5.2. ....	41
Fig. 5.6:	The effect of the renewal solution on the level of Na <sup>+</sup> saturation at higher temperature. Sample codes denoted in Table 5.2. ....	41
Fig. 5.7:	FTIR spectra: effect of solution molarity. Sample codes denoted in Table 5.1–5.3. ....	42
Fig. 5.8:	Time dependence of structural changes using 1M HCl solution. Sample codes denoted in Table 5.4. ....	44
Fig. 5.9:	Time dependence of structural changes using 2M HCl solution. Sample codes denoted in Table 5.4. ....	45
Fig. 5.10:	Effect of temperature on the structural changes using 1M and 2 M HCl solution. Sample codes denoted in Table 5.4. ....	45
Fig. 5.11:	FTIR spectra of HCl modified VMT. Sample codes denoted in Table 5.4. ....	46
Fig. 5.12:	SAXS of intercalated sodium VMT by CTAB for 5 hours. Sample codes denoted in Table 5.5. ....	48
Fig. 5.13:	SAXS of intercalated sodium VMT by CTAB for 24 hours. Sample codes denoted in Table 5.5. ....	49
Fig. 5.14:	FTIR spectra of organically modified sodium vermiculite. Sample codes denoted in Table 5.5. ....	49
Fig. 5.15:	SAXS of HCl treated and maleic anhydride modified VMT. Sample codes denoted in Table 5.4. ....	50
Fig. 5.16:	FTIR spectra of HCl treated and maleic anhydride modified VMT. Sample codes denoted in Table 5.4. ....	52
Fig. 5.17:	SAXS of sodium montmorillonite and its CTAB modified form.....	52
Fig. 5.18:	Interlayer distances for Cloisite 15A and Cloisite 20A.....	53
Fig. 5.19:	Comparison of filler intercalated by organic cations. ....	53
Fig. 5.20:	TGA curves for inorganic fillers. ....	54
Fig. 5.21:	TGA curves for organically modified VMT.....	55
Fig. 5.22:	TGA curves organically intercalated MMTs.....	56
Fig. 5.23:	Optical microscopy pictures (first approach to morphology) of Surlyn® 9020/Cloisite 20A compounds prepared on a) twin screw extruder, b) mixing chamber and c) double roll mill. ....	59
Fig. 5.24:	SEM pictures of Surlyn® 9020/Cloisite 20A compounds prepared on a) twin screw extruder, b) mixing chamber and c) double roll mill.....	60
Fig. 5.25:	X-ray diffraction of Surlyn® 9020 compounds with inorganic fillers. ....	63

Fig. 5.26: X-ray diffraction of Surlyn® 9020 compounds with organically modified clays.....	63
Fig. 5.27: Comparison of interlayer spacing between polymer–clay compound (full line) and filler (dot line).....	64
Fig. 5.28: Optical microscopy (first approach to morphology) of Surlyn® 9020 compounds filled by inorganic fillers, namely a) expanded VMT, b) NaVMT, c) HCIVMT 24 and d) Cloisite Na <sup>+</sup> .....	65
Fig. 5.29: Optical microscopy (first approach to morphology) of Surlyn® 9020 compounds with organic fillers a) HCIVMT 7, b) HCIVMT 24, c) o-NaVMT, d) o-NaMMT and e) Cloisite 20A.....	66
Fig. 5.30: SEM photos of Surlyn® 9020 compounded with inorganic fillers a) Cloisite Na <sup>+</sup> , b) NaVMT and c) HCIVMT 24.....	67
Fig. 5.31: SEM photos of cryogenically fractured Surlyn® 9020 compounded with organic fillers a) o-HCIVMT 24, b) o-NaVMT, c) o-NaMMT, and d) Cloisite 20A. ....	69
Fig. 5.32: SEM photos of selectively etched Surlyn® 9020 compounded with organic fillers a) o-NaVMT, b) o-NaMMT, and c) Cloisite 20A.....	70
Fig. 5.33: Detailed study of clay particles in cryogenically fractured polymer composites, a) o-HCIVMT, b) o-NaVMT, c) o-MMT and d) Cloisite 20A.....	71
Fig. 5.34: Detailed study of clay particles in selectively etched polymer composites, a) o-NaVMT, b) o-MMT and c) Cloisite 20A.....	72
Fig. 5.35: TEM photos of Surlyn® 9020 compounded with Cloisite 20A, a) surface of press moulded sheet and b) cut across the thickness of the sheet. ....	73
Fig. 5.36: TEM photos of Surlyn® 9020 compounded with MMT modified by CTAB, a) surface of press moulded sheet and b) cut across the thickness of the sheet. ....	73
Fig. 5.37: TEM photos of Surlyn® 9020 compounded with VMT modified by CTAB, a) surface of press moulded sheet and b) cut across the thickness of the sheet. ....	74
Fig. 5.38: Modulus increase in comparison to pure Surlyn® 9020 in %.....	76
Fig. 5.39: Yield stress increase in comparison to pure Surlyn® 9020 in %.....	76
Fig. 5.40: Break stress increase in comparison with pure Surlyn® 9020 in %.....	77
Fig. 5.41: Permeability decrease in %, in comparison to pure polymer Surlyn® 9020.....	79
Fig. 5.42: X-ray diffraction spectra of zinc and sodium Surlyn® filled by o-NaVMT and Cloisite 20A. ....	81

Fig. 5.43: Optical microscopy (first approach to morphology) of zinc and sodium ionomer compounds. Surlyn® 9910 filled by a) o-NaVMT, b) Cloisite 20A and Surlyn® 8920 compounded with c) o-NaVM and d) Cloisite 20A. ....	82
Fig. 5.44: SEM pictures of Surlyn® 9910 filled by a) o-NaVMT and b) Cloisite 20A and Surlyn® 8920 filled by c) o-NaVMT and d) Cloisite 20A .....	83
Fig. 5.45: Effect of filler addition on the modulus of Surlyn® 8920 and Surlyn® 9910.....	85
Fig. 5.46: Effect of filler addition on the yield stress of Surlyn® 8920 and Surlyn® 9910.....	86
Fig. 5.47: Permeability decrease in % for Cloisite 20A compounded with Surlyn® 9910 and Surlyn® 8920. ....	88
Fig. 5.48: Classification of Surlyn® in dependence on MAA content and level of its neutralization. ....	89
Fig. 5.49: Diffraction patterns of Surlyn® compounds with MMT based filler Cloisite 20A. ....	90
Fig. 5.50: Microscopy of Cloisite 20A compounds with a) Surlyn® 1605, b) Surlyn® 8920, c) Surlyn® 9020, d) Surlyn® 1705, e) Surlyn® 9721 and f) Surlyn® 9910. ....	91
Fig. 5.51: SEM photos of selectively etched compounds with Cloisite 20A in a) Surlyn® 1605, b) Surlyn® 8920, c) Surlyn® 1705, d) Surlyn® 9721 and e) Surlyn® 9910.....	92
Fig. 5.52: Modulus improvement of Surlyn® compounds with Cloisite 20A. ....	94
Fig. 5.53: Comparison of permeability decrease in % of filled compounds. ....	95

# LIST OF TABLES

Table 1.1:	Selected properties of Surlyn® (5).....	13
Table 4.1:	Properties of various types of Surlyn® [5, 72–76].....	26
Table 4.2:	Basic characteristic of MMT and VMT [52, 77, 78].....	27
Table 4.3:	Main characteristic properties of Cloisite 20A and Cloisite 15A [79].....	28
Table 5.1:	Preparation condition for 2M NaCl water solution.....	37
Table 5.2:	Preparation condition for 3M NaCl water solution.....	37
Table 5.3:	Preparation condition for 1M and 4M NaCl water solution.....	38
Table 5.4:	Condition of VMT preparation modified by HCl.....	43
Table 5.5:	Condition of preparation organically modified sodium VMT. ....	47
Table 5.6:	Content of water and organic component, calculated from TGA and burning test. ....	57
Table 5.7:	Compounding conditions for three methods. ....	59
Table 5.8:	Fillers compounded with polymers. Fillers short cuts are in brackets. ....	61
Table 5.9:	Compounding conditions for various types of Surlyn®.....	62
Table 5.10:	Tensile properties for the compounds containing 3 wt % of filler.....	74
Table 5.11:	Tensile properties for the compounds containing 5 wt % of filler.....	75
Table 5.12:	Permeability results for Surlyn® 9020 compounds. ....	78
Table 5.13:	Tensile properties of Surlyn® 8920 .....	84
Table 5.14:	Tensile properties of Surlyn® 9910 .....	84
Table 5.15:	Time dependence of modulus for samples filled by 5 wt %. ....	87
Table 5.16:	Permeability coefficient for Surlyn® 8920 and Surlyn® 9910 and their compounds with 5 wt % of fillers. ....	87
Table 5.17:	Modulus of pure polymer and filled by Cloisite 20A .....	93
Table 5.18:	Permeability coefficient of unfilled and filled Surlyn® compounds.....	95



# LIST OF SYMBOLS AND ABBREVIATIONS

MAA	-	methacrylic acid
WAXS	-	wide angle X-ray scattering
SAXS	-	small angle X-ray scattering
PE	-	polyethylene
MPa	-	megapascal
ASTM	-	American Society for Testing and Materials
DSC	-	differential scanning calorimetry
CEC	-	cation-exchange capacity
nm	-	nanometre
MMT	-	Montmorillonite
TEM	-	transmission electron microscopy
E	-	tensile modulus
MA	-	maleic anhydride
PP	-	polypropylene
IA	-	isobutyl acrylate
g	-	gram
cm	-	centimetre
min	-	minute
°C	-	Celsius degree
mm	-	millimetre
µm	-	micrometre
CTAB	-	cetyltrimethylammonium bromide
λ	-	wavelength
Θ	-	angle between incident beam of X-ray
d	-	spacing between crystal planes
FTIR	-	Fourier transform infrared spectroscopy
ATR	-	attenuated total reflectance
TGA	-	thermal gravimetric analysis
SEM	-	scanning electron microscopy
p	-	pressure
M	-	molar concentration, molarity
rpm	-	rotation per minute
VMT	-	Vermiculite
l	-	litre
mol	-	mole
s	-	second
XRD	-	X-ray diffraction
wt %	-	weight percentage
m	-	metre
Pa	-	pascal